High Speed Jet Turbine Test
Final Report

ME 430
Fall 2015

December 08, 2015

Ken Enstrom

Cameron Naugle

Isaac Thomas

Cody Lee

Project Manager:
Russell Westphal

Mechanical Engineering Department
California Polytechnic State University
San Luis Obispo

Contents

List of Tables

List of Figures

Nomenclature

Symbol	Description	Dimensions (FLT)	Units
α	Kinetic energy coefficient	-	-
ρ	Density	FL-4T2	lbf-s^2/ft^4
μ	Dynamic viscosity	FL-2T	lbf-s/ft^2
ε	Tube surface roughness	L	ft
Q	Volumetric flowrate	L3T-1	GPM
$\overline{V}$	Average velocity (axial)	LT-1	ft/s
A	Area (cross-sectional)	L2	ft^2
g	Acceleration of gravity	LT-2	ft/s^2
h	Air height in tank	L	ft
K_L	Entrance loss coefficient	-	-
f	Darcy friction factor	-	-
l	Length of tube	L	in
D	Inside diameter of tube	L	in
p	Pressure	FL-2	lbf/in^2
z	Elevation	L	ft
h_L	Head loss	L	ft
Re_D	Reynolds number	-	-
u	Uncertainty	Varied	Varied
$\dot{m}$	Mass flowrate	FTL-1	lbf-s/ft

1. Introduction

At high flight altitudes and speeds, external airplane elements are subject to immense loads. External devices must be put through testing that simulates these loads to ensure safety of the device. Our system will subject a device in need of testing to a jet of air, similar to wind seen on the surface of an airplane.

The High Speed Air Jet Turbine Test project team has been tasked to design, build, and test an apparatus capable of acquiring real world flight data for micro-ram air turbines (micro-RAT). The micro-RAT is a device that provides power to an electrical device by converting the kinetic energy of the wind into electrical energy. Currently the Cal Poly BLDS (Boundary Layer Development System) team has designed and is in the process of testing a micro-RAT to power an electronic BLDS on an airplane wing. Boundary layer development systems are used to gather flow data over airplane wings using various Pitot-static tubes. The apparatus will accurately measure thrust due to wind loads as well as torque developed by the rotor. Figure 1 identifies the main components of a micro-RAT. Each component is marked with a yellow number to distinguish and identify the main components of the device. Table 1 identifies the significance of each of the four main components.

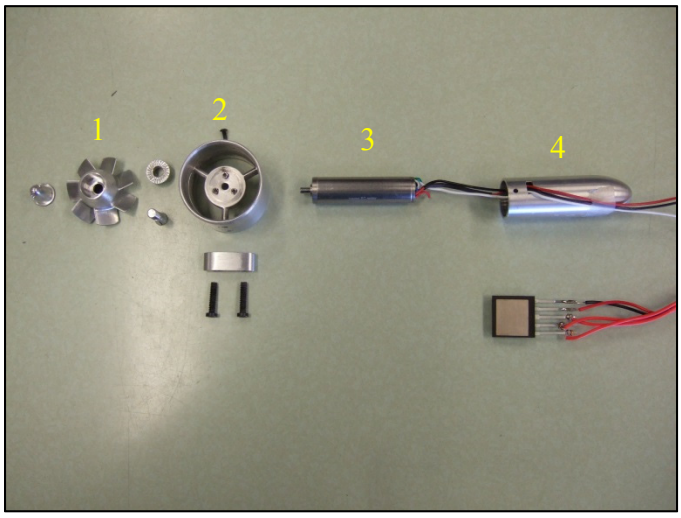

Figure 1. Components of a micro-RAT before assembly.

Table 1. (micro-RAT) component identification and description.

Figure Number	Component Name	Description of Device Function
1	Turbine Blisk	The turbine blisk is the collection of fan blades that diverts oncoming air. This diversion of air provides torque to the generator.
2	Turbine Shroud	The shroud increases turbine efficiency through contraction of the air stream.
3	Generator	The brushless three pole motor used to generate electricity when an input torque in provided.
4	Nacelle	Improves aerodynamic efficiency of the micro-RAT.

Currently the Cal Poly BLDS team is using the Cal Poly wind tunnel to test the micro-RAT shown in Figure 1. Unfortunately, the wind tunnel is only capable of creating wind speeds up to 100 mph. This velocity is far too low to recreate an adequate testing environment to simulate a high speed jet. The desired airstream velocity to simulate these environmental conditions is Mach 0.5 (380 mph). Figure 2 shows the micro-RAT mounted on an aluminum arm in the test section of the Cal Poly wind tunnel.

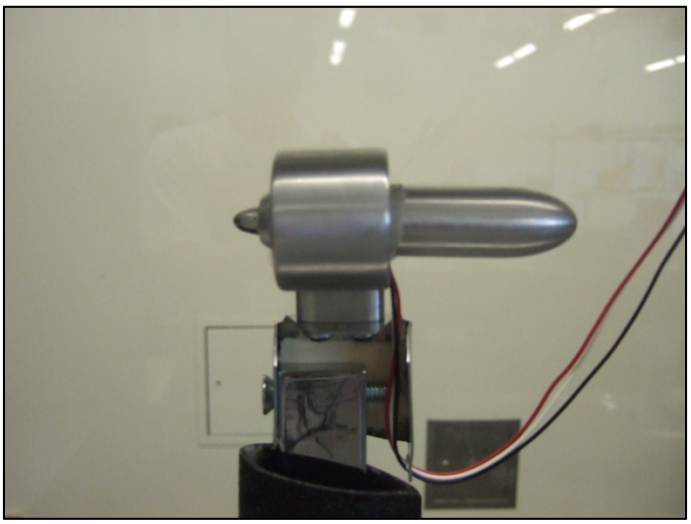

Figure 2. Assembled micro-RAT ready for testing in the Cal-Poly wind tunnel.

Dr. Westphal of Cal Poly will be our point of contact as well as our official sponsor for the project. He will make all financial and final design decisions. Potential clientele includes but is not limited to aircraft manufacturers and alternative energy wind farms. Wind turbine companies could

use this BLDS system to obtain data about flow over wind turbine blade tips and wing control surfaces for aircraft manufacturers. Large wind turbine blade tips can reach speeds over 100 mph, making high-speed tests appropriate for this industry. The FAA requires an extensive array of testing on any in-flight on-wing device. Convincing the FAA that implementing a micro-RAT on an airplane wing can be safe may be difficult to do. But data that this test rig will provide can convince the FAA to approve the device.

2. Background

2.1 Boundary Layer Development System

The Cal Poly BLDS team is currently having difficulty powering "on-wing surface electrical systems" at high altitude with an ample supply of electrical current. These electrical systems reside on the wings of airplanes and experience adverse environmental conditions negatively affecting battery performance. The cold environment and high altitude is hindering battery and sensor performance of the BLDS. The micro-RAT acts as a more reliable charging/power source for these delicate electrical systems while providing a heat source for the BLDS to maintain accurate readings. Currently, Cal Poly does not possess a wind tunnel capable of developing speeds that would satisfy interested parties' concerns of flight readiness of the micro-RAT. Figure 3 shows a typical BLDS system that traverses the wing.

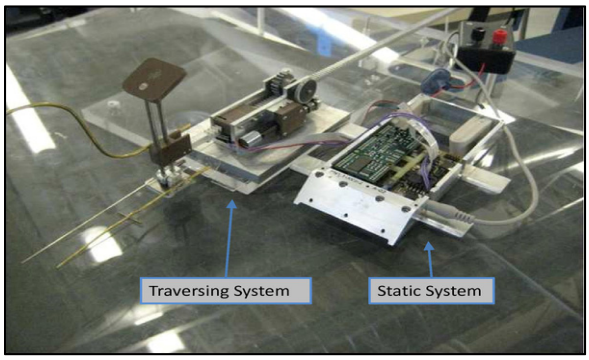

Figure 3. Typical on-wing BLDS electrical system. Photo courtesy of reference [2]

These BLDS systems use Pitot-static probes to measure how the boundary layer is developing over the wing of an airplane. By traversing the wing from leading to trailing edge (traversing system in Figure 3), a 2D cross section of pressure measurements of the air stream boundary layer can be obtained and transmitted by a system (Static system Figure 3) to a computer. These pressure measurements provide critical insight to how the boundary layer develops as it moves downstream on the wing. By knowing how the boundary layer develops, important performance metrics can be obtained regarding the control surface.

2.2 Existing Technology

Currently many institutions such as the NASA Langley Research Center, [3], have wind tunnels capable of reaching test section velocities of Mach speeds greater than 20. The Hot Shot wind tunnel located at NASA Langley's Hypersonic Facilities Complex can reach test section velocities greater than Mach 27. The facility is used to test flows past ballistic missiles, as well as

reentry of space shuttle. By utilizing an arc chamber to create a high-pressure region and creating a vacuum in large cylindrical silos known as the "Gun Barrel", where the ballistic missiles are placed, the air can reach these hypersonic speeds. The NASA facility is shown in Figure 4 in Langley, Virginia.

Some high-end, market available, wind tunnels are capable of producing Mach 0.5 speeds. Unfortunately these wind tunnels are extremely expensive and out of the budget of the BLDS team. No current patents are held on the general aspects of hyper and/or subsonic wind tunnels as they have been around for so long that the government no longer enforces monopolistic rights to previous patent owners. General Electric first patented the hypersonic wind tunnel in 1951[1]. The patent is included as Appendix A.

Figure 4. NASA Langley Hypersonic Facilities Complex, home to the "Hot Shot" Wind Tunnel [3].

Due to the extreme cost to operate such a facility demonstrated in Figure 4, it can readily be understood our limits on test section velocity (i.e. the cross section where the model requiring testing is placed, having the maximum velocity). Luckily, no patents exist on any pressure differential driven air streams so we can borrow from NASA's long tested concept and use the Cal- Poly air tanks located in the southwest corner of Building 13. These tanks will create a pressure differential great enough to obtain our required test section velocity.

Currently Ram Air Turbines are designed for use as emergency power generators on airplanes, shown in Figure 5. In the event of total power failure, the Emergency RAT is deployed and helps operate minimalistic functions of the airplane. Recently, emergency RAT's have shown the capability to save lives. In the case of U.S Airways flight 1549 [8], Capt. Chelsey B. Sullenberger III utilized the plane's on-board RAT to power hydraulic systems allowing him to control the descent of the airplane into the Hudson River. These RAT's are typically around 3 feet in diameter and contain no shroud. We hope to gain insight into just how valuable these micro-RATs can be on a smaller scale.

Figure 5. Emergency RAT on an airbus. Picture courtesy of [9].

The Cal Poly wind tunnel, located in building 192, as shown in Figure 6 is only capable of achieving wind speeds up to 100 mph. It is not practical to retrofit this wind tunnel to replicate real world flight conditions.

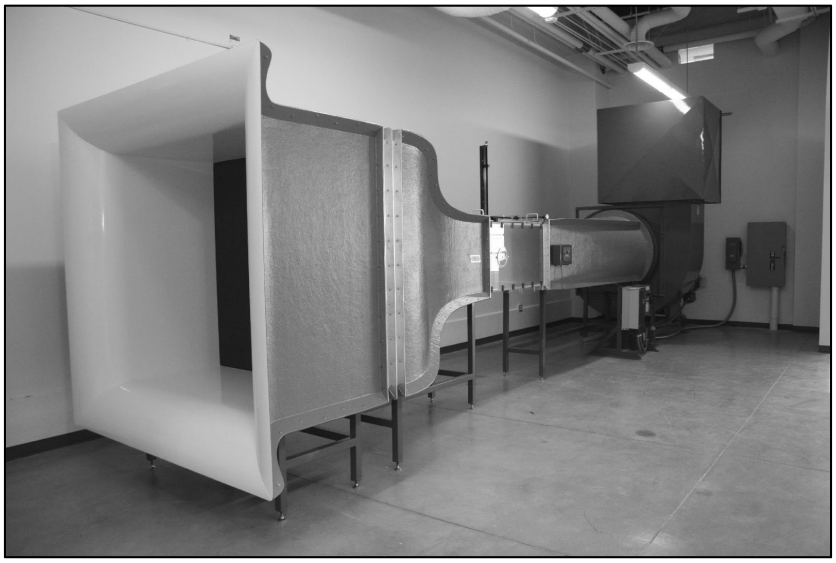

Figure 6. Cal Poly Mechanical Engineering Department wind tunnel.

All of the existing technologies discussed in this section do not meet our requirements and warrant the design and manufacture of a new system to test the micro-RAT. Among many of the existing wind tunnels flow straightening is applied to increase performance of the tunnel. Flow straightening is the reduction in secondary flow of the air stream (flow not in the downstream direction). This is typically done using a combination of steel mesh and a honeycomb structure. Utilization of these existing technologies in this project will improve the overall design.

2.3 Cal Poly Facilities

Our test device will utilize the air storage tanks that supply Building 13 of the Cal Poly campus to satisfy our pressure differential needs. These tanks are maintained at a constant 120 psig by a 75 h.p. compressor (shown in Figure 8). The storage tanks (shown in Figure 7), together, sum to an approximate volume of 14,000 gallons. The supply pipe feeding the lab is 4" in diameter and feeds several different flow regulators. One branch of the main pipe is a 3" line with pre-existing NPT (National Pipe Thread) connections. The other branch is a high SCFM (Standard Cubic Feet per Minute) 4" pipe with a larger 4" female NPT port. Both have electronically controlled ball valves that can be used to control the flow of air out of the branch of supply line. Either branch from the main pipe can be utilized to supply air to our micro-RAT test rig.

Figure 7. Cal Poly air supply for Building 13.

Figure 8. Compressor for Cal Poly Building 13 air supply tanks.

Due to the large volume of these tanks (Figure 7) we can assume a constant pressure source of 120 psig can be maintained by the compressor (Figure 8) through operation of our device for all intents and purposes of analysis in the following sections of this report.

2.4 Applicable Equations

The energy equation (head loss equation) [4] will be implemented in order to predict flow rates in this project. Assumptions made about the flow in order to validate the use of this equation include: incompressible fluid, steady flow, and application to a control volume with one inlet and exit.

$$\left(\frac{P_1}{\rho g}+\alpha_1\frac{\overline{V_1}^2}{2g}+z_1\right)-\left(\frac{P_2}{\rho g}+\alpha_2\frac{\overline{V_2}^2}{2g}+z_2\right)=h_L \tag{1}$$

In this equation P is pressure, ρ is density, g is acceleration due to gravity, α is the kinetic energy coefficient, $\bar{V}$ is average velocity, z is elevation, and h_L is the head loss term. The subscripts 1 and 2 indicate the inlet and exit conditions respectively. For this model, the control volume was taken with respect to a streamline that follows a path from the inside of the tank to the exit, where our testing will occur. With this particular control volume and streamline, $P_2=P_{ambient}$ because the exit condition is exposed to the atmosphere while $P_1=P_{tank}$. The head loss term, h_L, in Eq. (2) is composed of two distinct losses, major and minor head loss, which represent the amount of energy the fluid losses going through the control volume head loss. The major Head loss component of the term in Eq. (3) represents the energy expended by the fluid due to shear stress in the fluid from friction at the pipe wall. The major head loss is typically calculated using the Darcy friction factor, *f*, in the following equation [5]:

$$h_{L\,major}=f\frac{l}{D}\frac{\overline{V_2}^2}{2g} \tag{2}$$

In this equation *l* is the length of the pipe and *D* is the diameter of the pipe. The friction factor will be calculated using the Colebrook correlation. As the friction factor is a function of Reynolds number, which is a function of the flow rate, which is in turn a function of the friction factor as seen in Eq. (2), iterative solutions will be calculated with a MATLAB codes in Appendix B. The Colebrook correlation is as follows [5]:

$$\frac{1}{\sqrt{f}}=-2.0\log_{10}\left[\frac{\varepsilon/D}{3.7}+\frac{2.51}{\mathrm{Re}_D\sqrt{f}}\right] \tag{3}$$

In this equation, ε is the relative roughness of the pipe used. *ME 347 Fluid Mechanics Lab Experiments* provided the relative roughness of steel pipe in experiment as $\varepsilon = 150 \times 10^{-6}$ ft. [2]. Minor head losses are the second component of the head loss term in Eq. (2) and are due to physical pipe components such as entrance and exit conditions, pipe bends, valves, and fittings. The minor head loss is calculated using the following equation [6]:

$$h_{L\,minor}=K_L\frac{\overline{V_2}^2}{2g} \tag{4}$$

Engineering Calculator [7], provided the following useful equation involved in pipe and receiver design for particular applications. The following formula for minimum volume is used to help understand the change in pressure in the tank system for a given flow rate.

$$V = \frac{CP_a t}{(P_1 - P_2)} \tag{5}$$

In equation (5) V is in cubic feet, C is in SCFM, P_a is in psi and is ambient conditions, t is in minutes, and P_1 and P_2 are initial and final tank pressures respectively. From this equation the change in pressure can be approximated from our flow rate. *Engineering Calculator* [7], provided the following useful equation involved in pressure drop in pipes. The following formula for pressure drop is used to help understand the change in pressure in the line system for a given flow rate.

$$\Delta P = \frac{\rho \mu l v^2}{24 D g} \tag{6}$$

In equation (7) [7] ρ is density in lb./ft^3, D is diameter of the pipe in inches, μ is coefficient of friction, l is the length of the pipe in feet, v is the velocity of the air in ft./sec, P is pressure drop in psi, g is gravity in ft./sec^2. Sample lengths and associated pressure drops have been calculated. Equations (5) and (6) were used in Appendix C to approximately determine a capacity and pressure drop required for our design.

Operating the apparatus at speeds approaching Mach 0.5 brings with it certain difficulties in analysis. In general, when operating at flows higher than Mach 0.3 the effects of compressibility of the flowing fluid begin to become apparent. In our analysis though, we need not take the effects of compressibility into account. In order to understand why, we needed to first realize that dynamic pressure. Dynamic pressure, no wind speed is the governing factor to real world simulation. Appendix D demonstrates that in less dense air at lower elevations, a Mach speed of 0.3 is sufficient to replicate dynamic pressures created at Mach 0.5 at flight elevation.

3. Design Developments

3.1 Objectives

The desired end result from this project is a complete apparatus that is capable of simulating real world flight. Parties interested in utilizing the micro-RAT need to be completely satisfied that our micro-RAT will survive at load-free conditions at speeds approaching Mach 0.5 at cruise elevation. A load free environment would be when the micro-RAT turbine is freely spinning with no resistance from the generator. From basic Fluid Theory demonstrated in Appendix C it is shown that at cruising altitude of thirty to forty thousand feet, air is much less dense than at sea level. Therefore conditions emulating flight at altitude need only achieve dynamic pressures equivalent to those in a real flight. After consideration of dynamic pressure, it is understood that real world flight conditions can be tested with velocities of only Mach 0.3 at sea level.

With dynamic pressure still in mind, other factors may also affect the ideal representation of flight conditions. One major component of simulation is the straightness of the wind stream. The air needs to be sufficiently "cleaned" upstream of the test area of our device in order to simulate the actual fluid dynamics of the mostly static air that the airplane passes through.

Another major component of the simulation is completely enveloping the capture area of the RAT blades with our wind stream. We know from actuator disk theory, highlighted in Appendix E that the capture area upstream of an energy-capturing machine contracts and is slightly smaller than the total blade surface area of our micro-RAT. Keeping this reduced capture area in mind, we still need to allow for misalignment of the micro-RAT center of rotation to the center of the stream. We hope to create a stream diameter of at least 1.75 inches in diameter to ensure full envelopment of the micro-RAT and even factoring in minor misalignment.

With full envelopment of the micro-RAT in clean-dynamic pressure specific air, we can be sure to have a close representation of flight data to provide to interested parties. How we capture the data from our test rig now becomes the primary concern. The thrust exerted on the micro-RAT and torque induced from back EMF as well as friction in the bearings must both be measured to a degree of precision in order to satisfy the customer. Torque will ideally be measured in units of ounce-inch and drag measured in ounces.

In order to reach the testing stage, an accurate assessment of factor of safety on the entire device must be within a range of 3-5. A safe operating procedure must also be prepared before use. Operation of the device must include a way to quickly attach/detach the system from the Cal Poly air supply in the southwest corner of Building 13.

The project has a maximum budget of two thousand dollars. From quality functional deployment analysis, it has been determined that a significant amount of engineering specifications affect one another negatively and careful consideration of budget will be a constant problem limiting the scope of the project. As component performance goes up, so will the price, and over performing may not be an option in our price range without under performing in other aspects.

In order to fully understand the purpose of the House of Quality (QFD), an outline of its structure is necessary. The QFD is a means of directly incorporating customer needs into the design process. The normal approach is to design a product and then inspect to see if the product fulfills customer needs. The QFD allows us to identify these needs early on in the process of design iteration. By linking specific engineering specifications with engineering needs, it is possible to more directly incorporate the needs of the customer into the design process. The QFD first identifies the "Who" in the far left hand column of the table. This area identifies the various customers and identifies which customer requirements in the next section just to the right match up with each customer. By giving each a weighted score, it is easy to identify what customer requirement is valued most by each individual customer. The next important area is the engineering specifications that we have decided best suit the pursuit of meeting each customer requirement.

The weighted percentages of our QFD, located in Attachment F, bring about negative and positive correlations between engineering requirements. This project has numerous aspects that, if not completed, render the entire scope of this project invalid.

The matrix goes on to describe the relationship between each customer requirement and engineering specification. The correlations key shows the relationship symbols. If a customer requirement has no strong correlation to any engineering specification, a discussion should be had about adding a specification in order to facilitate the meeting of that requirement. Likewise, if an engineering requirement has no strong correlation to any goal; it may be a redundant specification and can be eliminated. The last important section of the QFD is the roof of the house which shows correlations between engineering specifications amongst themselves. Positive relationships may lead one to believe that by satisfying one requirement the other may also be improved. Negative relationships show that by satisfying one, the other may negatively be affected. Too many negative correlations can be an indicator that all the requirements may not be able to be met to the desired level. A discussion with your customer may need to occur regarding these negative correlations.

The following table (Table 3) helps encapsulate the size and scope of our engineering specifications. This table allows us to put quantifiable goals on some of our project requirements. We realize that not all of these specifications may be met due to a highly negative correlation between each goal. We must decide where budget must be used to maximize benefit to certain specifications, while limiting others. Before looking at Table 3, please use Table 2 as a legend to help facilitate your understanding of some Table 3 terms.

Table 2. Legend for Table 3, Formal Engineering Requirements

	Term	Definition
Risk	L	Low Risk Specification: These should be determined early so maximum effort can be concentrated on higher risk specifications.
	M	Medium Risk Specification: Careful consideration should be taken in order to ensure these are not passed off as low risk.
	H	High Risk Specification: High-risk requirements should be thoroughly discussed with the customer in order to ensure they can be met.
Compliance	A	Analysis: This specification requires analysis in order to determine if it is met.
	T	Test: This specification requires actual trial runs in order to determine if it is met.
	S	Similarity to existing design: This specification compares how well this design compares to other known solutions.
	I	Inspection: This specification requires visual inspection during a trial to determine if it is met.

Table 3. Formal Engineering Requirements

Specification Number	Parameter Description	Requirement of Target (Units)	Tolerance	Risk	Compliance (A,T,S,I)
1	Velocity	0.3-0.5 (Mach)	>0.3	M	T,I
2	Stream Diameter	2 (Inches)	+/- 0.5”	H	T,I
3	Factor of Safety Mounting	3-5 (//)	>3	L	A
4	Time Taken to Mount RAT	10 (min)	Maximum	L	T,I
5	Time to Install to Air	1 (hour)	Maximum	M	T,I
6	Time to Remove from Air	1 (hour)	Maximum	M	T,I
7	Pressure Capacity	360 (psi)	Minimum	H	A
8	Budget	2000 ($)	Maximum	H	I
9	Component Machine Time	10 (Hour)	Maximum	L	I
10	Thrust	(grams)	Maximum Resolution	L	S,T
11	Torque	(gram-inch)	Maximum Resolution	H	S,T
12	3” or 4” Pipe	N/A	Go No Go	L	I
13	% Difference in Velocity Profile	5 (%)	+/- 5	H	I,T
14	Number of Cycles to Failure	Infinite Life	Yes/No	H	A
15	Load Resistance	N/A	Yes/No	M	I

This project does not require much analysis beyond simple fluid calculations and will be almost entirely tested by trial based methods and inspections. We know that every additional component creates a probability for error. This information will guide us to a robust design that has no chance of failing. It was difficult to assign a customer weight to all of the different requirements because of this fact and we realize this section may not yield much valuable information.

With no comparable devices on the market, we realize that we may not yield too much insight into the design process from the competition section of the QFD either. We must look to component level, not entire design level, in order to find competitors that will influence our decision process. For instance, nozzle market competition may prove to be a valuable resource in order to save machine time, heighten manufacturability, and decrease overall budget for our design.

The final topic left undecided is the placement of the rig in respect to the engine lab. We can either use a flexible hose and route the air into the main area of the engine lab or directly connect to the air supply outside from a 4" male NPT fitting. This will be decided but space and access will be maximized according to our choice in placement.3.1 Concept Generation

3.2 Brainstorming

Brainstorming was initialized in lab by first determining a specific function to list solution methods for. Our group chose to list off various methods of straightening airflow between the air supply and our nozzle. The generated list is show in Appendix M.

Before ideation occurred, we had a natural inclination to re-create pre-existing flow straightening methods. In almost all cases a progressive stage honeycomb system is incorporated with finer and finer hexagonal features in order to condition the air. From the ideation process in Appendix M we were able to determine that a very course honeycomb pattern closely resembles a wire screen. We hope to be able to combine honeycomb as well as a screen to reduce cost instead of using multiple expensive honeycomb filters.

We also determined that reducing the surface roughness of the expansion chamber is worthwhile. There is almost zero cost associated with sanding down imperfections in the pipe wall and under any circumstances should be tried in testing to determine its effectiveness. We hope that minimal cost ideas like this can create visible results in the straightness of our airflow.

Next, our group chose to use a method of ideation that involved sketching of a specific function. The sketch was first drawn by a single individual then passed between the group members who would try to improve the idea with an additional sketch. This process is supposed to spark visual stimulation between group mates in order to refine a function of interest. In Appendix M, our group chose to sketch mounting methods for the micro-RAT.

From Appendix M, our group came to the realization that a linear slide mounting system may create too much stiction creating inaccurate results in the measurement of drag. To eliminate this stiction, Isaac suggested a circular mounting structure encapsulating the micro-RAT with ball bearings to eliminate some stiction and hysteresis.

3.3 Modeling

In Lab, our group was tasked to create a physical model out of relatively inexpensive materials in order to demonstrate one design solution. In class we used foam board, PVC fittings and pipe, drinking straws, and hot glue to create a model solution. The model is shown in Figure 9 and Figure 10.

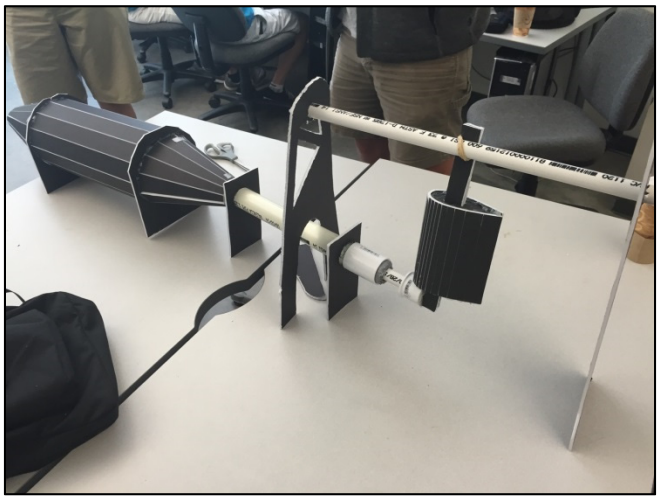

Figure 9. Physical Model of an expansion chamber flow straightener as well as a 90 degree lever arm method of Micro-RAT mounting.

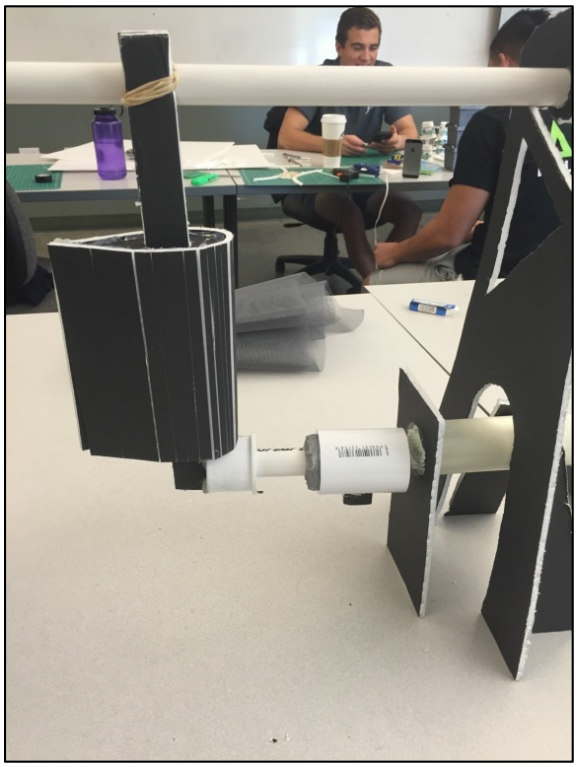

Figure 10. Close up of fairing design and torque transducer incorporation into physical model.

Both Figure 9 and Figure 10 show a physical representation of an initial design that would slowly mold into our final design selection. The design incorporates an expansion chamber for flow straightening. By doing flow straightening in an expansion chamber, the flow is slowed and the pressure drop across the straightening mechanism is reduced. By reducing pressure drop the straightening mechanism can be less robust and still hold up with a relatively high factor of safety. In this model, honeycomb was modeled by drinking straws. The micro-RAT mount incorporates a fairing to reduce drag from any air that wraps around the micro-RAT. By guiding this air gently past the support arm, additional drag is reduced and a more accurate drag measurement will be read by the load cell.

3.4 Sketching

Initially, most of our effort was focusing on defining the characteristics of the Cal Poly air supply to build familiarity. Through general background research and a tour of the system provided by Jim Gerhardt we were able to fully define the capabilities of the Building 13 air system. The General components of an industrial air supply system are laid out in the schematic in Figure 11.

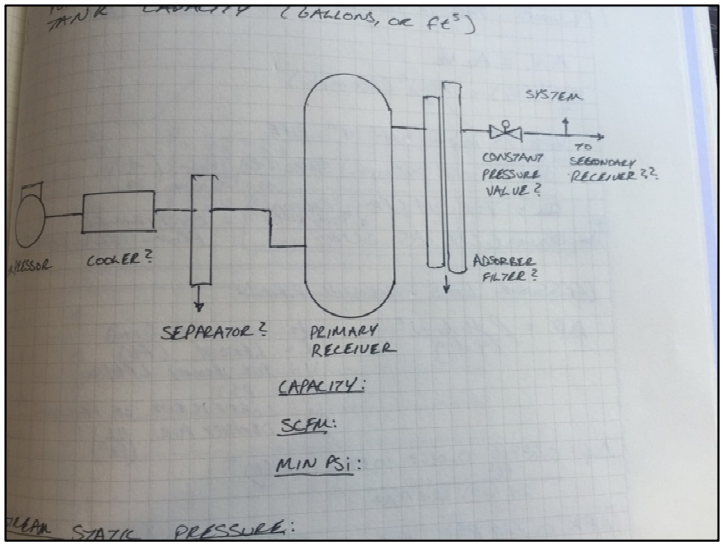

Figure 11. Schematic of general industrial air supply components.

The tour of the engine lab gave us valuable insight into the building's air supply system. Through inspection, it was determined that the system did not incorporate a cooler, separator, or absorber. These components are only used in much larger scale industrial air applications with a high duty cycle. When we asked Mr. Gerhardt the specific capacity of the air tanks he prompted us to take the measurements ourselves because he did not know. The rough estimates of tank capacity are shown in Figure 12.

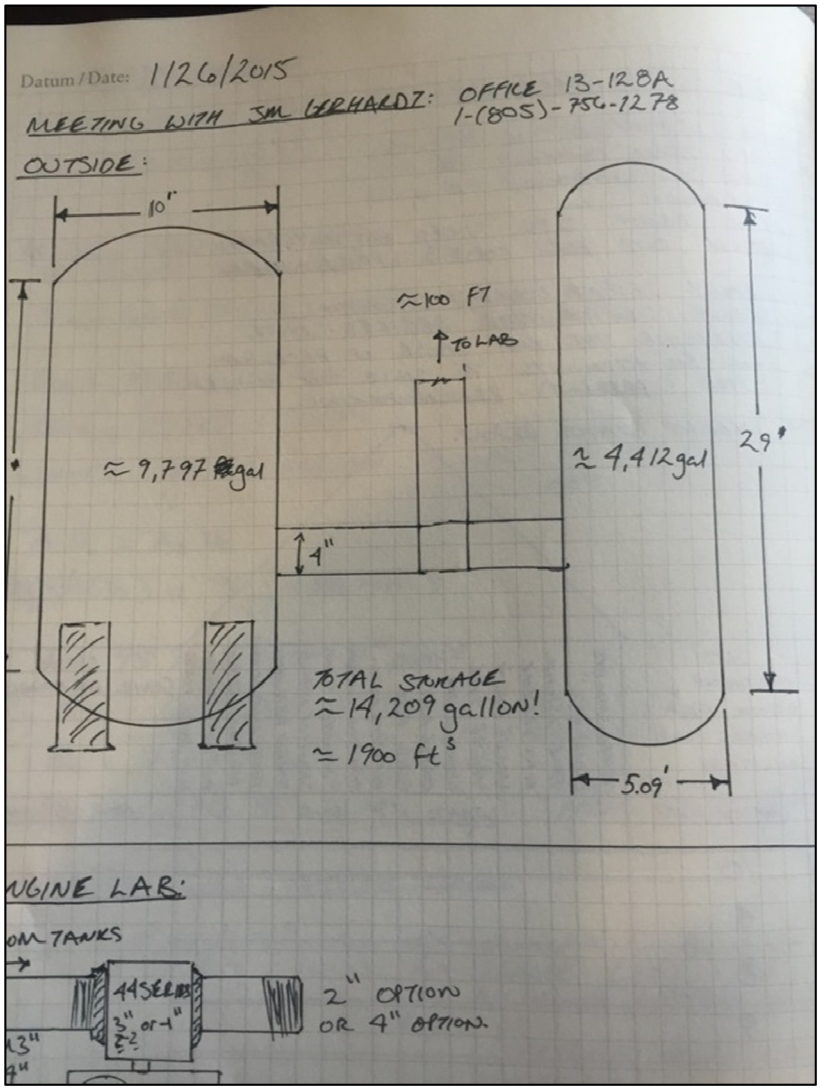

Figure 12. Cal Poly air supply general capacity estimations.

With the use of a tape measure we roughly estimated overall tank capacity to be a minimum of 14,000 gallons. By measuring the circumference of each tank and length a rough conservative estimate was established as shown in Figure 12.

With such a vast volume of air at our disposal, we realized that our design could easily be accomplished. Preliminary size requirements for our indicated SCFM flow rate amounts were calculated in Appendix C. As calculated, we only required around 2000 gallons to accomplish our test; luckily the tanks provide us with a buffer factor of 12,000 gallons.

The next task at hand was to divert our attention to mounting methods for our micro-RAT in the wind stream. The tour and following calculations had strengthened our confidence in the air systems ability to complete our task so we shifted gears into mounting methodology. Figures 13 and 13 show two designs that had arisen in brain storming methods.

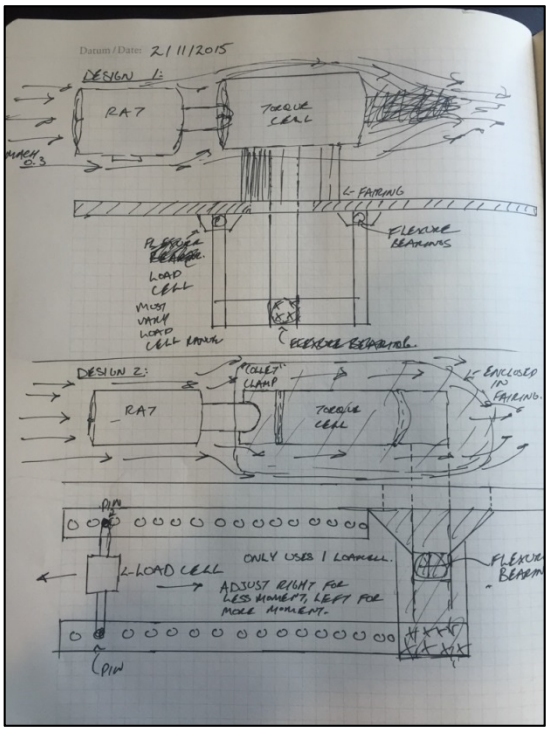

Figure 13. (Above) A cantilever lever arm design with a single pivot location.

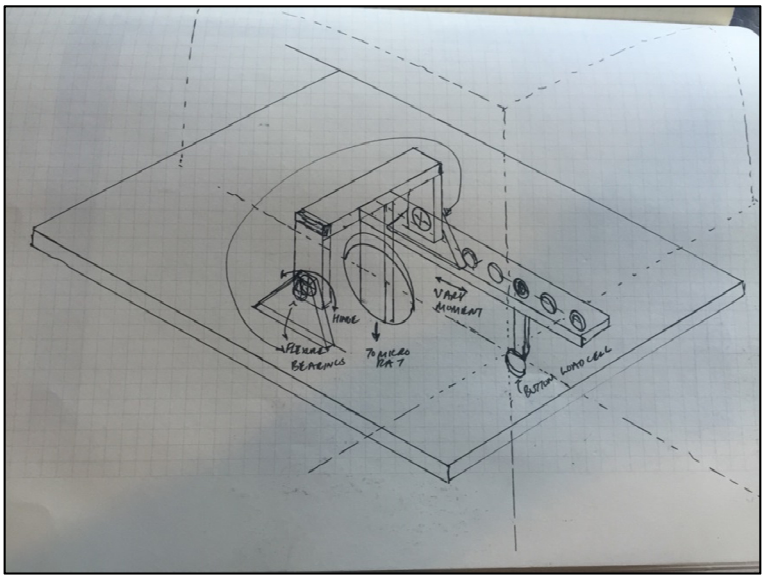

Figure 14. An isometric pictorial of the 90 degree lever arm design with an adjustable load cell location.

The two design sketches shown in Figure 13 and 14 both utilize flexure bearings at the pivot location in order to minimize hysteresis and stiction. The flexure bearing uses a cantilever design to create a quasi-frictionless pivot. The only difference between the (above) sketch in Figure 14 and the (below) design is that the (below) design incorporates an adjustable load cell location. The ability to adjust the location of the load cell on the moment arm allows a single load cell to be

used for various force ranges. By moving the load cell to the right of the arm visualized in Figure 14, the drag force is amplified; by moving the load cell to the left the drag force is reduced.

Both designs incorporate a torque load sensor to measure torque exerted on the motor by the blades of the micro-RAT turbine disk. The transducer is pictured and described in detail in the final design section of this report.

3.5 Concept Selection

3.5.1 Design Considerations

The following categories allowed us to compare different designs and evaluate the performance of each. The three categories used are: torque/drag measurement (subsection 3.5.1.1), straightening (3.5.1.2), and flow acceleration (3.5.1.3).

3.5.1.1 Torque/Drag Measurement

The first design pictured in this report (Figure 15) is a cantilever arm with an adjustable load cell location. This design incorporated hinge points with flexure bearings to eliminate stiction and hysteresis. The micro-RAT as well as the torque sensor are mounted at the end of the arm directly in the wind stream. The drag force is transferred through the cantilever arm and causes a moment to be applied to the hinge point rotating the assembly. This small rotation exerts a force on the load cell.

The load cell has the ability to be moved closer to the cantilever arm to increase the force exerted on it and vice versa it can be moved out to reduce the force placed on it. This ability to either magnify or reduce the force exerted on the load cell by drag is greatly beneficial allowing us to trim cost and only use one load cell for multiple ranges of input drag force. The design is shown in Figure 15.

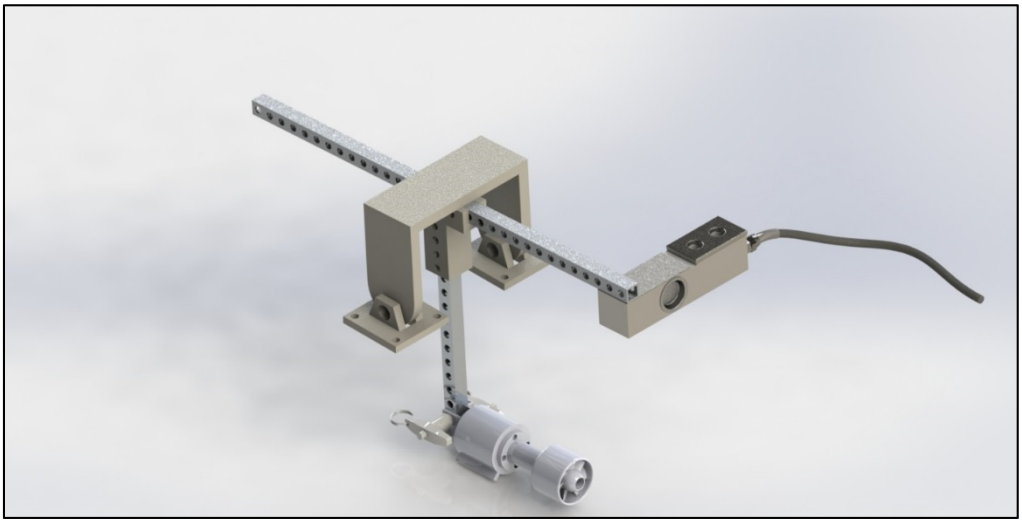

Figure 15. Cantilever arm with an adjustable load cell location design Solid Model.

The cantilever design, pictured above in Figure 15, was an iteration of the following design pictured in Figure 16. The 90 degree lever arm with a single pivot model requires that different load cells be used for different load ranges and lacks the ability to broaden the input range of a given load cell.

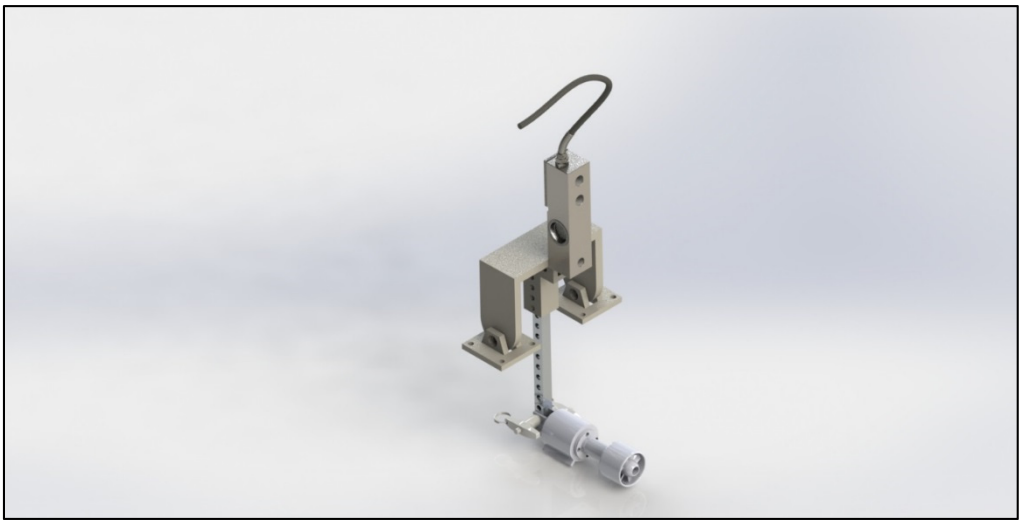

Figure 16. 90 degree lever arm with a single pivot design Solid Model.

Both the designs shown in Figure 15 and 16 stemmed from analysis of the current datum of drag measuring in wind tunnels. The cantilever design, shown in Figure 17, uses a flexible support made out of a material appropriately selected for the input drag force. The force causes the cantilever support arm to flex. This flex is captured by a strain gage on the arm itself. Using material constants and the strain gage deflection information, we can determine the input drag force causing the deflection. The drawback to this design is that once a material and geometry is selected for the cantilever support arm, the given drag force is permanently set. This is due to the limits in resolution of deflection set by the strain gage. In order to measure a larger drag force a more rigid cantilever arm must be used; in order to measure a smaller drag force a less rigid arm must be used. Also, the cantilever design presents a problem in vibration. By sticking a heavy mass at the end of a flexible cantilever arm, resonant frequency may be reached and large deflections in the micro-RAT at the end of the arm could be dangerous.

Figure 17. Cantilever design Solid Model.

The cantilever method shown in Figure 17 is included as a datum for reference and comparison to our other designs.

Sparked by insight obtained by the datum shown in Figure 17, our group created a linear dual cantilever support system for our micro-Rat. The sway in the dual cantilever supports will be suppressed by the load bearing at the end of the platform. This method, visualized by the solid model in Figure 18, takes our concerns about system vibration out of the system.

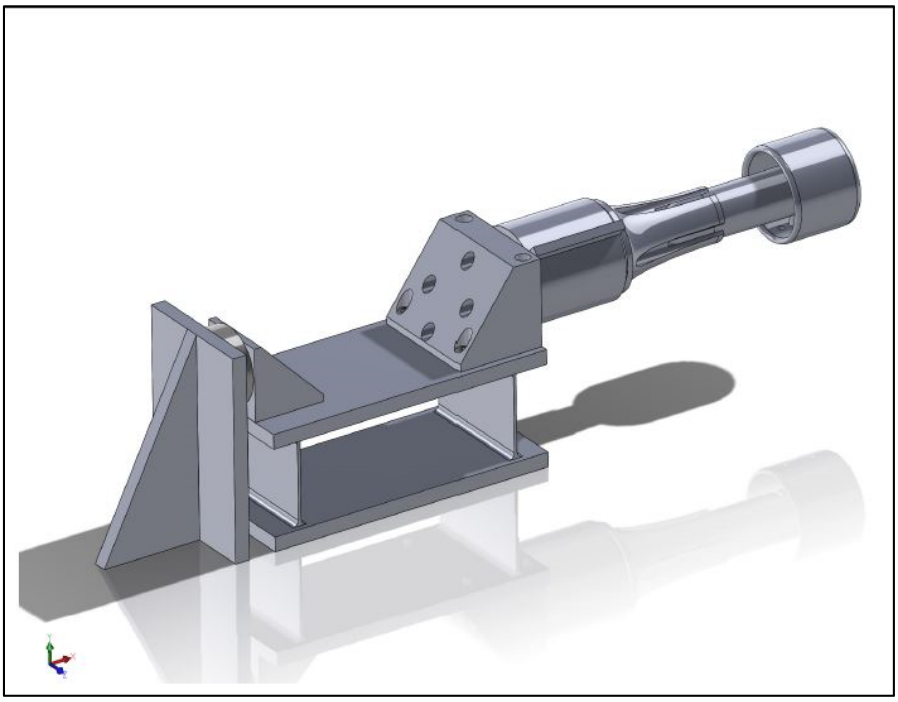

Figure 18. Linear Slide design Solid Model.

The design visualized in Figure 18, combined with our insight into the use of flexure bearings in Figure 15 and 16, brought us to a new design incorporating both a four bar linkage system shown in Figure 19. This system hinges about four axis of rotation and reduces the rinks of vibration compared to our datum.

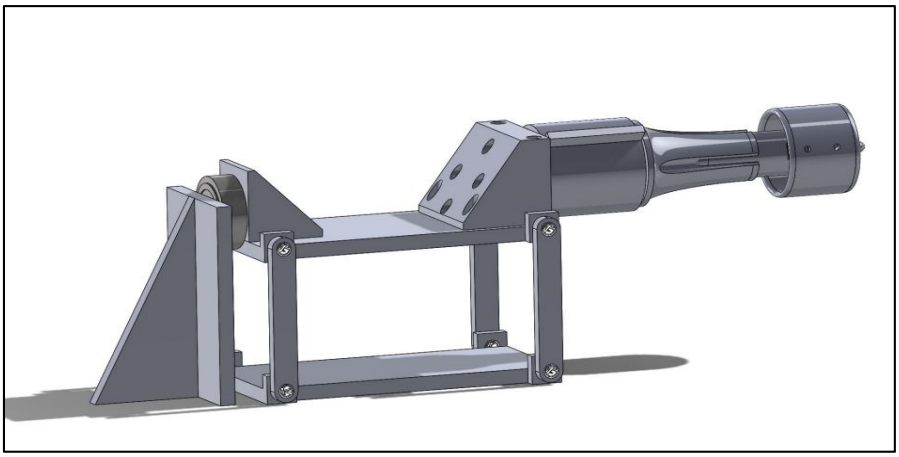

Figure 19. Four bar linkage design solid model.

The Pugh and weighted decision matrices in the following two sections of the report helped us identify how each of our four designs fulfilled customer specifications. These matrices identified how each design satisfied our customer requirement/engineering specifications in four distinct design functions: flow acceleration, flow straightening, torque measurement, and drag measurement.

3.5.1.2 Straightening

This section of the report identifies four ideas selected from the brainstorming process for further investigation for air flow straightening, sometimes referred to as "cleaning". The four methods chosen for further investigation are: honeycomb, wire mesh, perforated metal sheet, and drinking straws. In the following section of the report, these methods shown in Figure 20, are analyzed in Pugh in Appendix I and weighted decision matrices (Section 3.5.3) for greatest compliance and fulfillment of customer requirements.

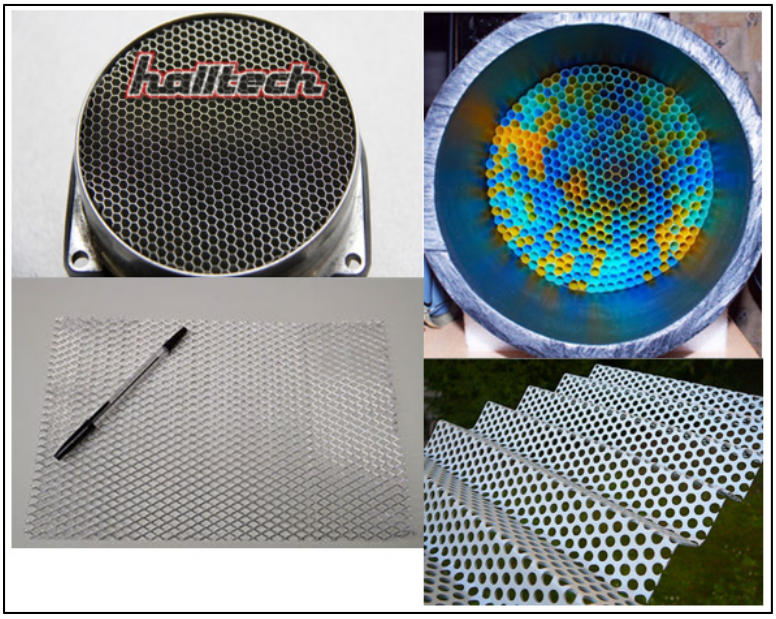

Figure 20. Top Lt.: Halltech honeycomb courtesy of [10]. Top Rt.: Honeycomb structure. Bottom Lt.: Steel mesh. Bottom Rt.: Steel mesh

We hope that some combination or adaptation of the methods proposed for flow straightening in Figure 20, will prove effective in satisfying our customer.

3.5.1.3 Flow Acceleration

This section of the report identifies five ideas selected from the brainstorming process for further investigation for air flow acceleration, sometimes referred to as “nozzeling”. The five methods chosen for further investigation are: Carbon fiber, a standard cast iron 6” to 2” Black pipe reduction, a machined nozzle with a bolted flange, a machined nozzle with a sanitary style quick connection, and a standard PVC pipe 6” to 2” reduction fitting. In the following section of the report these methods, shown in Figure 21, are analyzed in Pugh and weighted decision matrices for greatest compliance and fulfillment of customer requirements.

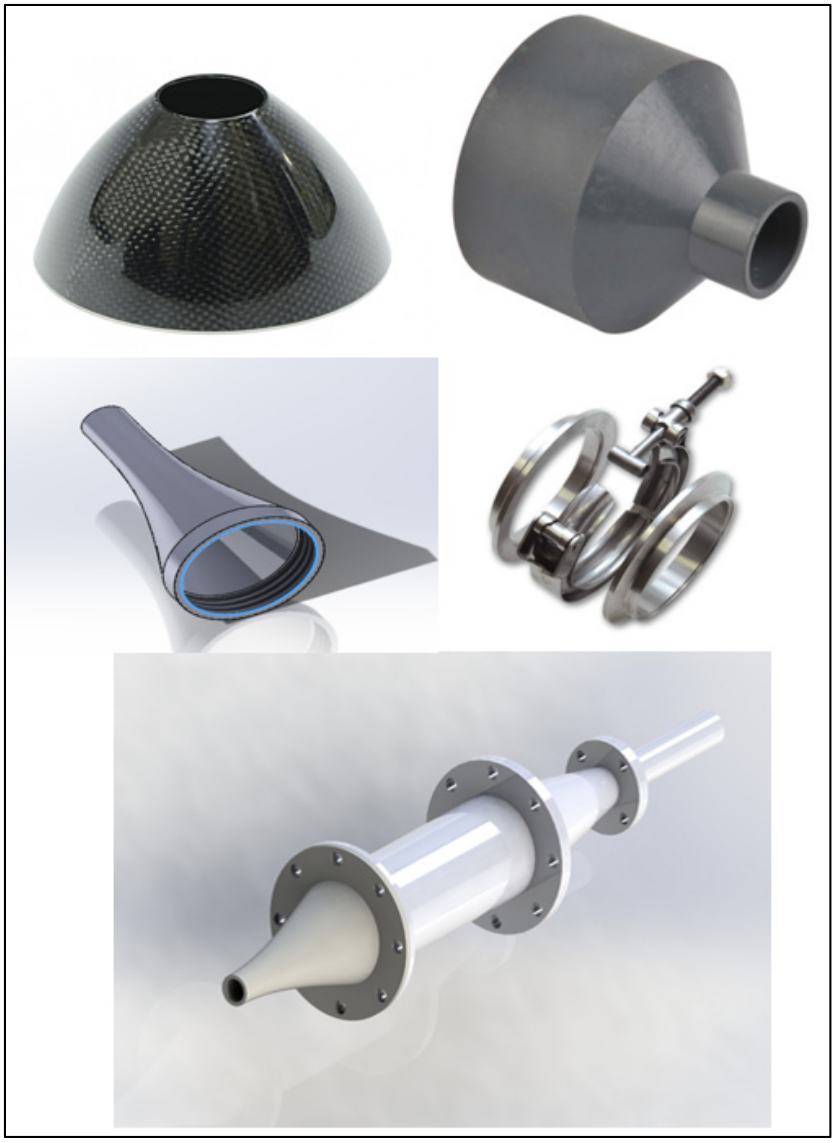

Figure 21. Nozzle Design Ideation. Above left: Carbon fiber [11]. Above right: Std. Black pipe reduction fitting. Middle left: PVC reduction fitting [13]. Middle Right: Sanitary quick clamp [12]. Bottom: Machined Nozzle with flange.

We hope that some combination or adaptation of the methods proposed for flow acceleration in Figure 21 will prove effective in satisfying our customer.

3.5.2 Pugh Matrix

Faced with making the difficult decision between the many designs generated in the brainstorming process, our group began to generate Pugh matrices for each individual function. The Pugh matrix is a way to effectively organize how each design fulfills customer requirements when compared to the current datum. By summing up all the ways the design works better, worse, and the same as the datum it may become apparent which design is best. The Pugh matrices for all of the following sections are attached as Appendix I.

Pugh matrices do not incorporate any weighting scale and more important customer requirements may be overshadowed by less important ones. It is important to keep the limitations of the Pugh matrix in mind when analyzing each design. Each Pugh matrix is expanded into a weighted decision matrix in the following section. It is important not to overlook the value of the Pugh matrix because it may spur new ideas and adaptations to designs in order to fully maximize their potential.

3.5.2.1 Straightening

The first Pugh matrix depicted in Table 4 compares four different air straightening designs to the current datum on the market. The four variants of flow straightening being analyzed are: Wire mesh, perforated metal sheet, small tubes, and a vortex generator. The following key for the Pugh Matrices should be studied before any further reading.

Table 4. Pugh Matrix Key

Matrix Entry	Meaning
S	Same as the current market Datum
+	Better performance than the market datum
-	Worse performance than the market datum

From inspection of the Pugh matrix for straightening in Appendix I, the vortex generator method immediately stands out as a top choice. Although this is true, they are extremely expensive to create and the affordability aspect of the customer requirement is vastly overshadowed. The affordability and reproducibility of the honeycomb and wire mesh combination are beginning to become the better solution when understanding that reproducibility of the test environment has a relatively high importance compared to other customer requirements.

3.5.2.2 Stream Acceleration

The first Pugh matrix depicted in the Pugh matrix for stream acceleration in Appendix I compares five different air accelerating designs to the current datum on the market. The five variants in design (Figure 21) are: machined nozzle with a flange, machined with a quick clamp, PVC reducer, composite reducer, and a cast aluminum nozzle.

From inspection of the Pugh matrix for stream acceleration in Appendix I, it is difficult to beat the market available datum. The PVC beats the datum in affordability and manufacturability, yet fails to satisfy the safety requirements regarding high pressure. With further investigation it may become apparent that buying a nozzle will be our best option.

3.5.2.3 Drag Measurement

The first Pugh matrix depicted in the Pugh matrix for drag measurement in Appendix I compares four different drag measurement designs to the current datum on the market. The five variants in design are: a linear slide, 90 degree lever arm with a single pivot, cantilever with a four bar linkage, and a cantilever arm with an adjustable load cell location. Both the Pugh matrix for

Drag Measurement and Torque Measurement Pugh matrices in Appendix I are extremely similar so they will be discussed in tandem.

3.5.2.4 Torque Measurement

Both the torque measurement and drag measurement will both be incorporated into five different micro-RAT mounting designs. In regards to the torque measurement is has become apparent that there is not much variation between each design in fulfilling the customer requirements. The difference in each individual design lies in how it satisfies the measurement of drag. This Pugh matrix, the Pugh matrix for torque measurement in Appendix I, will be discussed in detail. The ability of the cantilever arm design to adjust the load cell location greatly enhances the affordability by allowing one load cell to act over a variety of input force ranges. While the cantilever arm datum is more affordable, the danger in vibration and the required multiple support arms to vary the load range have caused us to favor the adjustable load cell design.

3.5.3 Weighted Decision Matrices

While the Pugh matrices proved somewhat effective in design consideration, weighted decision matrices proved more useful. Some customer requirements should take higher precedence in the comparison of different designs and the weight factors were carefully chosen to account for this. Each category of evaluation on the top row of the weighted decision matrix stresses the relative importance of those particular criteria, all criteria importance sum to one. Then each alternative is given a percentage of satisfaction to each of the design criterion, this is the value in the top left corner of each box. The satisfaction is multiplied by the importance and summed across a row in order to attain the alternative's overall satisfaction of the design criterion.

3.5.3.1 Straightening

Table 5. Weighted decision Matrix for air flow straightening selection among various techniques.

Design Criteria / Weighting Factor / Alternatives	Ral world wind velocity	Envelopment of wind turbine in air stream	Utilization of Cal Poly air supply	Safe Operating Procedure	Hard stop safety	Symmetric windstream	Durability	Affordability	Overall satisfaction
	0.30	0.10	0.05	0.10	0.05	0.30	0.05	0.05	1.00
Honeycomb	100% / 30%	100% / 10%	100% / 5%	75% / 8%	100% / 5%	50% / 15%	75% / 4%	35% / 2%	78%
Wire Mesh	100% / 30%	100% / 10%	100% / 5%	75% / 8%	100% / 5%	25% / 8%	75% / 4%	100% / 5%	74%
Perforated metal sheet	100% / 30%	100% / 10%	100% / 5%	100% / 10%	100% / 5%	25% / 8%	100% / 5%	40% / 2%	75%
Honeycomb/Mesh combination	100% / 30%	100% / 10%	100% / 5%	100% / 10%	50% / 3%	75% / 23%	75% / 4%	35% / 2%	86%
Small Tubes	75% / 23%	100% / 10%	50% / 3%	25% / 3%	10% / 1%	25% / 8%	25% / 1%	100% / 5%	52%

After careful selection of weighting factors in Table 5 for each customer requirement, the honeycomb and wire mesh combination has taken the lead in straightening. Due to its high performance in straightening the airflow into a symmetric stream and ability to handle the required air velocity, it has come out on top as the clear choice. The only drawback to this design is the relatively expensive nature in honeycomb capable of handling this high air flow. Luckily, the school has extra honeycomb leftover from another project and we will be able to use it at no cost. This affordability and exceptional performance when paired with the wire mesh puts the design at the top of our list for further pursuit.

3.5.3.2 Stream Acceleration

The following decision matrix, Table 6, is for the comparison of different flow acceleration designs. The various designs' abilities to satisfy customer requirements are highlighted by the percent of total satisfaction on the right hand column.

Table 6. Weighted Decision Matrix for air flow acceleration selection among various techniques.

Design Criteria / Weighting Factor / Alternatives	Ral world wind velocity	Envelopment of wind turbine in air stream	Utilization of Cal Poly air supply	Safe Operating Procedure	Hard stop safety	Symmetric windstream	Durability	Affordability	Overall satisfaction
	0.30	0.10	0.05	0.10	0.05	0.30	0.05	0.05	1.00
Threaded reducer	100% / 30%	100% / 10%	100% / 5%	100% / 10%	100% / 5%	75% / 23%	100% / 5%	100% / 5%	93%
Machined with bolted flange	100% / 30%	100% / 10%	100% / 5%	100% / 10%	100% / 5%	85% / 26%	50% / 3%	50% / 3%	91%
Machined with quick clamp flange	75% / 23%	100% / 10%	75% / 4%	75% / 8%	100% / 5%	25% / 8%	25% / 1%	25% / 1%	59%
pvc	25% / 8%	100% / 10%	0% / 0%	0% / 0%	0% / 0%	75% / 23%	0% / 0%	100% / 5%	45%
composite	50% / 15%	100% / 10%	50% / 3%	50% / 5%	50% / 3%	25% / 8%	10% / 1%	75% / 4%	47%

By inspection of Table 6, the threaded reducer design is the best design for flow acceleration. The ability of nozzle to create a relatively symmetric windstream at an extremely low cost compared with all other designs pushes it to the top of the list. By machining our own nozzle we may be able to slightly enhance the straightness of our flow. However, this greatly enhances our cost. The ability of the threaded reducer to satisfy customer requirements already eliminates the need to spend any more money. If in the case the threaded reducer fails to satisfy our requirements, the part can be returned to the vendor and alternate ideas can be explored such as the machined nozzle with a bolted flange.

3.5.3.3 Drag Measurement

The following decision matrix, Table 7, is for the comparison of drag measurement designs. The various designs' abilities to satisfy customer requirements are highlighted by the percent of total satisfaction on the right hand column.

Table 7. Weighted Decision Matrix for micro-RAT drag measurement selection among various techniques.

Design Criteria / Weighting Factor / Alternatives	Effective mounting	Safe operating procedure	Retrieve sufficient test data	Measurement of unloaded vs. loaded	Durability	Affordability	Manufacturability	Reproducability of test environment	Overall satisfaction
	0.10	0.15	0.30	0.05	0.10	0.05	0.05	0.20	1.00
Cantilever	100% / 10%	100% / 15%	100% / 30%	50% / 3%	100% / 10%	100% / 5%	100% / 5%	60% / 12%	78%
Linear slide	25% / 3%	100% / 15%	25% / 8%	50% / 3%	25% / 3%	75% / 4%	50% / 3%	25% / 5%	36%
90º Lever arm with a single pivot	75% / 8%	100% / 15%	75% / 23%	75% / 4%	50% / 5%	75% / 4%	75% / 4%	50% / 10%	61%
Cantilever arm with a four bar linkage	75% / 8%	100% / 15%	100% / 30%	100% / 5%	50% / 5%	50% / 3%	75% / 4%	100% / 20%	69%
Cantilever are with an adjustable load cell location	75% / 8%	100% / 15%	100% / 30%	100% / 5%	75% / 8%	75% / 4%	75% / 4%	100% / 20%	73%

By inspection of Table 7 the cantilever arm (datum) proves most effective in drag measuring. This chart does not incorporate the effects of adding torque measurement to the design. If we add a large mass to the end of the cantilever arm to measure torque, the design quickly loses its ability to compete with the runner up design: cantilever arm with an adjustable load cell location. With a large mass at the end of a cantilever arm, vibration becomes a concern and data may become flawed due to oscillation. The cantilever arm with an adjustable load cell location allows us to increase the rigidity of the arm and eliminate oscillation concerns by using a load cell to measure drag instead of a strain gage. The deflection of the arm is greatly reduced in the load cell case. The cost of the cantilever design is also comparable. Further analysis into how each of these designs satisfies the ability to measure torque may make the decision more clear cut.

3.5.3.4 Torque Measurement

The following decision matrix, Table 8, is for the comparison of torque measurement designs. The various designs' abilities to satisfy customer requirements are highlighted by the percent of total satisfaction on the right hand column.

Table 8. Weighted Decision Matrix for micro-RAT torque measurement selection among various techniques.

Design Criteria / Weighting Factor / Alternatives	Effective mounting	Safe operating procedure	Retrieve sufficient test data	Measurement of unloaded vs. loaded	Durability	Affordability	Manufacturability	Reproducability of test environment	Overall satisfaction
	0.10	0.15	0.30	0.05	0.10	0.05	0.05	0.20	1.00
Cantilever	50% / 5%	100% / 15%	50% / 15%	50% / 3%	100% / 10%	100% / 5%	100% / 5%	50% / 10%	58%
Linear slide	25% / 3%	100% / 15%	25% / 8%	50% / 3%	25% / 3%	75% / 4%	50% / 3%	25% / 5%	36%
90º Lever arm with a single pivot	75% / 8%	100% / 15%	75% / 23%	75% / 4%	50% / 5%	75% / 4%	75% / 4%	50% / 10%	61%
Cantilever arm with a four bar linkage	75% / 8%	100% / 15%	100% / 30%	100% / 5%	50% / 5%	50% / 3%	75% / 4%	100% / 20%	69%
Cantilever are with an adjustable load cell location	75% / 8%	100% / 15%	100% / 30%	100% / 5%	75% / 8%	75% / 4%	75% / 4%	100% / 20%	73%

By inspection, previous concerns in design selection have been eliminated. The cantilever arm now is the dominant design for the ability to measure torque. When combining the designs ability to eliminate oscillation and ability to satisfy customer requirements with torque measurement, the design outweighs the lower cost of the market datum. Considering a torque cell costs upwards of 800 dollars. It may be worth spending extra money in the micro-RAT mounting design to make sure it will produce the required data. In the following section we analyze a few mounting techniques in Abaqus to determine some rough estimations of deflection.

3.6 Preliminary Analysis

3.6.1 3D Abaqus FEA Models

A simple FEA model of the cantilever idea was created. This allowed us to investigate potential vibration or compliance issues. The system was found to have modes occurring at very low frequencies. The low natural frequencies thus eliminate this system from consideration as an effective method of measuring drag. Figures 22 and 23 show the first and second modes of vibration.

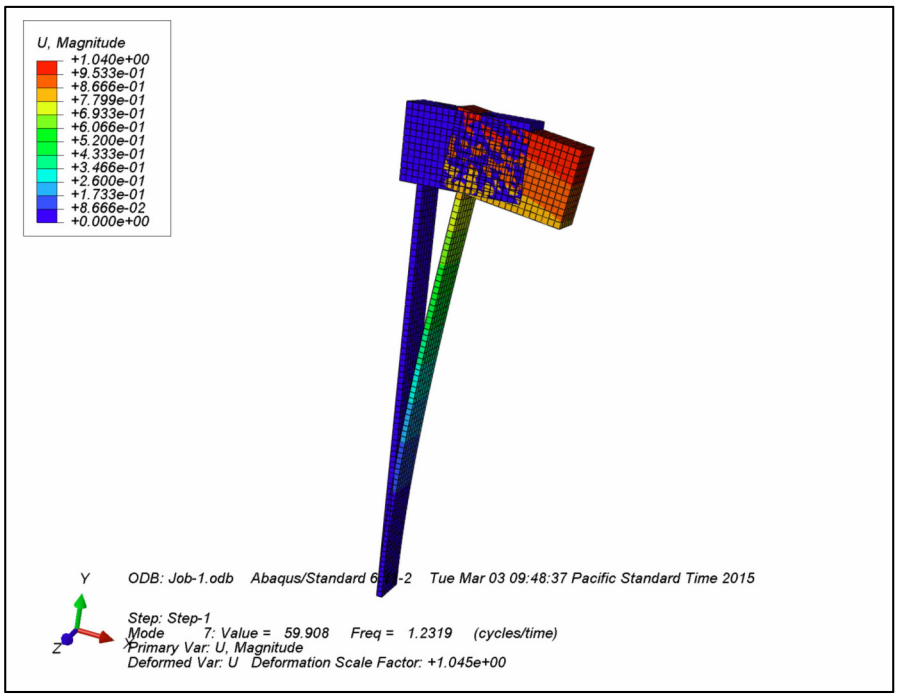

Figure 22. First mode of natural frequency occurs at 1.23Hz. The mass of the micro-RAT was approximated as a solid block.

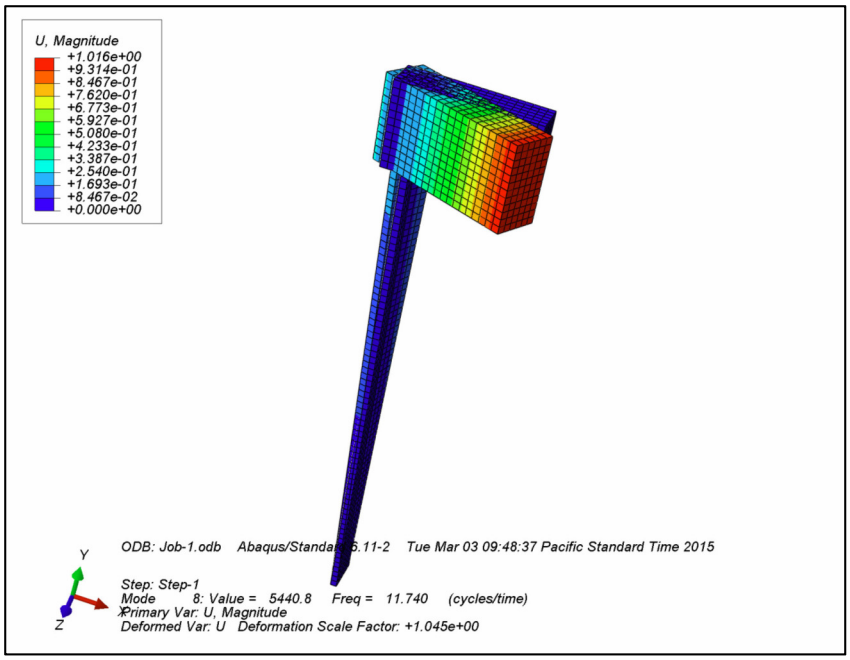

Figure 23. The second mode is torsional and occurs at 11.7Hz

An FEA model was also created for the linear flexure bearing system. The system was found to behave linearly for small loads. Since the system is rigidly mounted through a load cell, vibrations were not a concern. Table 9 and Figure 24 show the how the spring rate was determined for low loads. Although the system sees a higher load than shown below, most of the load is resisted by the load cell and not the flex bearing itself. Figures 24 and 25 show the FEA model and the dimensions used.

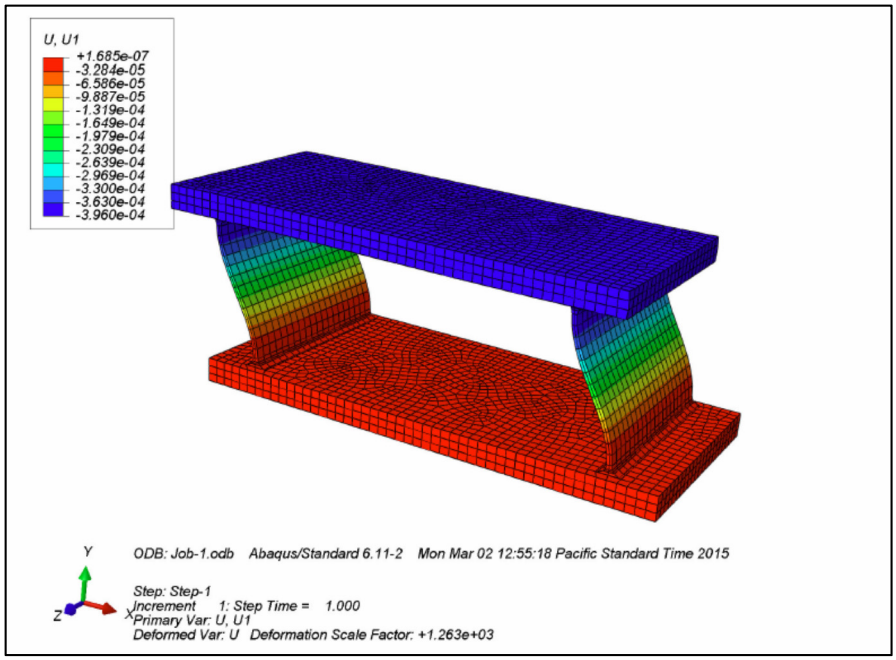

Figure 24. FEA displacement model of Linear Flexure.

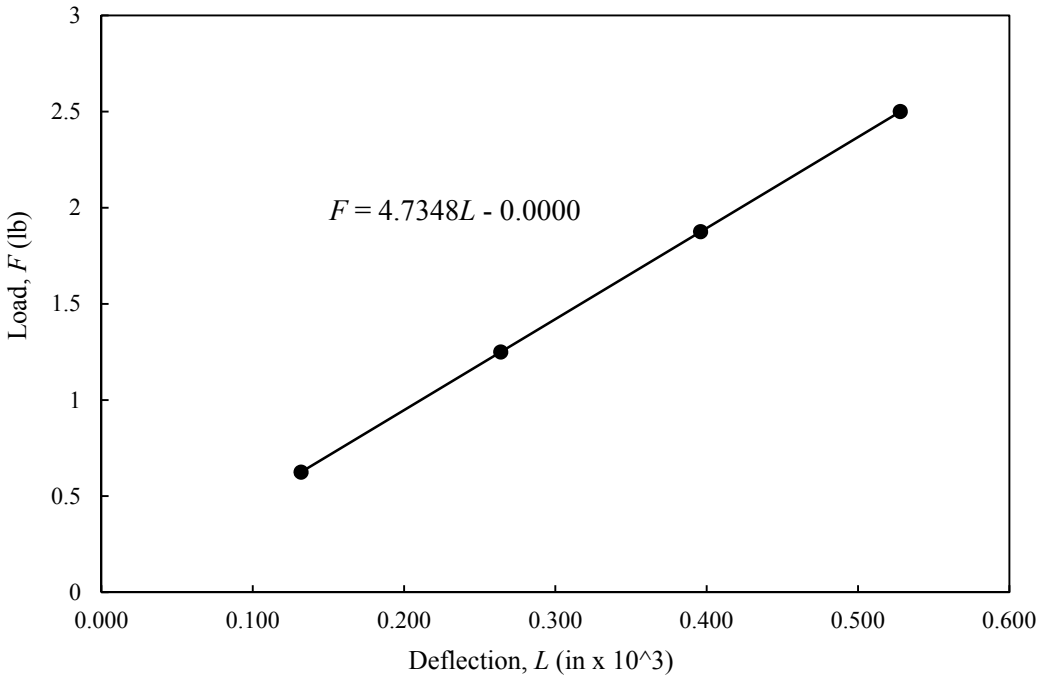

Figure 25.Load and corresponding deflection in thousandths of an inch as determined form the ABAQUS FEA model. Spring rate is linear for this range and is 4.7348 pounds per thousandths of an inch. The flexure should not deflect more than a few thousandths of an i

Table 9. Load and deflection for linear flex bearing with two 0.050 inch thick flexures.

Load (Lb.)	Deflection (in x 10^3)
0.625	0.132
1.250	0.264
1.875	0.396
2.500	0.528

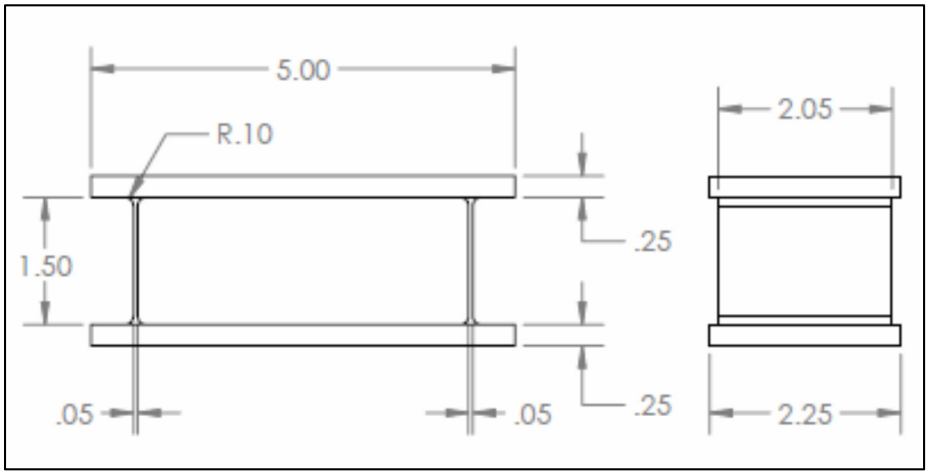

Figure 26. Dimensions of linear flexure used for ABAQUS FEA Model.

As proven by FEA analysis, careful consideration must be taken to avoid resonant frequencies in our system. These frequencies, if low enough, will have the ability to vastly skew results of our measurement devices.

3.6.2 Solid Works Flow Express Pipe Model

Solid Works Flow Express was used as a quick analysis of incompressible flow. A constant pressure sink of 120 psig was added to the blue side of the pipe and atmospheric conditions were applied to the red side. It was determined in Figure 27 that 120 psig with minor losses factored out would prove sufficient to choke the flow out of a 2" nozzle.

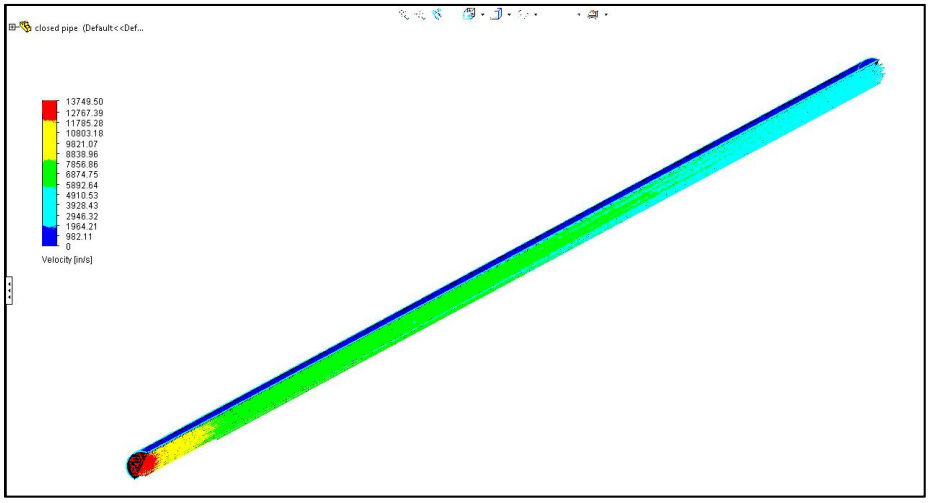

Figure 27. Flow Express Flow Report through a 100' length of 4" Pipe. A pressure sink of 120 psig was used.

Using incompressible equations, Flow Express determined that Mach speed and hence, choked flow could be obtained with 120 psig and a 2" nozzle as seen in Figure 27. Flow Express uses computational fluid dynamics to calculate the velocities of the fluid from inlet of the pipe to outlet. The outlet can be identified in Figure 27 as the red (higher velocity) and the inlet as the blue (lower velocity).

4. Top Design Selection

After analysis of the weighted decision matrices and FEA modeling we have concluded that the cantilever arm with an adjustable load cell location is our best design for drag and torque measurement. It most readily handles the mass of the torque sensor and micro-RAT. This system can be produced at a relatively low cost minus the requirement of the two flexure bearings at the hinge points (flexure bearing located in Attachment H for visualization and comprehension courtesy of [15]). This design allows us to use one load cell to measure a variety of drag ranges by moving it along the moment arm indicated by the blue arrow in Figure 28.

Figure 28. Prototype of Final design selection. Cantilever arm with an adjustable load cell Location

The final design selection in Figure 28 was created using a 3D printer for all components that are black. The square tubing is made out of 0.5” x 0.5” steel tube and the mock flexure bearings are visualized by brass bushings. The next component of our design is the flow straightening and acceleration design. The clips in Figure 29 characterize our final design selection.

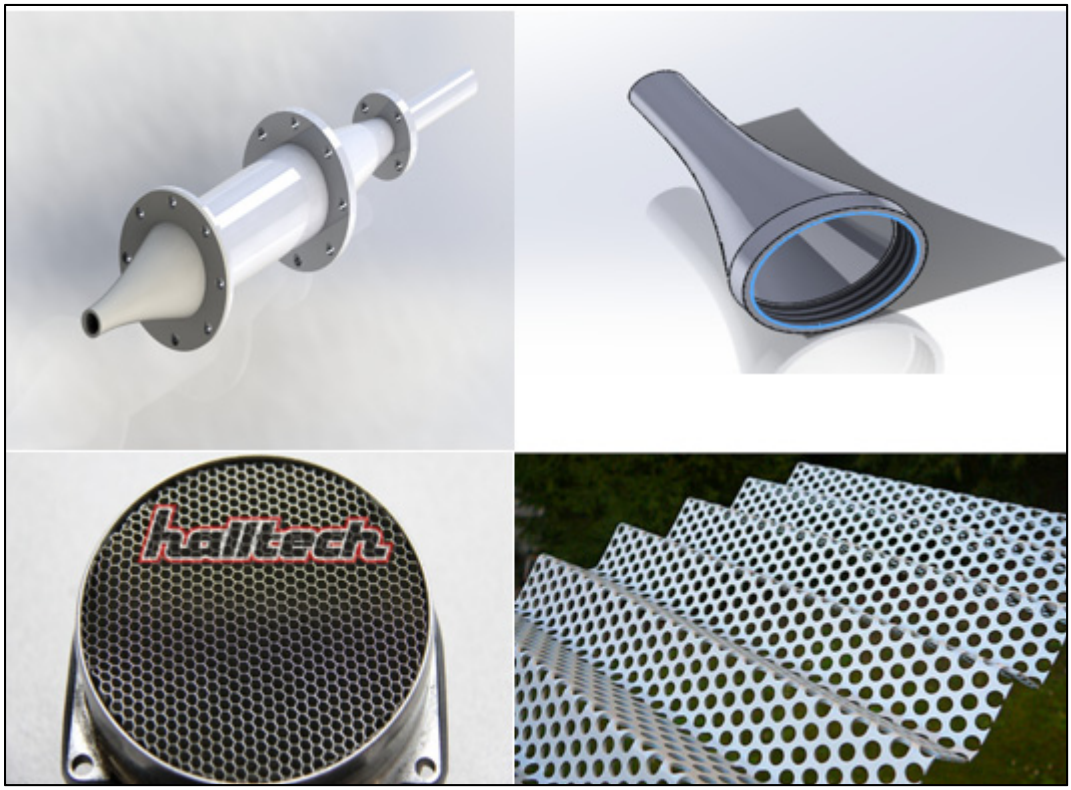

Figure 29. Top Lt.: First design iteration. Top Rt.: Nozzle. Bottom Lt.: Honeycomb example. Bottom Rt.: Steel mesh example

The load cell and torque cell have both been selected based on input range from Appendix F.

The blade angle of the micro-RAT was used to generate a rough estimate of torque development. This information was used to size the torque sensor. A 1.5” disk with a coefficient of one was used to develop a drag force in order to size the load cell. Both sensors shown in Appendix F will be large components to the overall cost of our design. The sum total of both components is approximately $1000 U.S.D.

5. Conceptual Design

5.1 Design Specification Fulfillment

Overall our design strongly satisfies the customer requirements laid out in the QFD. By utilizing an expansion chamber, combined with honeycomb and perforated mesh we simulate a high speed flight environment with straight “conditioned” air at the appropriate wind speed. The two inch nozzle diameter completely envelops the micro-RAT in this stream and allows for some miss-alignment of the micro-RAT. By using Black Sch. 40 Pipe we are completely satisfied that the straightening and acceleration device will provide an adequate factor of safety allowing us to utilize the Cal Poly air supply at pull 120 psig. The durable nature will make it easy to provide a safe operating procedure for use.

Our micro-RAT mounting system will adequately measure thrust and drag from the micro-RAT in the wind stream without creating too much cost in manufacturing. The overall repeatability of this test rig should be sufficiently high enough to satisfy our customer as well as any other stakeholders that arise along the way.

The ability of the final design to adapt to a variety of load ranges by manipulating load cell location on the lever arm greatly reduces the cost involved with ordering multiple load cells for multiple load ranges.

The use of flexure bearings for hinge mounts reduces stiction and hysteresis and should create extremely accurate graphs of both torque and drag when the data is normalized.

Overall we hope this design will satisfy the holistic goal of subjecting the BLDS team micro-RAT to typical in flight conditions on the wing of an airplane. The torque and drag measurements will us characterize micro-RAT performance as well as make improvements to them in the future.

6. Design Realization

6.1 Management Plan

In order to complete the design and planning of our senior project, we decided to divide the entire project into smaller subtasks. Each subtask will have a manager in charge of the planning and making sure everything runs smoothly for that task. Ultimately each task will be a collective team effort lead by the subtask manager. Cameron will be in charge of leading the testing plans and the micro-RAT mount design. These testing plans include a written set up, test, and cleaning procedure. Cody will be in charge of budget and schedule as well as a safety procedure when running the experiment. Ken will be in charge of the manufacturing considerations, the nozzle design, and the torque test design. Isaac will be in charge of the thrust test design and the system mounting design.

As of now, Ken has the strongest handle on the necessary steps to accomplish the goal of this project which is why he has been given three subtasks. Ken also has access to a machine shop with many CNC's which is why he is in charge of manufacturing considerations. The thrust test design task involves extracting load data induced by the airstream onto the micro-RAT. Figuring out a way to attach our system to the existing piping in the engines lab is the system mounting task. We will all be responsible for doing background research and documenting the design process in our lab notebooks as the project progresses. Table 10 below summarizes the work division for our senior project team.

Table 10. Summary of work division among Jet Rats.

Team Member	Task
Whole Team	Information Gathering
	Documentation of Design Process
	Testing

Ken	Manufacturing Considerations
	Nozzle Design
	Torque Test Design
Cody	Budget and Scheduling
	Safety Procedure
Isaac	System Mounting Design
	Thrust Test Design
	Torque Test Design
	Engineering Analysis
Cameron	Testing Plans
	Micro-RAT Mounting Design
Sponsor	Purchasing

Concentrating on each subtask one at a time will allow for full concentration of all of the team members and allow us to work efficiently.

6.2 Method of Approach

The first step we took in completing this project was defining the problem. The development of the High Speed Air Jet Turbine is the problem, and the objectives which outline this problem have clearly been stated in this report. In order to transform the objectives of the problem into a reality we defined attributes of the device to be built that fit into the objectives. We then identified metrics we used to quantify these attributes. Idea generation was then performed followed by exploration of different ideas. Eventually a final idea was selected using these methods. Forthcoming methods of completing this project will include method of construction, prototyping and refining of the design. This approach is outlined in Figure 30, a design approach from NASA.

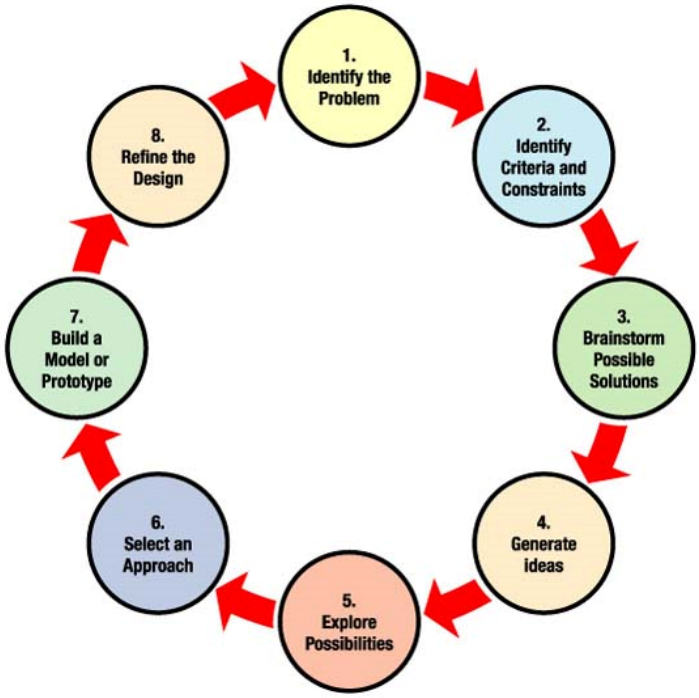

Figure 30. A flow diagram outlining the eight steps of the engineering design process [14]

Background research was performed in order to gain a complete understanding of all aspects of the problem. Research has allowed us to identify ways of solving the problem based on existing designs or theory involved. Idea generation coincided with and followed background research. We individually developed ideas on how to best solve the problem. The process involved calculations, and estimations, of the metrics as well as conceptual drawings. We, as a team, discussed and critiqued different ideas leading to an arrival at an agreed design concept outlined in this report. The report explicitly outlines the intended design and the expected outcome.

Design tasks will be split up among the team members and development of the actual design of the device will commence. Completing design tasks will be an iterative process in which a specific revision process will be adhered to. An initial draft of a document will be revision A and will be submitted for review by one of the other team members. A team member will review the document and identify changes that are needed. The document is now revision B and will be

submitted for review again. The document can iterate until a review justifies no changes. Then a document is ready for final draft and is labeled as revision 0, if any revisions are necessary after this point, the document will count up from 0 in an identical iterative process as before. All documents will combine to make up the final design report that will detail exactly what we are intending to construct.

After review of this report we will have a well-defined solution to the problem and a defined method of construction. We will proceed to construct the system while maintaining checks on quality and safety. We will provide status reports keeping all involved parties aware of the current status of the project during the construction. After construction we will develop a testing procedure and test the device. Testing will allow us to determine how well our construction met our metrics as well as evaluate safe function of the device. Changes will be made as required. Then, a safe operating procedure will be created. This detailed procedure will allow future students and faculty to operate the device.

6.3 Gantt Charts

The following Gantt charts highlight the major milestones and sections of our design process. Figures 31 through 33 depict each individual quarter and how we have decided to manage our time.

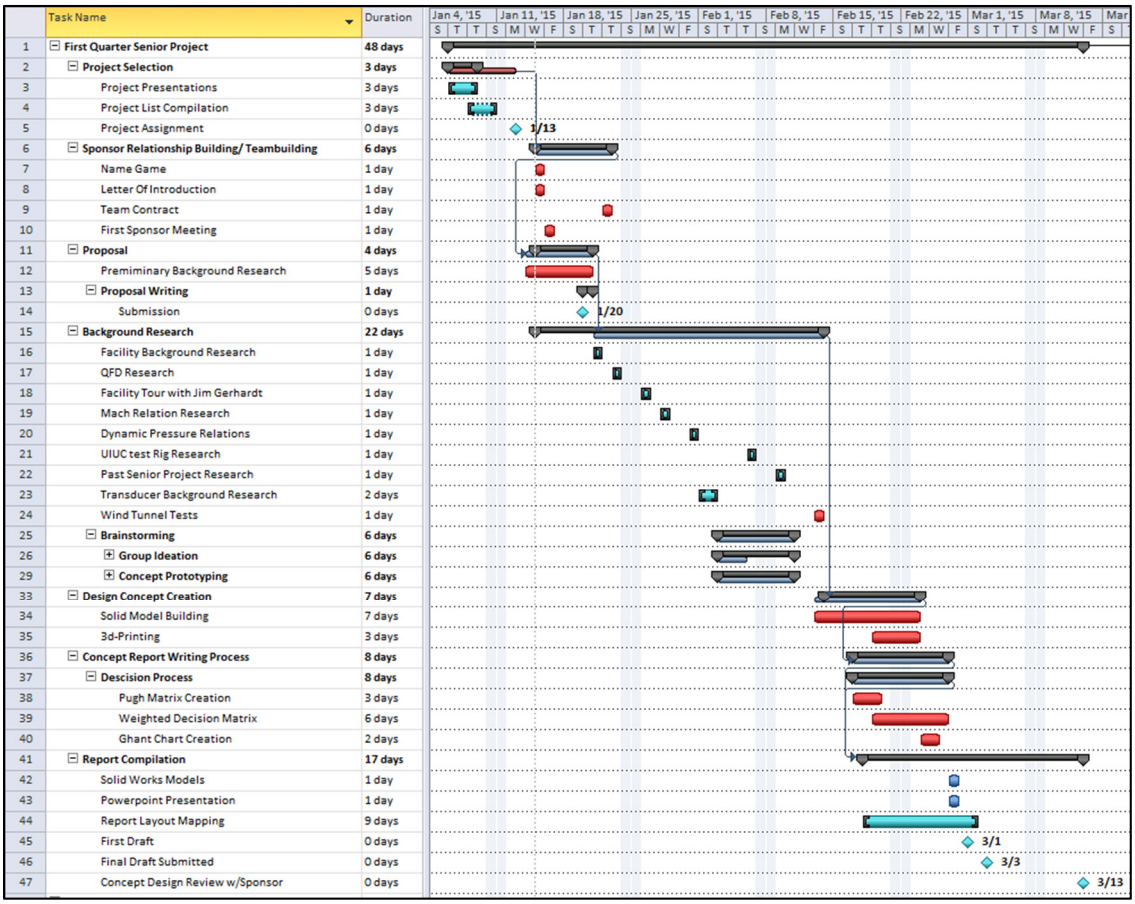

Figure 31. Gantt chart Quarter one.

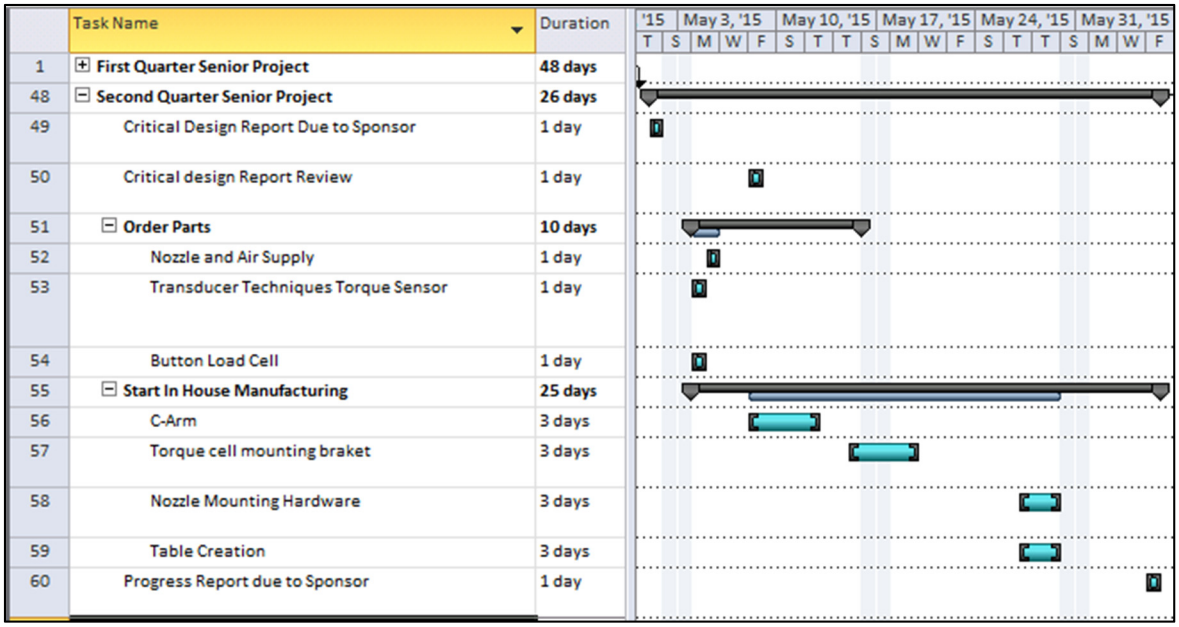

Figure 32. Gantt chart Quarter two.

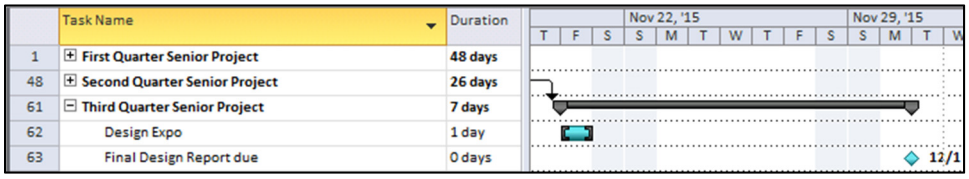

Figure 33. Gantt chart Quarter three.

The Gantt charts show items that will be addressed and referenced in our construction plan in the following section. We realize these divisions of time are very difficult to determine and may have to be adapted in the future due to setbacks in communication of manufacturing processes.

6.4 Construction Plan

Construction of the testing device will be split up into either manufacturing or purchasing of three main components. The nozzle, the expansion and straightening chamber, and the micro-RAT mounting and measurement rig. Cost and effectiveness evaluated in the weighted decision matrices included previously in this report have allowed us to make a decision on whether to manufacture or purchase each component.

The weighted decision matrix for the nozzle lends us to conclude that optimum performance and cost efficiency is best fulfilled through purchase of the component. Purchasing the nozzle also allows us flexibility in altering the nozzle design in future iterations by purchasing different configurations. A six inch to two inch NPT will be purchased to serve as the nozzle.

The expansion and straightening chamber will be purchased as well. The weighted decision matrix for these components led us to this decision because the components are readily available on the market. The components that are available are adequate for our design and are cheaper due

to large scale production. Construction is also simplified by using standard pipe threading to join the components.

Due to the complexity of the mounting for the micro-RAT, we will custom manufacture the mounting system. Access to CNC mills and lathes will allow us to accurately fabricate the necessary components. We plan to use 6061 aluminum as the material. Precise tolerances will be necessary because the torques and forces we will be measuring with the mounting system will be very small. Luckily, the machines we have available to us will allow us to achieve these tolerances.

The first constructed test rig will serve as a prototype if testing reveals that the design or the construction process needs to be altered. Testing will also allow us identify potential areas of improvement to better our original design.

7. Final Design

7.1 Final Design Description

After careful consideration of customer requirements and analysis, a final design has been procured. The final design is broken into two sub-assemblies incorporated into one final mechanism for testing our micro-RAT device. The two sub-assemblies consist of: a flow straightening mechanism utilizing stainless steel off the shelf pipe fittings, and a micro-RAT mounting and measurement system consisting of a mix of manufactured and purchased items.

The first sub-assembly to consider is the flow straightening mechanism. It is rendered in Figure 34.

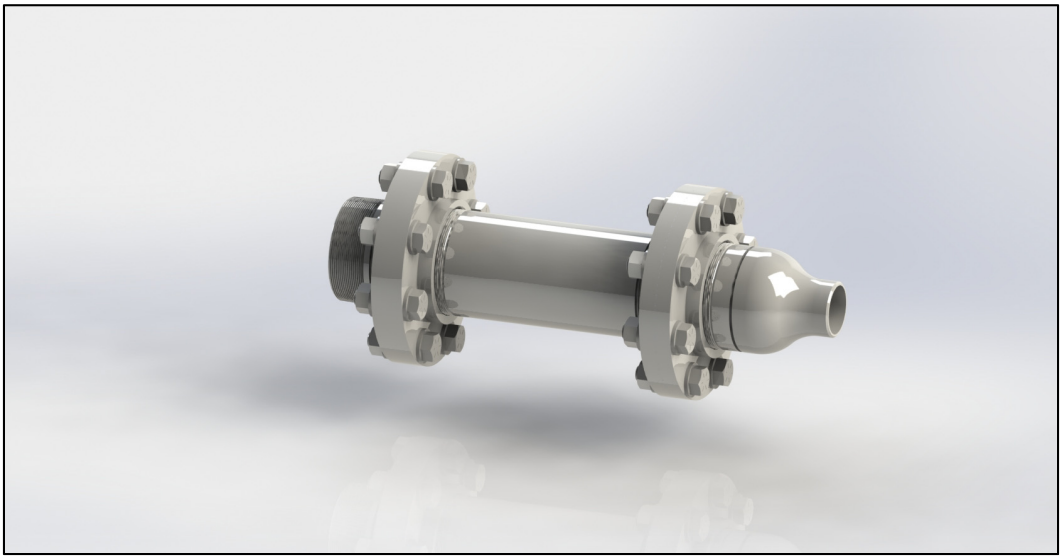

Figure 34. Flow Straightening Mechanism Render

This assembly will partially attach to a female NPT ball valve located on the Cal Poly air supply system. The flow straightening will be achieved using straightening mesh and aluminum

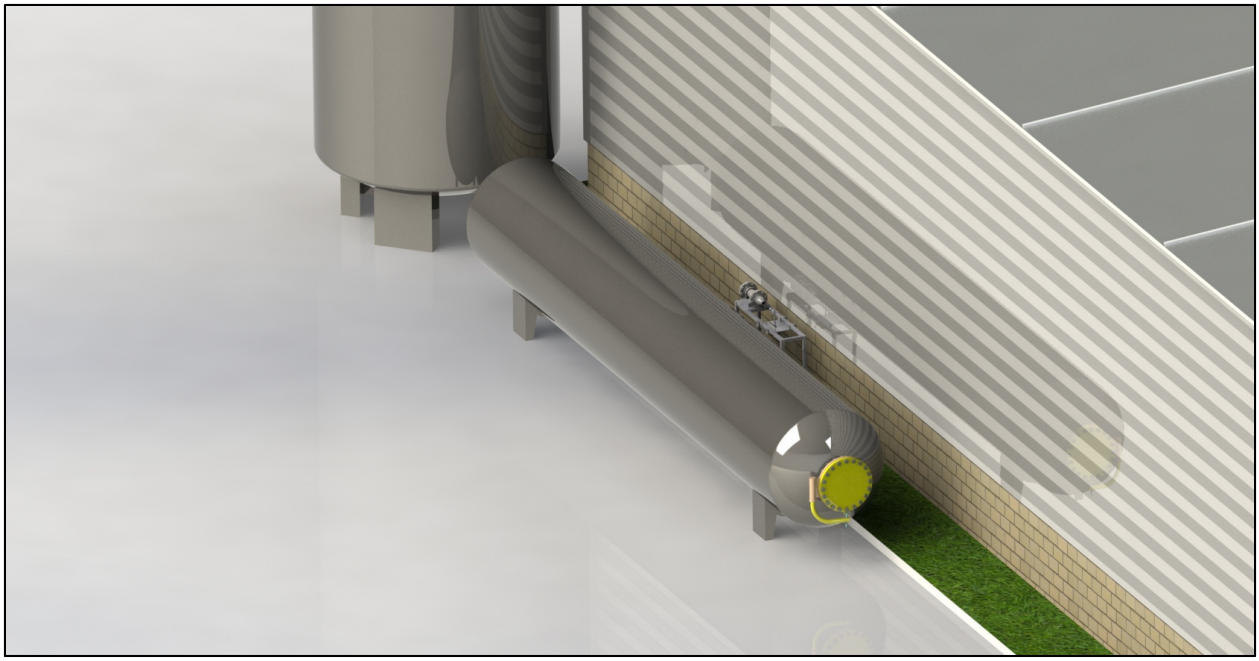

Figure 35. Schematic of Cal Poly Air System Interface

honeycomb. For visualization of the connection to Cal Poly air supply, Figure 35 has been included for reference.

The next sub-assembly in our system is the micro-RAT mounting and measurement apparatus. The sub assembly is capable of measure both torque developed by the rotor of the RAT in units of inch-ounce as well as drag exerted on the micro-RAT in units of pounds-force. The sub-assembly is featured as a Solidworks render in Figure 36.

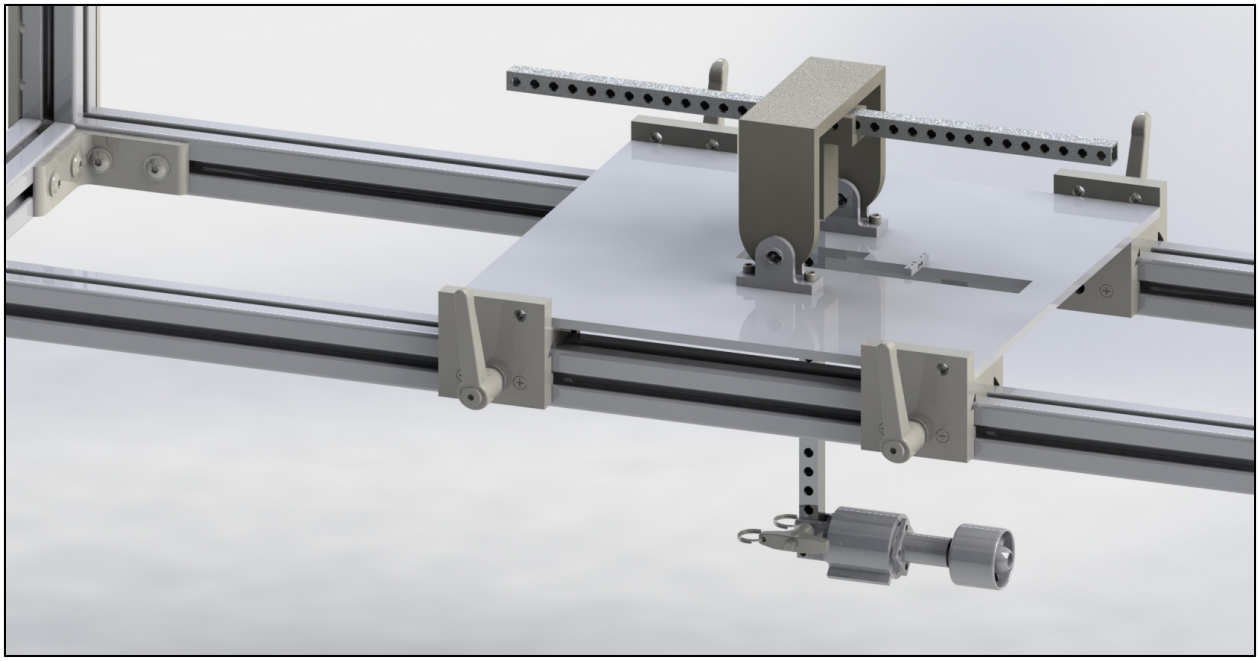

Figure 36. Micro-RAT mounting mechanism rendering

This Sub-assembly, highlighted in section 4 of this report, now incorporates 4 linear bearings enabling us to slide parallel our micro-RAT parallel to the flow. This feature enables us to ramp up flow velocity when the micro-RAT is at a safe distance away from the nozzle. As soon as we are comfortable with flow conditions we can slide the RAT and immerse it in the high velocity stream at a rate allowing the blades to spool up at a safe rate. Both the flow straightening sub-assembly and micro-RAT mounting sub assembly are contained in the final assembly consisting of an extruded aluminum jig. The final assembly is featured as a render in Figure 37.

Figure 37. Final Assembly Test Rig Assembly

Technical Details of the final assembly, pictured in Figure 37, will be discussed thoroughly in the proceeding subsections of chapter 7 of this report.

7.2 Final Design Analysis

Analysis was done on the proposed structure to ensure that it is safe to operate and that it will perform as desired. A calibration curve for measuring the drag on the Micro-RAT was also developed.

Since there is a significant amount of pressure in the flow straightening and nozzle section, hoop stress and longitudinal stress in the stainless pipes was calculated along with the stress experienced by the bolts in the flanges holding the assembly together. The factors of safety were determined to be much larger (at least one order of magnitude) than the minimum factor of safety for the pressurized sections requested by the customer.

The test stand was also analyzed in order to determine if it would hold up to the loads applied to it. Of primary concern was the weight of the flow straightening and nozzle assembly. The minimum force required to tip the structure was also calculated. The calculated force was determined be lower than would be desired and as such it was decided that the test stand would not be carted with the flow straightening assembly in place. This assembly should be placed on the bottom shelf of the stand or on a separate cart during transportation to avoid damage to the

stand or personal injury. Table 11. and Table 12. show the calculated stresses and forces on the structure. The lowest factor of safety calculated was 72 for the hoop stress.

Table 11. Calculated stresses on structure

Loading Condition	Stress (psi)	FOS
Bolt Stress	845	142
Hoop Stress	1019	72
Longitudinal Stress	510	144
Compressive Stress	32	1200
Buckling	40 (lb)	485

Table 12. Calculated force on structure

Loading Condition	Forces (lb)
Minimum Tipping of Stand	26
Maximum Drag Force on Micro-RAT	4.6
Flex Bearing Load	4.4

An Excel spreadsheet was developed to determine the correct calibration curve to use for determining the drag force acting on the Micro-RAT. This was necessary because the load cell does not directly read the drag force on the Micro-RAT. The curve will also change depending on the location of the load cell on the lever arm. Since the load cell is initially in tension and then is loaded in compression as the drag force increases, the zero loading crossover point was of concern. It was determined that this crossover point corresponded to a very low drag that it would not be necessary to counterweight the assembly such that the load cell is always in compression.

If a heavier Micro-RAT were to be tested, a counter weight could very easily be added to the lever arm to negate this issue. Since the bearings being used have a torsional stiffness, it would be feasible that the additional load due to this torsional spring rate would need to be calibrated out. However, the torsional spring rate is very low and presence of the load cell means that the deflection of the flex bearings is extremely low. As such, it is not necessary to calculate the force on the load cell due to the flex bearings. Any force present in the system due to the flex bearings will just be accounted for as an initial offset and will be zeroed out with the rest of the initial offset before the beginning of a test run. A sample of the spreadsheet is shown in Table 13. h is the distance of the micro-Rat from the pivot of the test stand. l is the distance of the load cell from the pivot and x is the amount of overhang of the micro-Rat Assembly.

Table 13. Sample of spread sheet for determining calibration curve and offset of load cell

Flex Bearing Loads and Drag Force Calibration Curve						
Inputs				Outputs		
h	8.26	in		Max Force on each Bearing	4.4	lbf
l	6.75	in		Drag force slope	0.817	lbf
x	2.5	in		Drag force offset	0.061	lbf
Max Drag force	4.6	lbf		Max force on Load Cell	5.6	lbf
Frame weight	1.7	lbf		Drag force for load cell		
MicroRAT weight	0.2	lbf		zero point	0.061	lbf

In order to size the Torque Sensor for the Micro-RAT measuring device, a detailed analysis using Euler Turbo-machinery equations. From analysis a set of curves was developed, (Figure 38), showing a relationship between torque and oncoming airspeed for various fixed rotor RPMs. This allowed us to choose the torque sensor load input range in units of ounce inch.

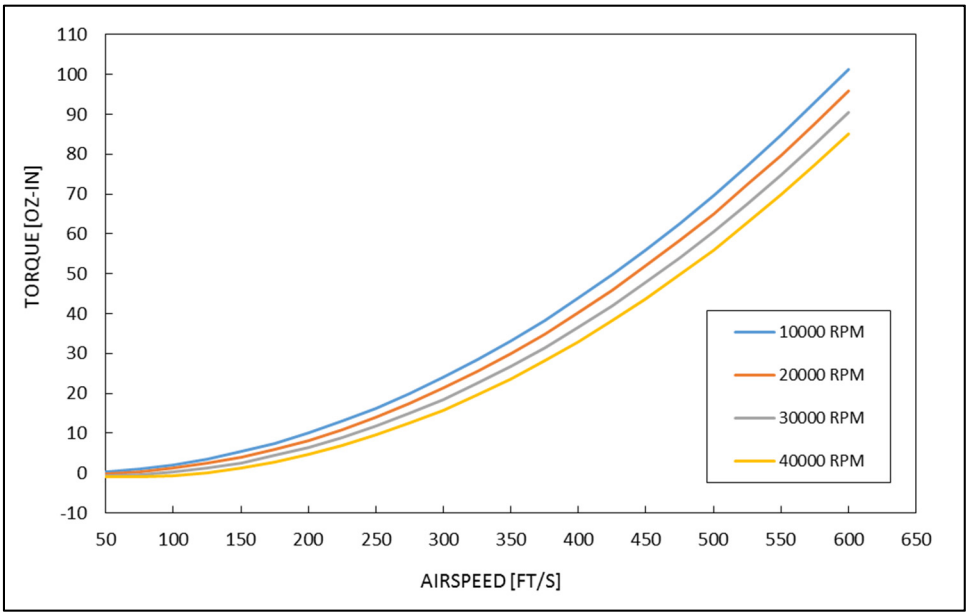

Figure 38. Torque developed at the rotor of a micro-RAT vs. oncoming airspeed for a range of design point RPM

All other analysis is located in Appendix G Each analysis page not referenced here has adequate explanatory notes to enable comprehension. The most notable and important takeaways from analysis have been chosen to be included above in the body of the report.

7.3 Final Design Assembly Drawings

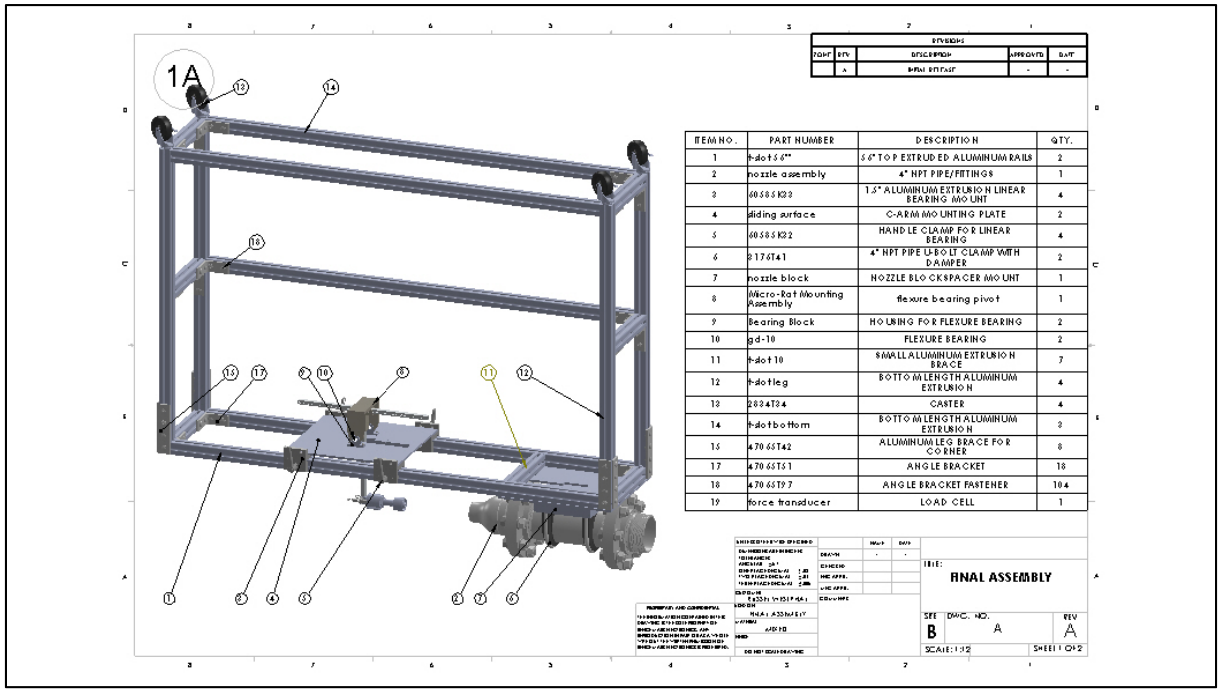

Figure 39. Final Assembly Bill of Materials

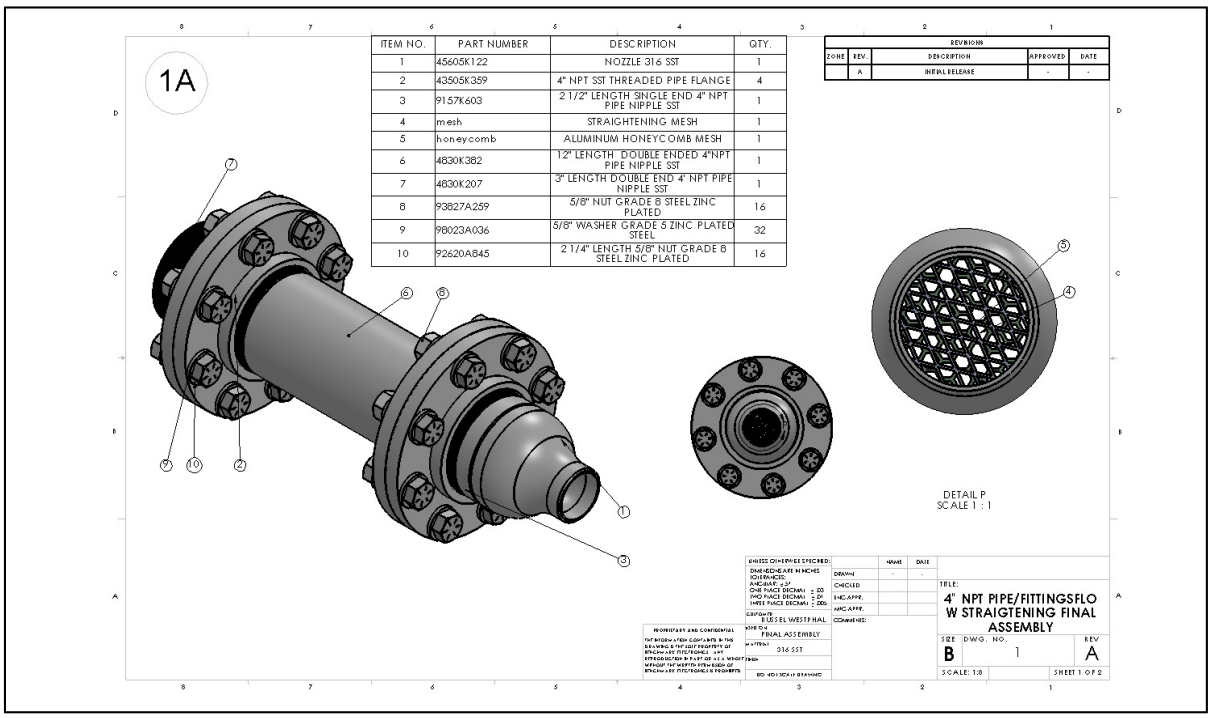

Figure 40. Flow straightening Bill of Materials Sub-Assembly

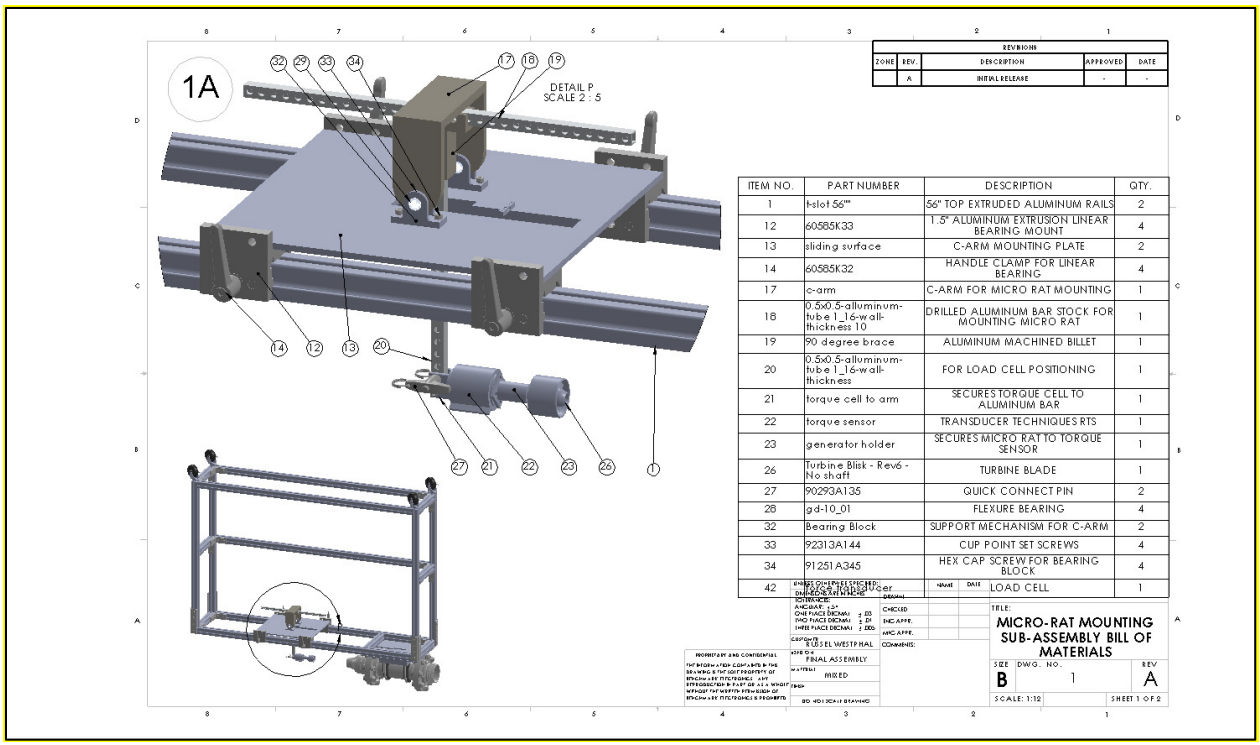

Figure 41. Micro-RAT mounting Bill of Materials Sub-Assembly

For sub-assembly component detail drawings please reference Appendix K.

7.4 Final Design Vendor Information/ Costing Analysis

A detailed Bill of Materials including Vendor information as well as a component costing sheet have both been included in Appendix L.

7.5 Final Design Manufacturing Plan

All parts requiring manufacturing will be run on the HAAS VF2 located in the IME building. Creo software has been used to generate tool path geometry. The following figure is of the HASS VF2.

Figure 42. HAAS VF2 CNC Mill

Detailed design drawings for parts too simple to warrant the tool path being created by Creo have been included for manual machining located in Appendix K. For parts too complex for manual machining Creo has been used to create G-Code to control the HAAS tool path. The following three snapshots, Figures 43-45, demonstrate the tool path geometry for three sample Creo simulations.

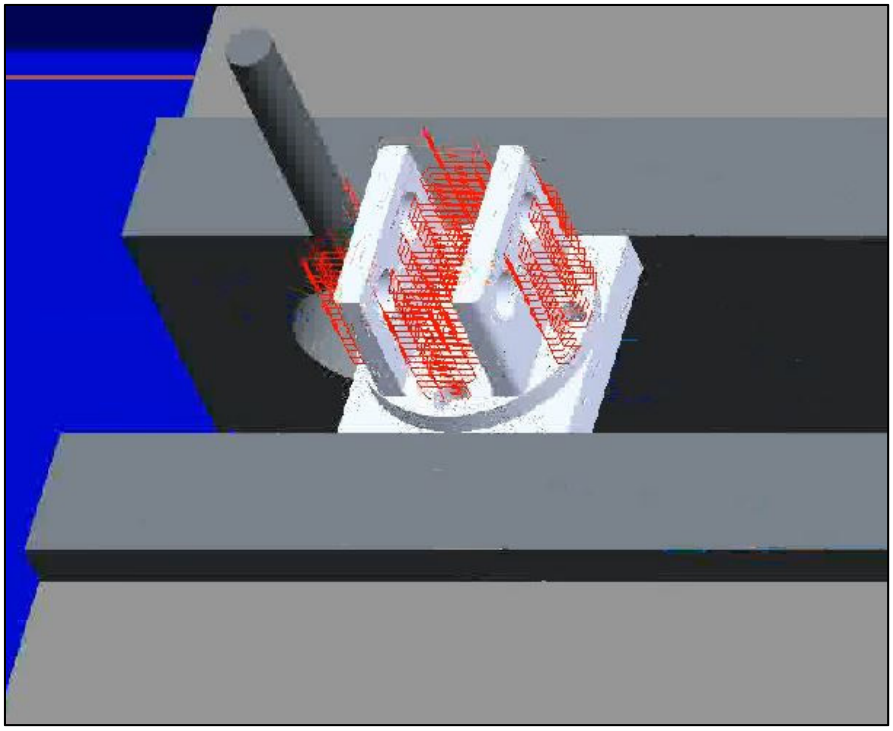

Figure 43. Creo CNC Toolpath rendering for Torque cell to C-Arm Part

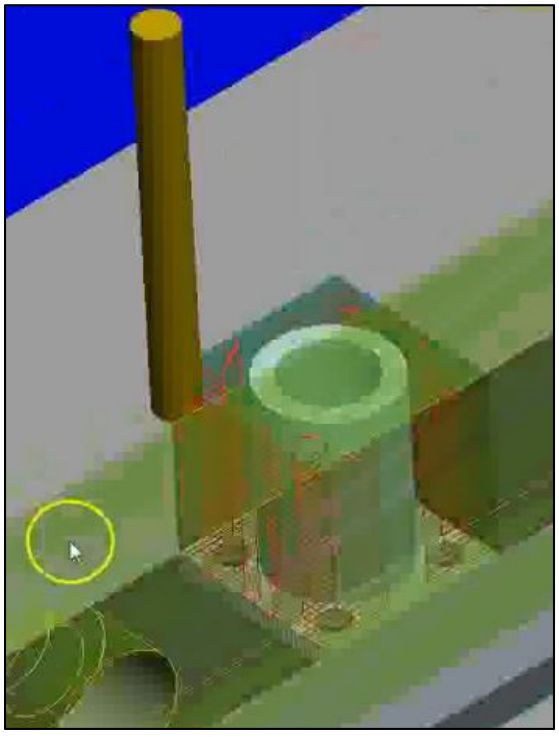

Figure 44. Creo CNC Tool path Rendering for Bearing Block Part.

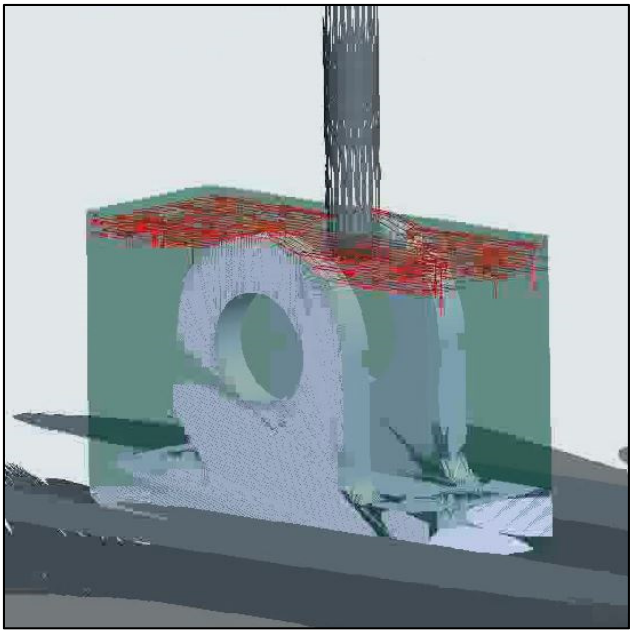

Figure 45. Creo CNC Tool path rendering for Torque Cell to Micro-RAT part.

All machined components will be made from 6061 aluminum stock located in the IME shop. All profile tool paths were created using a ¼" HSS Ball end mill at 4800 rpm and 14 i.p.m (inch per minute) velocity. The rough stepping depth per pass was 50 thousands of an inch.

7.6 Final Design Verification Methodology and Failure Analysis

To verify the design both a DVP&R and a FMEA were conducted on our device. Both are included as Appendix O and Appendix P respectively. A hydraulic pressure testing procedure for the flow straightening subsystem was also included as Appendix N. A general safety Precaution checklist also been included in Appendix J.

In order to improve comprehension of the Failure Modes and Effects Analysis document, we find it helpful to introduce the methodology behind its implementation. Our design was divided into two component systems for analysis: flow system, and Micro-Rat mounting. Each subsystem has individual components with respective modes of failure. The effects of these failure modes were looked at and assigned a severity rating in the off chance that the failure did occur. In order to determine a criticality of this failure mode, a probability of occurrence value from one to ten was multiplied by the severity. The components with the highest criticality must be further investigated and a recommended action developed.

8. Product Realization

Manufacturing of most components was completed in house, by the team. The Haas CNC Milling machine, Figure 42, was used for the bearing blocks seen in Appendix K, Item 32. The bearing blocks were the most challenging to manufacture. This was due to the fact that the housing for each of the two flexure bearings had to be concentric to not cause any off-axis torque on the bearings. The product of machining can be seen in the final bearing block depicted in Figure 46.

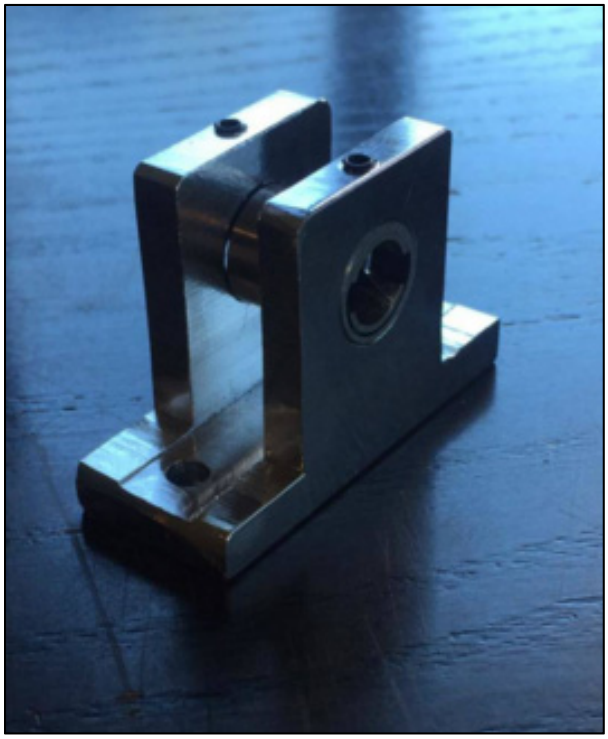

Figure 46. Bearing block, bearing fit test.

The CNC Mill was critical in providing the accuracy necessary to accomplish this task. A Blanchard ground plate was used for the C-Arm mounting plate (Appendix K, Item 17) and the features were cut using the CNC Mill. Figure 47 depicts the milling process of the torque cell mounting block.

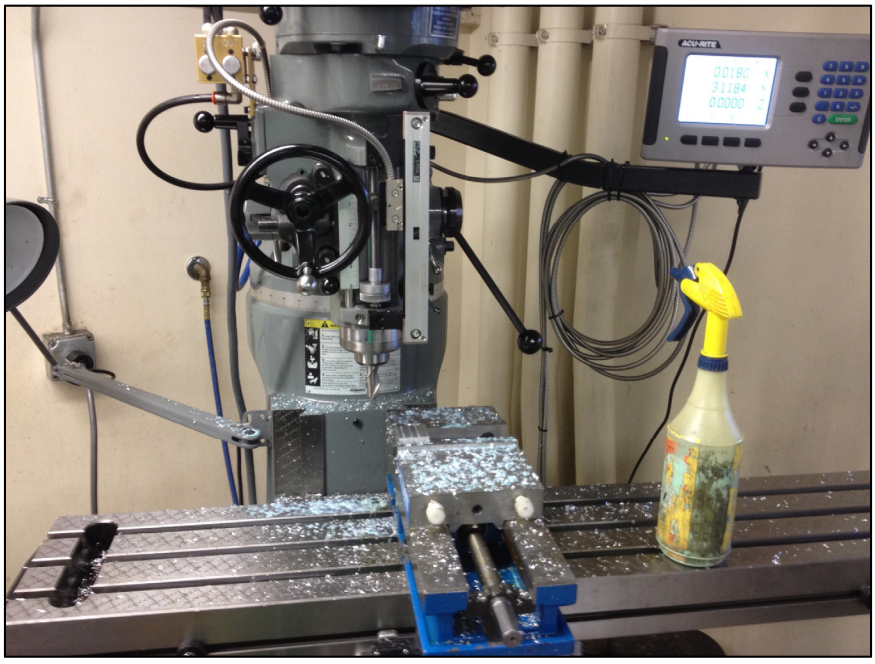

Figure 47. Torque cell mounting block milling process.

The C-Arm for Micro-RAT Mounting (Appendix K) design was changed to be manufactured in 3 parts; two bearing mounts and a connecting plate between. This was done so that the hole for each bearings did not have to be machined as accurately as previously thought. All of the moment Arm mountings were cut from ½" aluminum tubing (Appendix K, Items 18, 20) and the connecting pieces (Appendix K, Items 19, 21) were milled from aluminum blocks. Solid tubing instead of slotted tubing was used to increase the adjustability of the mounting location. The mounting apparatus can be seen in Figure 48 and 49.

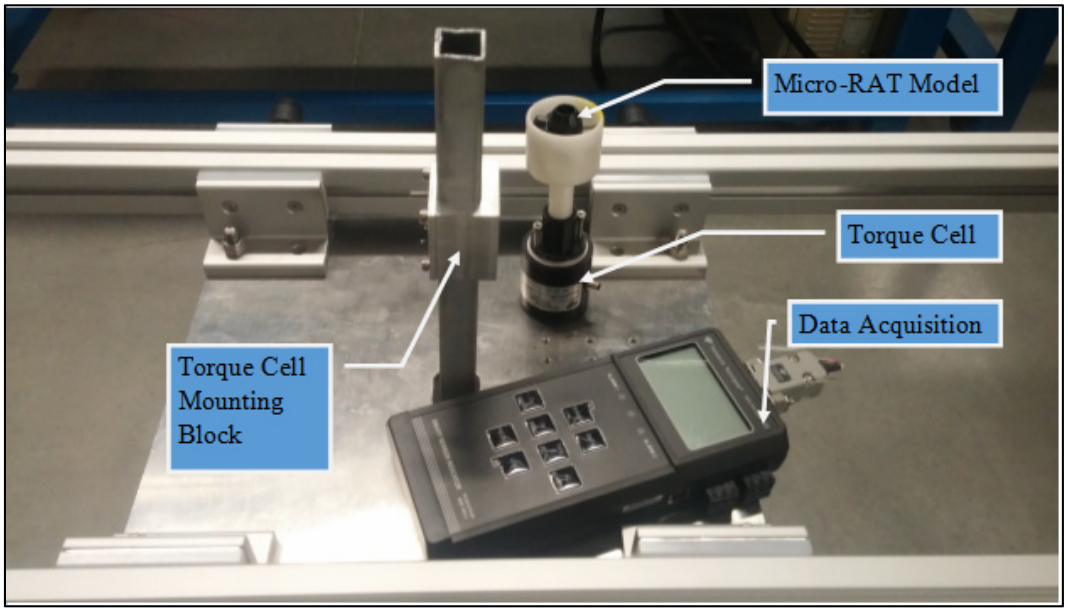

Figure 48. Mounting Apparatus, Air flow side.

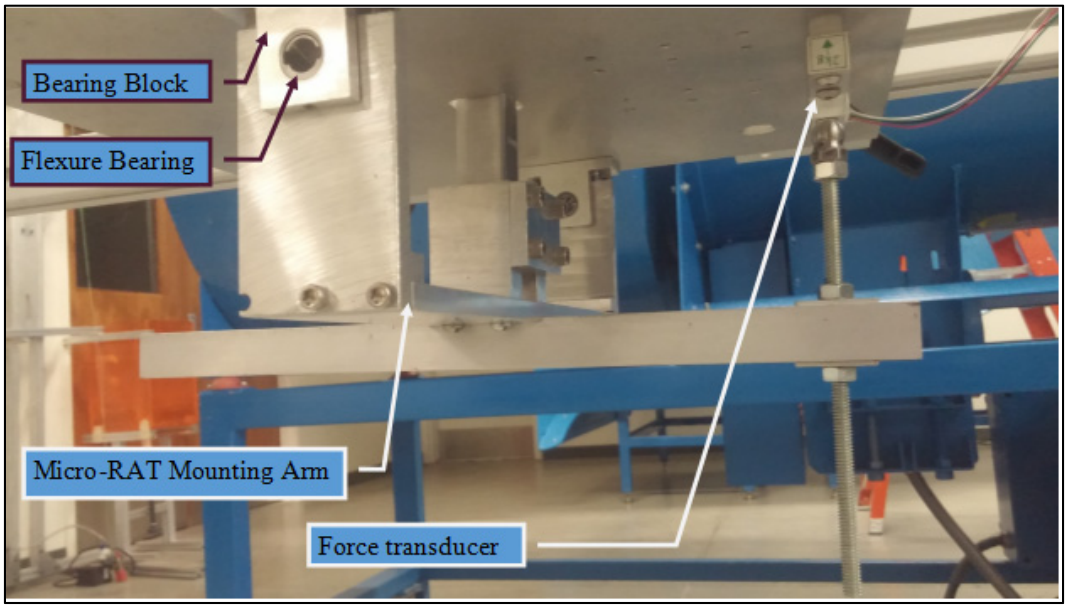

Figure 49. Mounting Apparatus, Bottom side.

The Cart was assembled from prefabricated and cut to length aluminum rails and gussets purchased from TSLOTS (Futura Industries). Teflon linear slide bearings, also from TSLOTS, were used to allow the C-Arm mounting plate to slide along the aluminum rails. The cart with the flow straightening piping and the mounting apparatus installed can be seen in Figure 50.

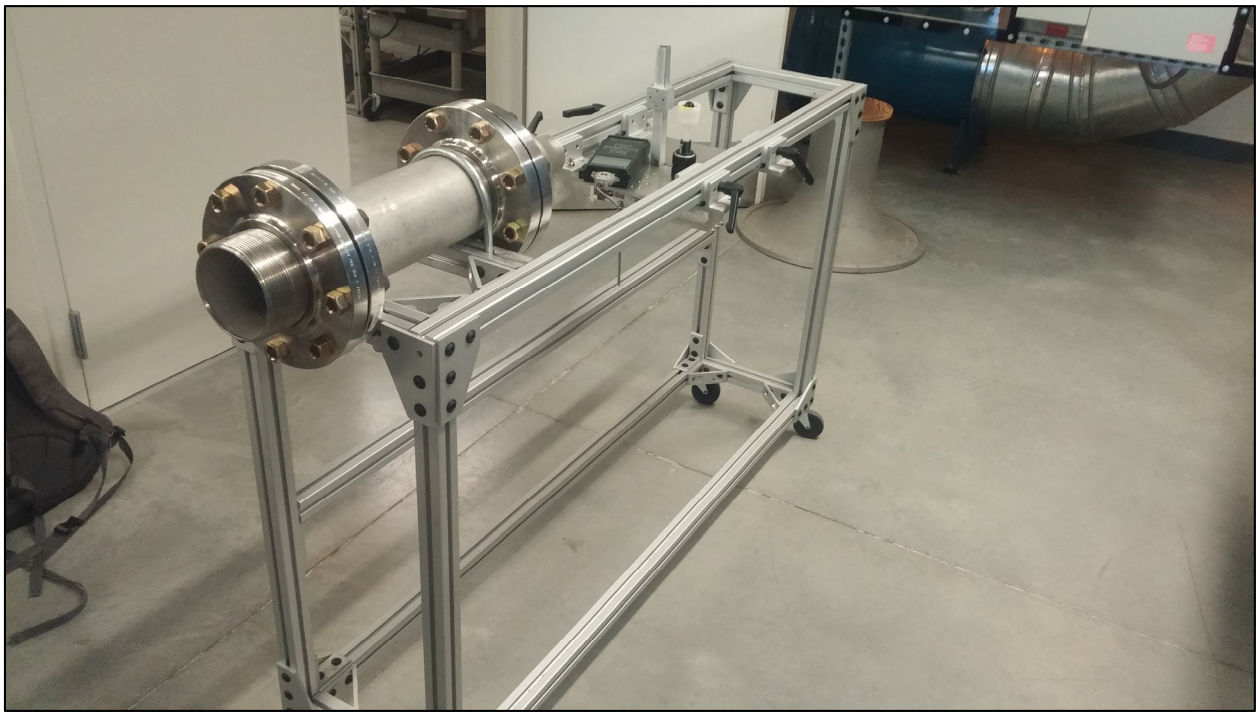

Figure 50. Final Design test rig photograph.

The nozzle at the end of the flow straightening portion of pipe was welded on to the end of the stainless steel pipe. Due to the complexity of this weld and the quality necessary, we outsourced the welding to the welding instructor Kevin Williams. Kevin welded the nozzle and the pipe together with high enough quality to withstand a hydrostatic test on the pipe network. This weld as well as the other Pipe components can be seen in detail in Figure 51.

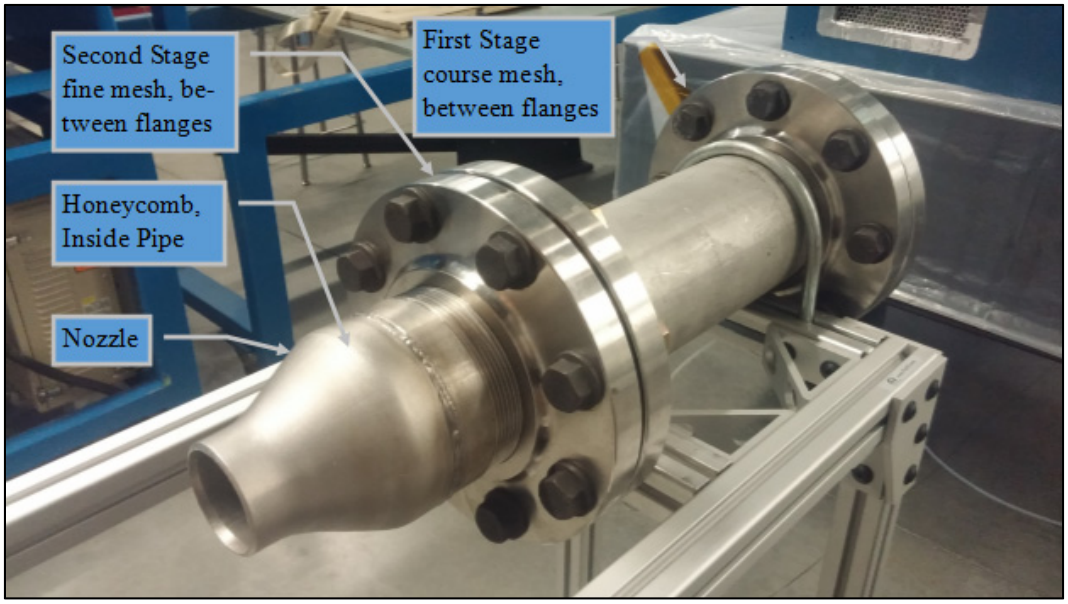

Figure 51. Flow straighteneing pipe network

A threaded rod was used to transfer the drag force onto the force transducer seen in Figure 48. This rod had a ball welded to the end to contact the transducer. The welding can be seen in progress in Figure 52.

Figure 52. Threaded rod welding.

9. Testing

Originally we were to test our rig with air from the air supply located outside of the engines lab. This air is pressurized at 120 psi and the flow rate is controlled using a ball valve. While running this test we were to collect thrust and torque data using our Micro-Rat mounting sensors. However, our team did not receive permission to run this test for safety reasons. Our sponsor was unable to get school approval to run the test. Also, a hydrostatic pressure test on our flow straightener to make sure that it could withstand 120 psi pressure needs to be completed before a test can be performed.

We set up the rig and used a spring scale to pull on the micro-RAT in order to test the sensor and lever arm against a varying load. We recorded data with the load cell and used the spring scale with a resolution of 0.1 pounds and a set moment arm length of 8 inches. We applied loads to the micro-RAT in 0.1 pound increments up to 2.0 pounds using the spring scale. The results from this test can be seen in Table 14. We then plotted the force we applied with the spring scale versus the force seen on the readout seen in Figure 53. We got the equation of the line and compared it to the ratio of the moment arms as this is the factor between the two forces. The two moment arms were vertical distance between the point on the micro-RAT where the force was applied to the center of the flexure bearing and the horizontal distance from the center of the flexure bearing to the point where the lead cell contact hits the load cell. The ratio of these two moment arms were 0.578125 and the equation of the line from the experiment was 0.5717. Because these two values are so close to one another we can conclude that the moment arm transfers the force with no other factors that need to be considered.

We also performed a functionality test. To do this we used a leaf blower to provide the air stream over the mirco-RAT. The leaf blower had the capability to move air at 70 mph. We set up a rig for the leaf blower over our cart and put it directly in front of the micro-RAT. We blew air at 70 mph over the micro-RAT and measured torque and drag on the Micro-RAT. To get varying loads on the generator of the Micro-RAT we connected a rectifier and a variable resistance. We decided to minimize the resistance to create a maximum load on the shaft. The data that we were able to obtain from the sensors proved that there will be significant resolution of the torque and drag measurements to provide information on the relation between resistance of the generator, dynamic pressure and torque/drag of the Micro-RAT. This test also verified that the rig will withstand at least a fraction of the wind speeds that will be present in the full scale test.

Table 14. Raw data from load cell calibration test.

Force Applied (lbs)	Force On Readout (lbs)
0.1	0.043
0.2	0.135
0.3	0.189
0.4	0.243
0.5	0.305
0.6	0.350
0.7	0.412
0.8	0.448
0.9	0.526
1	0.588
1.1	0.645
1.2	0.689
1.3	0.762
1.4	0.818
1.5	0.849
1.6	0.917
1.7	0.971
1.8	1.028
1.9	1.100
2	1.171

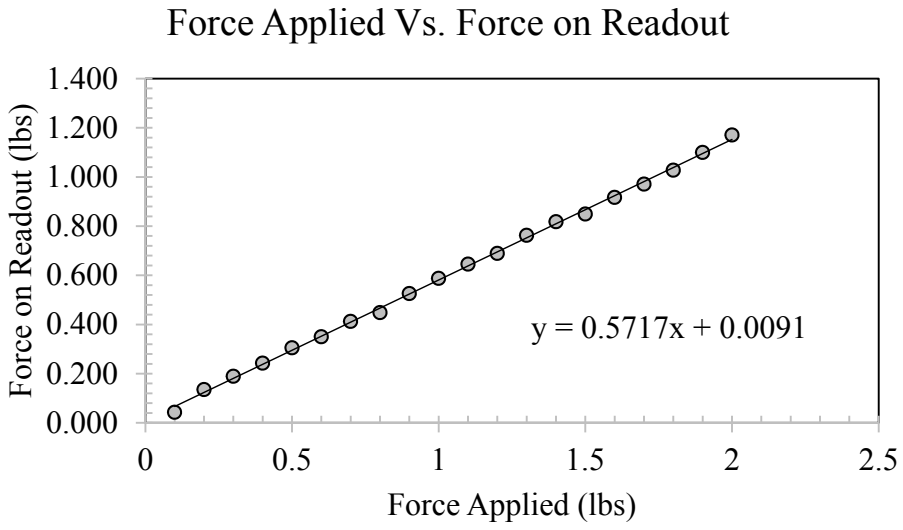

Figure 53. Plot to Determine Moment Arm Ratio for Load Cell Calibration Test.

References

[1] "Patent US2592322 - Rocket Motor Pumped Supersonic Wind Tunnel." *Google Books*. N.p., n.d. Web. 02 Mar. 2015.

[2] "Picture of the Bombardier CRJ-200ER (CL-600-2B19) Aircraft." *Photos: Bombardier CRJ-*

[3] "1247 Hypersonic Facilities Complex." - *NasaCRgis*. N.p., n.d. Web. 02 Mar. 2015.*200ER (CL-600-2B19) Aircraft Pictures*. N.p., n.d. Web. 02 Mar. 2015.

[4] Munson, Bruce R., Theodore H. Okiishi, Wade W. Huebsch, and Alric P. Rothmayer. "Viscous Flow in Pipes." Fundamentals of Fluid Mechanics. 7th ed.: R.R. Donnelley/Jefferson City, 2013. Print.

[5] Cal Poly Mechanical Engineering Department. "Pipe Flow Analysis." ME 347 Fluid MechanicsLab Experiments. San Luis Obispo: Cal Poly University Store, 2010. Print.

[6] Rennels, Donald C., and Hobart M. Hudson. "Entrances." Pipe Flow: A Practical and Comprehensive Guide. Hoboken, N.J.: John Wiley & Sons, 2012. Web. 4 May 2014.

[7] "Engineering Calculator." *Engineering Calculator*. TLV, n.d. Web. 31 Jan. 2015.

[8] Robert. "Pilot Is Hailed After Jetliner's Icy Plunge." *The New York Times*. The New York Times, 15 Jan. 2009. Web. 02 Mar. 2015.

[9] "CONCORDE SST : FLIGHT SYSTEMS." *CONCORDE SST : FLIGHT SYSTEMS*. N.p., n.d. Web. 02 Mar. 2015.

[10] "Halltech Honeycomb™1/8." *Halltech Systems Performance Products*. N.p., n.d. Web. 02 Mar. 2015.

[11] "Spinner Cone 3,2" with Cooling." *Spinner Cone 3,2" with Cooling*. N.p., n.d. Web. 02 Mar. 2015.

[12] "Single Pin Sanitary Hinge Clamp." *Single Pin Sanitary Hinge Clamp*. N.p., n.d. Web. 02 Mar. 2015.

[13] "NIBCO 4 In. X 2 In. PVC DWV Hub X Hub Reducing Coupling-C4801HD42 - The Home Depot." *The Home Depot*. N.p., n.d. Web. 02 Mar. 2015.

[14] Dunbar, Brian. *NASA*. NASA, n.d. Web. 02 Feb. 2015.

[15] "Patent US5492313 - Tangential Linear Flexure Bearing." *Google Books*. Web. 3 Mar. 2015. <http://www.google.com/patents/US5492313>.

[16] "LOW CAPACITY (INCH-OUNCE) REACTION TORQUE SENSOR." *RTS Series Low Capacity (In-oz) Reaction Torque Sensor*. Web. 3 Mar. 2015. <https://www.transducertechniques.com/rts-torque-sensor.aspx>.

Table of Appendices

April 8, 1952 A. J. NERAD 2,592,322

ROCKET MOTOR PUMPED SUPERSONIC WIND TUNNEL

Filed Sept. 2, 1948

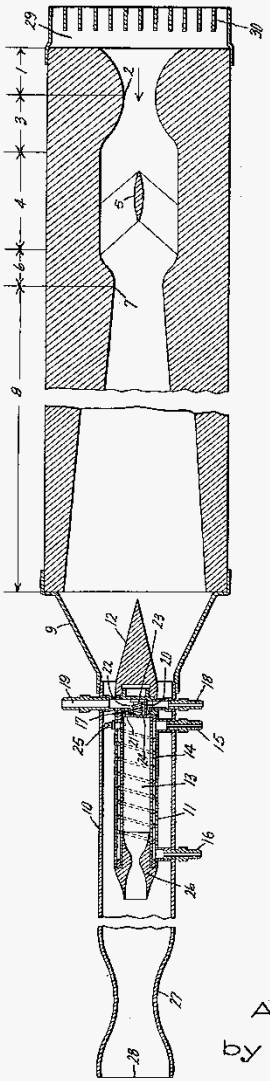

Inventor:
Anthony J. Nerad,
by Richard E. Hosley
His Attorney.

Contents


```
% pipeflow.m
% Ken Enstrom
% ME 428


clear all

% Given/measured values
rho = 1.936; % Density of water at 68 deg F, slugs/ft^3
mu = 2.037E-5; % Kinematic viscosity of water at 68 deg F, lbf*s/ft^2
D = 0.264/12; % Inside diameter of pipe, ft
ed = 0.227E-3; % Surface roughness/I.D. using given e, (-)
A = (pi/4)*D^2; % Pipe cross-sectional area, ft^2
g = 32.17; % Acceleration of gravity, ft/s^2
a = 1; % Turbulent kinetic energy factor, (-)
K_L = 0.1; % Entrance loss coefficient, (-)
L_D = 30/.264; % Length/Diameter Ratio, (-)

% Input experimental flowrate and initial friction factor guess
% Use f1 = 0.015 for all data poitns
f1 = 0.015; % Initial friction factor guess, (-)
f2 = 1; % Arbitrary new friction factor for while loop, (-)
Q_1 = input('Enter experimental flowrate (gpm): ');
Q_2 = 5000; % Arbitrary initial Q_2 for while loop, gpm
```

```
Attempt to execute SCRIPT pipeflow as a function:
/Users/kennyenstrom/Downloads/pipeflow.m
```

Begin while loop for convergence %%

```
% Input uncertainty of flowrate
Q_unc_input = input('Enter flowrate uncertainty (gpm): ');

Q_unc = abs(Q_2-Q_1); % Difference between new and old flowrates, gpm
f_unc = abs(f2-f1); % Difference between new and old friction factors, (-)

% Input water height
h = input('Enter water height (ft): '); % Water height, ft

% Track number of iterations
i1 = 1;

while Q_unc >= Q_unc_input && f_unc >= 0.10*f2

    % Calculate Reynold's Number
    V = (Q_1/470)/A; % Flow speed, ft/s
    Re = ((rho*V*D)/mu); % Reynold's Number, (-)
```

```
    % Calculate Darcy Friction Factor
    f2 = (-2.0*log10(((0.277E-3)/3.7)+(2.51/(Re*(f1^0.5)))))^-2;

    % Calculate Flowrate
    Q_2 = (((2*g*h)/(a+K_L+f2*L_D))^0.5)*(pi/4)*D^2*(470); % New flowrate, gpm

    % Calculate iteration differences and re-assign Q_1 and f1
    Q_unc = abs(Q_2-Q_1); % Calculate new difference
    Q_1 = Q_2; % Re-assign Q_1 to new flowrate
    f_unc = abs(f2-f1); % Calculate new difference
    f1=f2; % Re-assign f1 to new friction factor
    i = i1+1; % Add one to iteration
    i1 = i; % Reset i1 to new i
end

Reynolds_number = Re
Flowrate_GPM = Q_2
Darcy_friction_factor = f2
Number_iterations = i1
```

Published with MATLAB® R2013a

VELOCITY STARTING POINT = 0.5 MACH

0.5 MACH = 33,464 FT/MIN
= 380 MPH
= 557 FT/SEC

* FOR A 2" STREAM OF AIR

AREA = πr^2

AREA = $\frac{\pi D^2}{4}$

2" = 2/12' = 0.16667' = DIAMETER

AREA = $\frac{\pi (0.16667')^2}{4}$

AREA = 0.021817 ft^2

SCFM = AREA (ft) · VELOCITY (ft/m)

SCFM = (0.021817 ft^2) · (33,464 ft/min)

SCFM = 730.071 (SCFM)

* COMMON RECEIVER SIZING FORMULA:

$t = V(P_1 - P_2) / C P_a$

WHERE
V = VOLUME OF TANK (CUBIC FEET)
t = TIME FROM UPPER TO LOWER PRESSURE LEVEL (MIN)
C = SCFM REQUIRED
P_a = 14.7 psia (ATM.)
P_1 = MAX TANK PRESSURE
P_2 = MIN TANK PRESSURE

$\therefore V = \frac{C P_a t}{(P_1 - P_2)}$

$V = \frac{(730.071 \text{ SCFM})(14.7 \text{ psi})(0.5 \text{ min})}{(120 - 100) \text{ psi}}$

$V = 268 ft^3$ 1) FOR 30 SECONDS
2) MIN TANK PRESSURE 100 psi

1 CUBIC FOOT = 7.48 GALLON

$\therefore$ V = 2006 GAL

MAYBE A LITTLE BIG?!!

V = AIR VELOCITY (FT/S)
Qa = AIR FLOW RATE (ACTUAL

* FOR ANSI SCH80 NPS4
@ 120 PSI, 70°F, 380 mph

$Q_a = 60\pi\ 380(\text{mph/hour})\ 5280\left(\frac{\text{ft}}{\text{MILE}}\right)\frac{1\text{ hour}}{3600\text{ sec}}\left(\frac{4}{24}\right)^2$

$Q_a = 2955.6$ CFM

$Q_a = 25147.4$ SCFM

!! WHOOPS THIS IS ASSUMIN 380 MPH IN PIPE (4") NOT (2")

$A_1V_1 = A_2V_2$

$\frac{\pi(4)^2}{4}(V_1) = \frac{\pi(2)^2}{4}(380\text{ mph})$

$V_1 = 95$ mph IN 4" PIPE

$\therefore Q_a = 60\pi\ (95\text{mph})\ 5280\left(\frac{\text{ft}}{\text{m}}\right)\frac{1\text{ hour}}{3600\text{sec}}\left(\frac{1}{24}\right)^2$

$Q_a = 738.9\pi$ CFM (ACTUAL) ← NOTE DIFF.

$Q_a = 6286.85$ SCFM

CONFIRMED FROM TLV.com

PRESSURE LOSS THROUGH PIPING:

$$\Delta P = \frac{\rho \mu L V^2}{24 d \cdot g}$$

d = diameter (in)
L = LENGTH (FT)
V = AIR VELOCITY (FT/SEC)
ΔP = PSI
μ = COEFFICIENT OF FRICTION
ρ = DENSITY AIR $\left(\frac{\text{lb}}{\text{ft}^3}\right)$

$$\Delta P = \frac{0.687\frac{\text{lb}}{\text{ft}^3}\ 0.0167\ 10\text{ ft}\left(139.33\frac{\text{ft}}{\text{s}}\right)^2}{24\ (4")\ 32.2\ \text{ft/s}^2}$$

ΔP ≈ 0.724 PSI FOR 10 FEET
ΔP ≈ 1.448 PSI FOR 20 FEET
ΔP ≈ 3.62 PSI FOR 50 FET

NOTE NEG. PRESSURE DROP FROM 4" PIPE

$V^* = c^* = \sqrt{kRT^*}$

$V^* = \left[1.4 \cdot 287 \frac{J}{kgK} \cdot T^*\right]^{1/2}$

$T^* = \left(\frac{T^*}{T_0}\right) T_0 = 0.8333 \cdot 294.3 = 245.24\,K$

$\frac{T^*}{T_0} = 0.8333$

$\therefore V^* = 315\ m/s$

$V^* = 704.635\ MPH$

* PRESS HAS NO AFFECT SO LONG AS $P_{amb} < P^*$

P_0: IF CHOKED, $\dot{m} \propto P_0$

T_0: IF CHOKED, $\dot{m} \propto \frac{1}{\sqrt{T_0}}$

$\dot{m}_{CHOKED} = 4.435\ kg/s$

$\rho_{-20°F} = 1.395\ \frac{kg}{m^3}$

$\dot{m}_{CHK} = 4.435\ \frac{kg}{s} \cdot \frac{m^3}{1.395\ kg} = 3.18149\ \frac{m^3}{s} \cdot \frac{35.3147\ ft^3}{1\ m^3}$

$\dot{m}_{CHK} = 112.353\ CFM$

11/30/2015

FOR $M = 0.5$; $\frac{P}{P_t} = 0.843$; $\frac{\rho}{\rho_t} = 0.8852$; $\frac{T}{T_t} = 0.9524$; $\beta = 0.8660$

$\frac{A}{A_0} = 1.3398$; $\frac{V}{a_0} = 0.53452$

* REALLY IT'S A COMPARISON OF DYNAMIC PRESSURE P_t THAT MATTERS. MACH 0.5 AT ALTITUDE OF 11,000 FT MAY EQUAL MACH 0.3 P_t at SEA LEVEL.

11/31/2015

$P_{dynamic} = \frac{1}{2} \rho V^2$

$\therefore$ CHANGE IN VELOCITY IS PROPORTIONAL TO CHANGES IN ρ

ρ @ 35,000 ft = 7.38×10^{-4} SLUGS/Ft^3

ρ @ 0 Ft = 23.77×10^{-4} SLUG/FT^3

* DYNAMIC PRESSURE NEEDS TO SIMULATE ALTITUDE CONDITIONS AND BE EQUAL NOT NECESSARILY VELOCITY.

$$\frac{1}{2}\rho V^2 = \frac{1}{2}\rho V^2$$

$$7.38 \times 10^{-4}(0.5)^2 = 23.77 \times 10^{-4}(M)^2$$

$$M_{0\,ALT} = 0.2786$$

$M_{compressible} \approx 0.3 \approx$

Mach # $\approx 0.3 = 0.2786$

$V \simeq 230$ MPH.

* SINCE DYNAMIC PRESSURE RELATES REAL WORLD CONDITIONS AT ~~A~~ & CHANGES IN ALTITUDE WE REALLY DON'T NEED SPEEDS EQUIVALENT TO FLIGHT SPEEDS TO CORRECTLY SIMULATE. WE ONLY PROPORTIONALLY NEED VELOCITY TO RELATE TO CHANGES IN DENSITY.

∴ SIMULATION SPEED AT SEA LEVEL COULD BE $\approx$ 230 MPH

BASIC ← NO SWIRL OR FRICTION ACTUATOR DISK THEORY ← FOR BARE ROTOR

WESTPHAL ADT 1/5

* Application of conservation of mass/momentum/energy for 1-D, steady, uniform flow analysis
* "Rankine-Froude" model

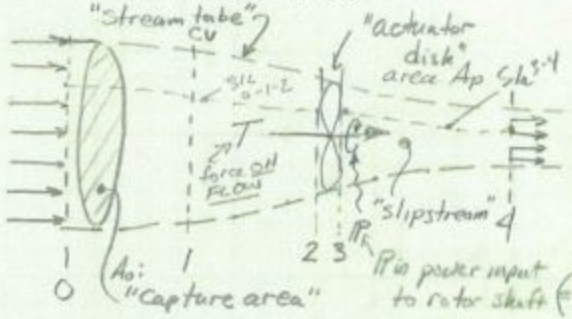

assumptions... (*** Swirl?!)

- C.V. fixed to prop.
- steady, incompressible, (1-D)
- uniform, no losses ($h_L = 0$)
- pressure jump @ disk
- $P_0 = P_4$ = atmospheric
- bare rotor - no shroud or duct

P_{in} = power input to rotor shaft (= torque × rot. speed)

- conservation of MASS: mass flowrate through rotor disk $\equiv \dot{m}$

$$\dot{m} = \dot{m}_0 = \dot{m}_1 = \dot{m}_2 = \dot{m}_3 = \dot{m}_4 \Rightarrow \rho A_0 u_0 = \rho A_1 u_1 = \rho A_2 u_2 = \rho A_3 u_3 = \rho A_4 u_4 \quad (A_p = A_2 = A_3)$$

- Newton's 2nd Law – MOMENTUM / FORCES:

$$T = \dot{m}(u_4 - u_0) = A_p(P_3 - P_2)$$

- conservation of ENERGY (1st Law)

$$\mathcal{P} = \dot{m}\left(\frac{u_4^2}{2} - \frac{u_0^2}{2}\right)$$

Bernoulli on S/L's 0-1-2 & 3-4:

$$P_0 + \tfrac{1}{2}\rho u_0^2 = P_2 + \tfrac{1}{2}\rho u_2^2$$
$$+ \quad P_3 + \tfrac{1}{2}\rho u_3^2 = P_4 + \tfrac{1}{2}\rho u_4^2$$
$$\therefore P_3 - P_2 = \tfrac{\rho}{2}(u_4^2 - u_0^2)$$

NOTE: $u_2 = u_3$, $P_0 = P_4$

$$\Rightarrow T = \dot{m}(u_4 - u_0) = A_p(P_3 - P_2) = A_p \cdot \tfrac{\rho}{2}(u_4^2 - u_0^2) = A_p \tfrac{\rho}{2}(u_4 + u_0)(u_4 - u_0)$$

($\dot{m} = \rho A_p u_2$)

$$\therefore \rho A_p u_2 (u_4 - u_0) = \rho A_p \left(\frac{u_4 + u_0}{2}\right)(u_4 - u_0) \quad \text{so} \quad \boxed{u_2 = \frac{(u_4 + u_0)}{2}}$$

$$\therefore \boxed{\dot{m} = \rho A_p \frac{(u_4 + u_0)}{2}}$$

$$\boxed{T = \rho A_p \frac{(u_4^2 - u_0^2)}{2}}$$

$$\boxed{\mathcal{P} = \rho A_p \frac{(u_4 + u_0)}{2}\frac{(u_4^2 - u_0^2)}{2}}$$

{ Key results of Actuator Disk Theory – inter-relate velocity rise in slipstream to $\dot{m}$, T, $\mathcal{P}$ }

{ SIGN convention: T is + for propeller & $\mathcal{P}$ + for power INput to prop }

* alternatively, write $\mathcal{P}$ in terms of T & $\dot{m}$:

$$\mathcal{P} = \dot{m}(u_4 - u_0)\left(\frac{u_4 + u_0}{2}\right) = T \cdot \tfrac{1}{2}(u_4 - u_0 + u_0 + u_0) = T\,\tfrac{1}{2}\left((u_4 - u_0) + 2u_0\right)$$

$$\therefore \boxed{\mathcal{P} = T u_0 + \tfrac{1}{2}\frac{T^2}{\dot{m}}}$$

← Power input for given thrust will be smallest when mass flowrate is LARGEST

$\therefore T = \dot{m}(u_4 - u_0)$, we favor ↑$\dot{m}$ & ↓$(u_4 - u_0)$ to achieve desired T

APPLICATIONS OF "BASIC" ← NO SWIRL OR FRICTION
ACTUATOR DISK THEORY - [PROPELLER] (UNDUCTED) WEYPHR 4/5

I. PROPULSIVE AIRSCREW – "PROPELLER"

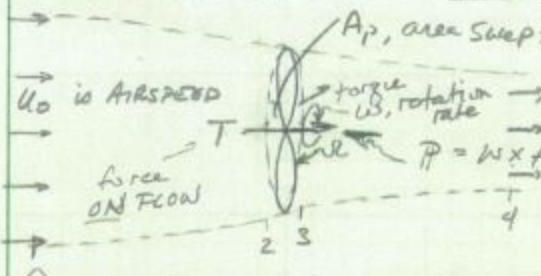

objective: provide propulsive thrust for given brake power input

$$T = \rho A_p \left(\frac{u_4^2 - u_0^2}{2}\right)$$ ← for specified T, A_p, u_0 find required u_4 slipstream velocity

$$\Rightarrow \dot{m} = \rho A_p \left(\frac{u_4 + u_0}{2}\right)$$ ← mass flowrate

$$\& \quad P = \rho A_p \left(\frac{u_4+u_0}{2}\right)\left(\frac{u_4^2-u_0^2}{2}\right) = \dot{m}\cdot\frac{T}{\rho A_p} = Tu_0 + \frac{1}{2}\frac{T^2}{\dot{m}}$$ ← brake power input

CASE: $u_0 \neq 0$ ... define $\eta_p = T\cdot u_0 / P$ "propulsive efficiency"

$$\eta_p = \frac{T\cdot u_0}{P} = \frac{\rho A_p \left(\frac{u_4^2-u_0^2}{2}\right)\cdot u_0}{\rho A_p \left(\frac{u_4+u_0}{2}\right)\left(\frac{u_4^2-u_0^2}{2}\right)} = \frac{2u_0}{(u_4+u_0)} = \frac{2}{\left(\frac{u_4}{u_0}+1\right)}$$

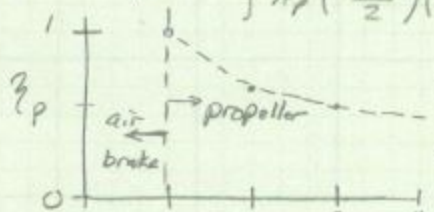

- $\frac{u_4}{u_0} > 1$ for $T > 0$
- for given T, want $\frac{u_4}{u_0} \to 1$ which will require large A_p & $\dot{m}$
- min possible $P = Tu_0$

CASE: $u_0 = 0$ ... static thrust is required

$$T|_{u_0=0} = \rho A_p \frac{u_4^2}{2} = \dot{m} u_4$$

$$\dot{m}|_{u_0=0} = \rho A_p \frac{u_4}{2}$$

$$P|_{u_0=0} = \rho A_p \frac{u_4^3}{4} = \frac{T^2}{2\dot{m}}$$

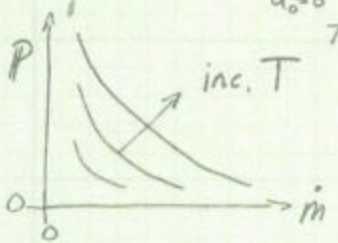

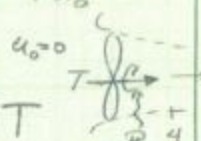

Power required to obtain a specified static thrust drops with increasing $\dot{m}$. implies smaller u_4 since $T|_{u_0=0} = \dot{m}u_4$ & increasing A_p!

APPLICATIONS OF "BASIC" ACTUATOR DISK THEORY — WIND TURBINE (UNDUCTED) WESTRAM ADT 3/5

II WIND TURBINE

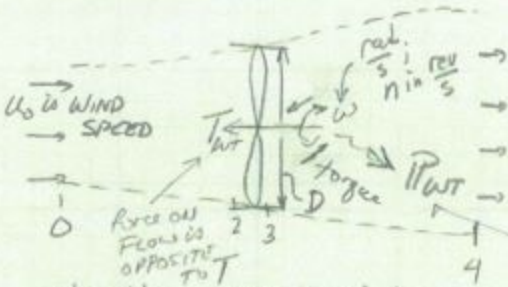

$\mathcal{P}_{WT}$ is $-\mathcal{P}$, ie, + OUT

$$\mathcal{P}_{WIND} \equiv \rho A_p U_0 \cdot \frac{U_0^2}{2} = \rho A_p \frac{U_0^3}{2}$$

↑ power available within the free-flowing wind in an area equal to rotor swept area A_p

objective: convert wind energy to brake power output

$$-T = T_{WT} = \rho A_p \left(\frac{U_0^2 - U_4^2}{2}\right) = (p_2 - p_3) A_p$$ thrust reaction on rotor disk (bending moment on tower!)

$$\dot{m} = \rho A_p \left(\frac{U_4 + U_0}{2}\right)$$

$$-\mathcal{P} = \mathcal{P}_{WT} = \rho A_p \left(\frac{U_4 + U_0}{2}\right)\left(\frac{U_0^2 - U_4^2}{2}\right)$$ power production $\mathcal{P}_{WT}$ is +, $\mathcal{P}$ is −

$\div \mathcal{P}_{WT}$ by $\left(\frac{1}{2}\rho A_p U_0^3\right) = \mathcal{P}_{WIND}$:

$$\eta_{WT} \equiv \frac{\mathcal{P}_{WT}}{\mathcal{P}_{WIND}} = \frac{1}{2}\left(\frac{U_4}{U_0} + 1\right)\left[1 - \left(\frac{U_4}{U_0}\right)^2\right]$$ { wind turbine efficiency vs. U_4/U_0 } graph

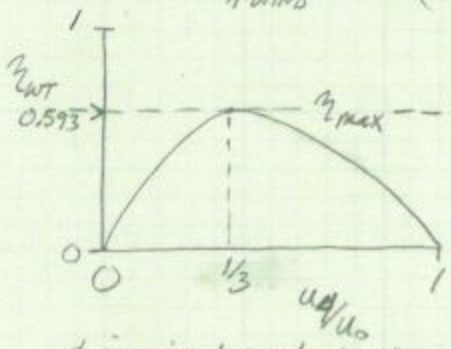

"Betz Limit" for bare rotor wind turbine efficiency = $\frac{16}{27}$ (= 59.3%) @ $\frac{U_4}{U_0} = \frac{1}{3}$

dimensional analysis gives... (Reynolds number)

$$\eta_{WT} = \text{fcn}\left[\text{SHAPE}, \frac{\omega(D/2)}{U_0}, \left(\frac{U_0 D}{\nu}\right)\right]$$

SHAPE: # blades, blade shape; $\frac{\omega(D/2)}{U_0}$: tip speed ratio (used instead of advance J)

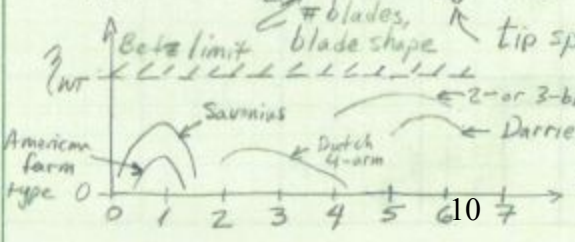

{ 2- or 3-bladed propeller type have become the most common }

APPLICATIONS OF *BASIC* ACTUATOR DISK THEORY – FAN (UNDUCTED + DUCTED)

ADT 4/5

WESTDYNE

IIIa. FAN

UNDUCTED ("bare rotor")

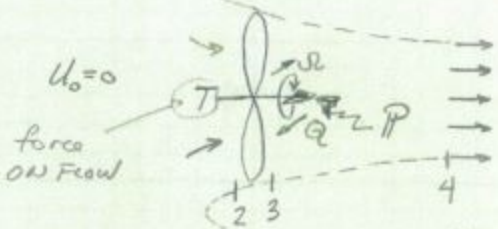

- Benefit = $\dot{m}$ (or U_4) $= \rho \dot{V}$
- Cost = $\mathcal{P}$, brake power input
- applications:
  - ✓ ventilation
  - ✓ freeze protection

objective: provide air flow using brake power input

$$T = T_{fan} = \rho A_p \frac{U_4^2}{2} = (P_3 - P_2) A_p$$

$$\dot{m}_{fan} = \rho A_p \frac{U_4}{2} \; ; \; \dot{V}_{fan} = \frac{\dot{m}_{fan}}{\rho} = A_p \frac{U_4}{2}$$

($\dot{V}$ is volume flowrate)

$$\mathcal{P} = \rho A_p \frac{U_4^3}{4} = \dot{m} \frac{U_4^2}{2} = \frac{2\dot{m}^3}{\rho^2 A_p^2} = \frac{2\rho \dot{V}^3}{A_p^2} = T \cdot \frac{U_4}{2} = \frac{T^2}{2\dot{m}}$$

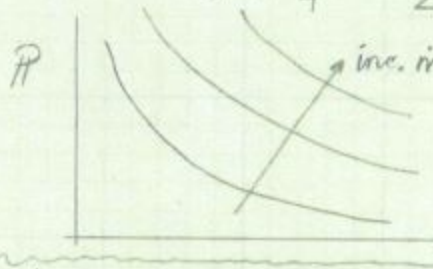

Fan drive power required decreases rapidly as A_p increases for given $\dot{m}$ – favors LARGE FAN

b. DUCTED FAN

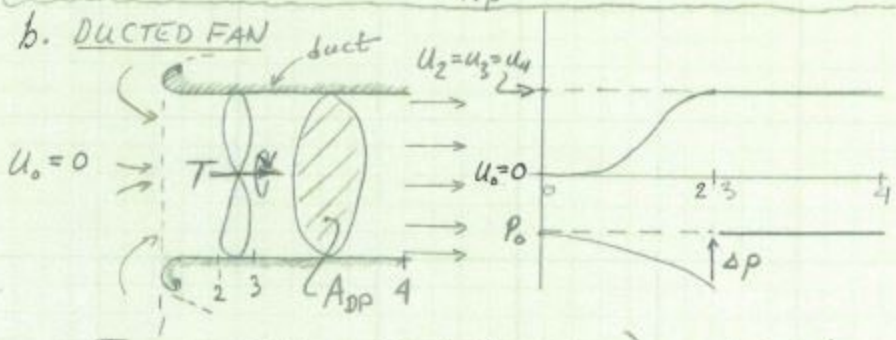

$$T_{\substack{ducted \\ fan}} = \dot{m} U_4 = \rho A_{DP} U_4^2 = (P_3 - P_2) A_{DP}$$

$$\dot{m}_{\substack{ducted \\ fan}} = \rho A_{DP} U_4$$

$$\mathcal{P}_{\substack{ducted \\ fan}} = \dot{m}\left(\frac{U_4^2}{2}\right) = \rho A_{DP} \frac{U_4^3}{2} = T \cdot \frac{U_4}{2} = \frac{T^2}{2\dot{m}}$$

∴ ducted fan achieves same result as a bare rotor of ½ the area given same U_4

"BASIC" ACTUATOR DISK THEORY for BARE ROTOR: CAPTURE, SLIPSTREAM, VELOCITY & PRESSURE — WESTPHAL — ADT 5/5

PROPELLER

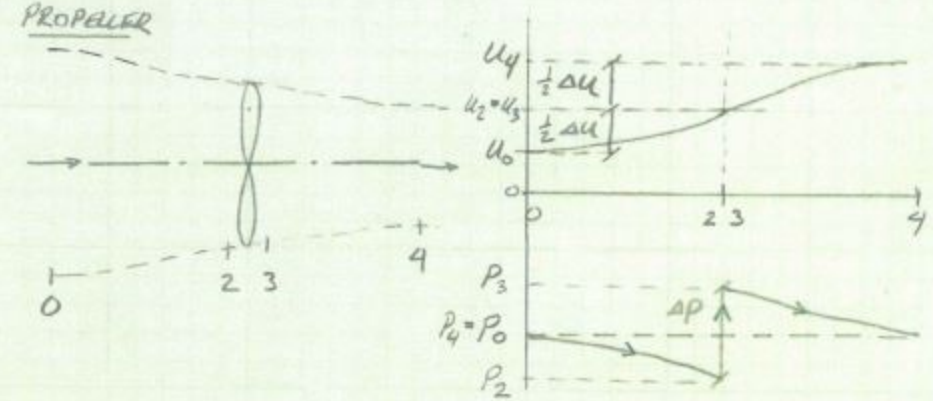

WIND TURBINE

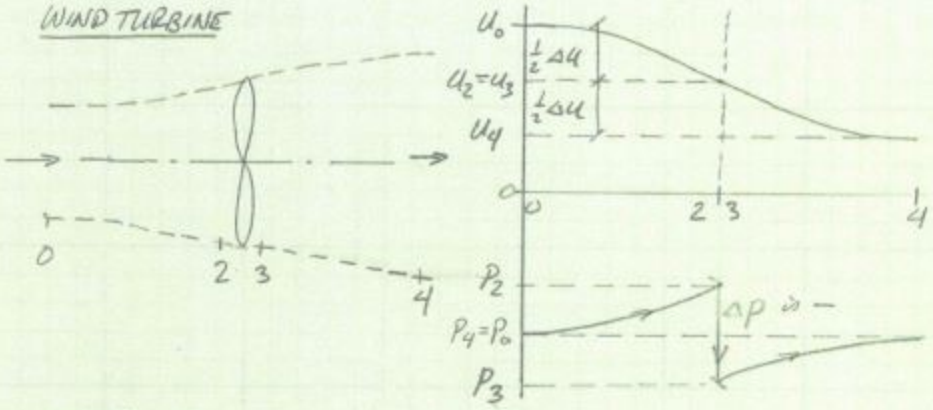

FAN (or STATIONARY PROP)

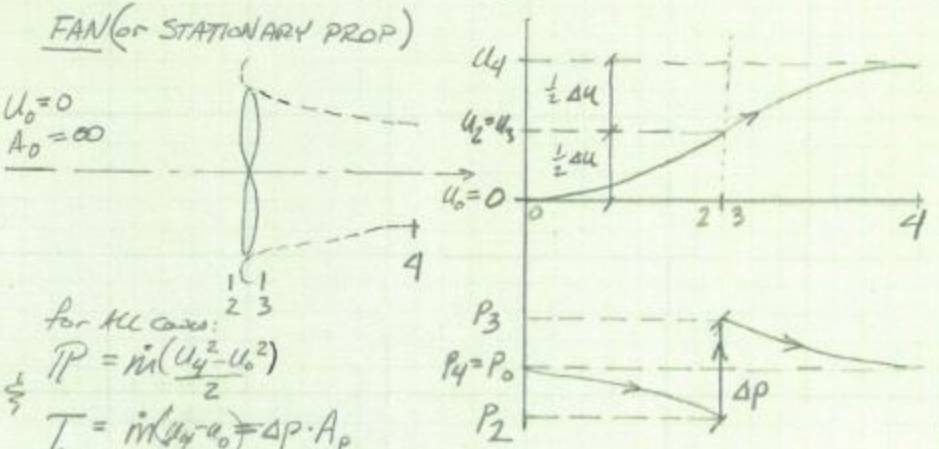

for ALL cases:

$$\mathcal{P} = \dot{m}\left(\frac{u_4^2 - u_0^2}{2}\right)$$

$$T = \dot{m}(u_4 - u_0) = \Delta p \cdot A_p$$

Thrust; "Δu"; rotor swept area

(for wind turbine, T, Δu, & Δp all NEGATIVE)

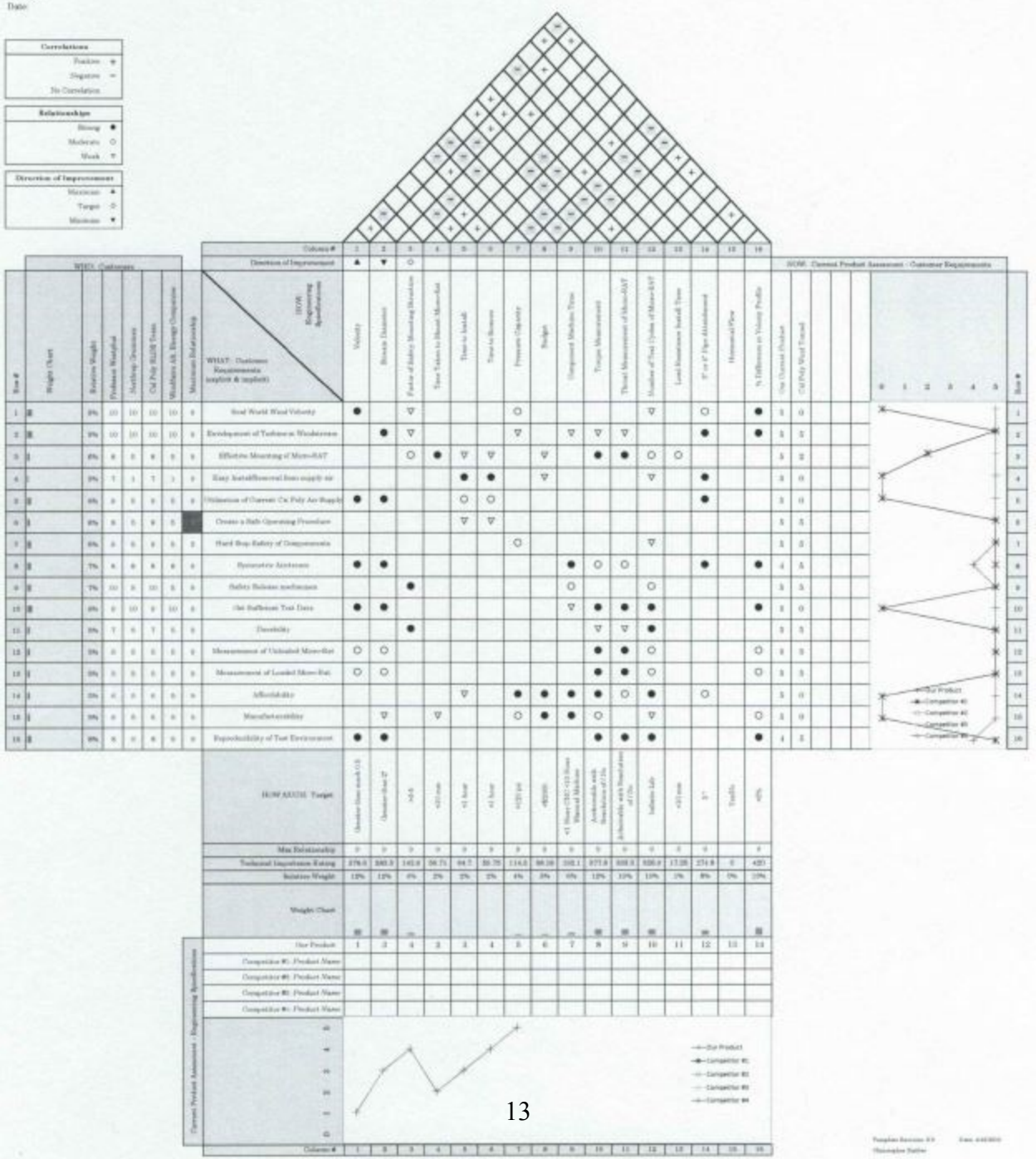
QFD: House of Quality
Project:
Revision:
Date:
Correlations
Positive +
Negative −
No Correlation
Relationships
Strong ●
Moderate ○
Weak ▽
Direction of Improvement
Maximize ▲
Target ◇
Minimize ▼
WHATs: Customer Requirements
HOW: Engineering Specifications
WHAT: Customer Requirements (explicit & implicit)
Row #
Weight Chart
Relative Weight
Preference Weighted
Marketing Questions
Old Poly HAM Tests
Modified Alt. Energy Comparison
Maximum Relationship
Velocity
Rotation Diameter
Factor of Safety Mounting Hardware
Time Taken to Mount Motor/Set
Time to Install
Time to Remove
Pressure Capacity
Weight
Computed Machine Time
Torque Measurement
Thrust Measurement of Motor/BAT
Number of Test Cycles of Motor/BAT
Load Maximum Install Time
1" or 4" Pipe Attachment
Horizontal Flow
% Difference on Volume Profile
Our Current Product
Old Poly Wind Tunnel
HOW: Current Product Assessment - Customer Requirements
Real World Wind Velocity
Development of Turbine in Weatherstem
Effective Mounting of Micro-BAT
Easy Install/Removal from supply air
Utilization of Current On Poly Air Supply
Create a Safe Operating Procedure
Hand Stop Safety of Components
Innovative Assistance
Safety Solution mechanism
Get Sufficient Test Data
Durability
Measurement of Unloaded Motor/Set
Measurement of Loaded Motor/Set
Affordability
Manufacturability
Reproducibility of Test Environment
HOW ASSESS: Target
Max Relationship
Technical Importance Rating
Relative Weight
Weight Chart
Our Product
Competitor #1: Product Name
Competitor #2: Product Name
Competitor #3: Product Name
Competitor #4: Product Name
Current Product Assessment - Engineering Specifications
Our Product
Competitor #1
Competitor #2
Competitor #3
Competitor #4
Column #

Estimate of Torque on Micro-RAT turbine — Isaac Thomas

Axial flow turbine

approximate dimensions:

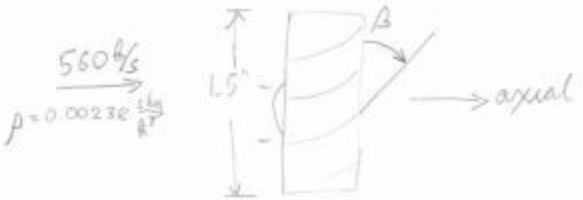

mean radius $r \approx 0.5"$

let $\omega = 20\,000$ rpm - approximate value

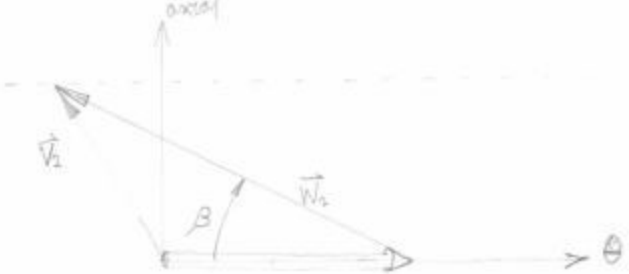

$U = r\omega$

$$\tan\beta = \frac{V_{2\,axial}}{-V_{2\theta} + U}$$

$$V_{1\theta} = U - \frac{V_{2\,axial}}{\tan\beta}$$

$$U = r\omega = \left(\frac{.5}{12}\,ft\right)\left(20000\,\frac{rev}{min}\cdot\frac{2\pi\,rad}{rev}\cdot\frac{min}{60\,s}\right) = 87.3\,ft/s$$

$T_{shaft} = \rho\, Q\,(r\,V_{2\theta})$ (assuming no swirl on inlet)

$$T_{shaft} = (0.00238\,slug/ft^3)(560\,ft/s)\left(\frac{\pi}{4}(1.5^2 - .5^2)\,in^2\cdot\frac{1}{12^2}\,ft^2/in^2\right)\left(\frac{.5}{12}\,ft\right)V_{\theta_2}$$

$$T_{shaft} = 0.0006058\,V_{\theta_2}$$

$$V_{2\theta} = 87.3\,ft/s - 560\,ft/s\cdot\frac{1}{\tan\beta}$$

$$T_{shaft} = 0.0006058\,\left(87.3\,ft/s - \frac{560\,ft/s}{\tan\beta}\right)\cdot\frac{12\,in}{ft}$$

β (deg)	T (in-lbf)
20	10.55
30	6.42
40	4.22
50	2.78
60	1.71
70	0.85
80	0.083

- Approximate range of torque required to be tested as a function of blade angle at a fixed RPM and flow rate

Isaac Thomas

Approximate drag on Micro-RAT

let $C_d = 1$

$A = \frac{\pi}{4}(1.5in)^2 = 1.77in^2 = 0.0123ft^2$

$\rho_{air} = 0.00238 slug/ft^3$

$V = 560 ft/s$ (Mach 0.5)

$$C_d = \frac{D}{\rho A \frac{V^2}{2}}$$

$$D = C_d \rho A \frac{V^2}{2}$$

$$D = (1)(0.00238 \frac{slug}{ft^3})(\frac{lbf\,s^2}{slug\,ft})(0.0123ft^2)(\frac{560 ft/s)^2}{2}$$

$\boxed{D = 1.6 lbf}$ at Mach 0.5

② Mach 0.75:

$\boxed{D = 10 lbf}$

Flex Bearing Loads and Drag force Calibration Curve.

Isaac Thomas

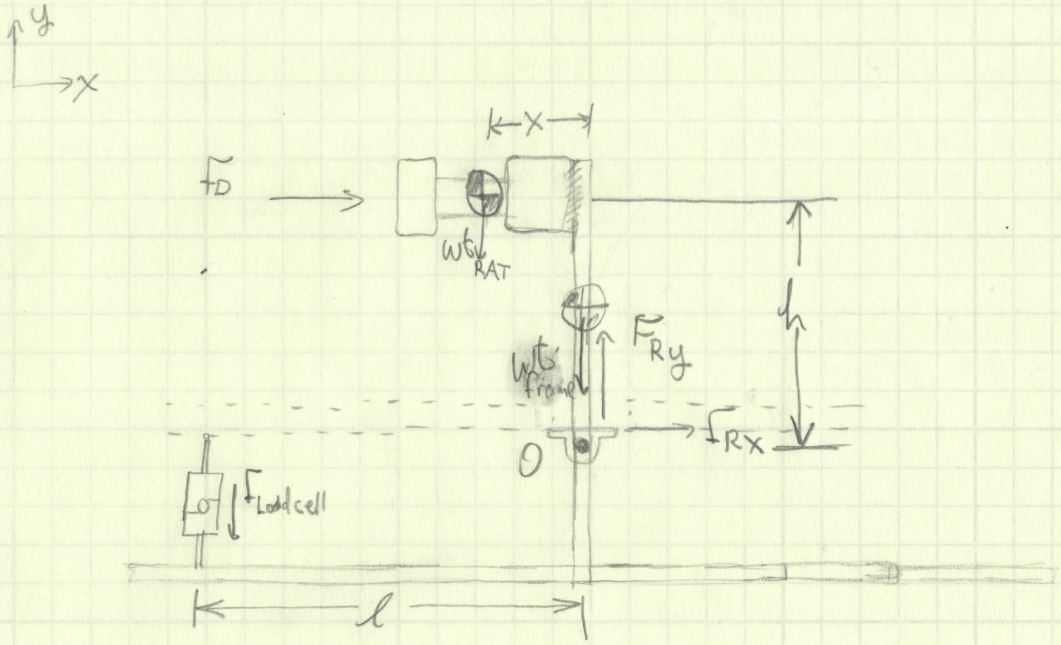

Sum forces:

$$\Sigma F_y = 0 = F_{Ry} - F_{load\,cell} - wt_{frame} + wt_{RAT}$$

$$F_{Ry} = F_{load\,cell} + wt_{frame} + wt_{RAT}$$

$$\Sigma F_x = 0 = F_{RX} + F_D$$

$$F_{RX} = -F_D$$

Moments about O:

$$\circlearrowleft \Sigma M_O = -F_D \cdot h + F_{L.C.} \cdot l + wt_{RAT} \cdot X = 0$$

$$F_{LC} = \left(-wt_{RAT} X + F_D h\right) \frac{1}{l}$$

$$F_{LC} = F_D \cdot \frac{h}{l} - \frac{wt_{RAT} X}{l}$$

slope — offset → easily measure statically and calibrate out

$$F_D = F_{lc} \cdot \frac{l}{h} + wt_{RAT} \frac{X}{h}$$

when $F_{lc} = 0$,

$$F_D = wt_{rat} \frac{X}{h}$$

Once $wt_{RAT} \cdot X$ is calibrated out. drag force can calculated as follows:

$$F_D = F_{lc} \cdot \underbrace{\frac{l}{h}}_{\text{gain}}$$

O - point crossover occurs when $F_{LC} = 0$:

$$F_D = \frac{wt_{RAT} \cdot X}{h}$$

Bolt Stress in Flanges

8 bolt flange, 4" pipe

Bolt size: 5/8-11, GRADE 5

Pipe ID: 4.026"

MAX PRESSURE: 120 PSI

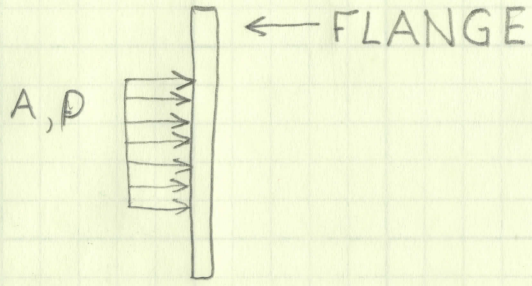

$F = PA$

$F = (120 \frac{lbf}{in^2}) \times \frac{\pi}{4}(4.026\,in)^2)$

$F = 1530\,lbf$, TOTAL FORCE ON BOLTS

FORCE ON EACH BOLT

$F_{BOLT} = \frac{1530\,lbf}{8}$

$F_{BOLT} = 191\,lbf$

Stress: MINOR DIAMETR: 0.5119 in, $A = 0.2260\,in^2$

$\sigma_{BOLT} = \frac{191\,lbf}{0.2260\,in^2} = 845\,psi$

$FOS = \frac{120e3\,psi}{845\,psi}$

FOS = 142

Buckling Estimation

Simplification: all the weight on two uprights

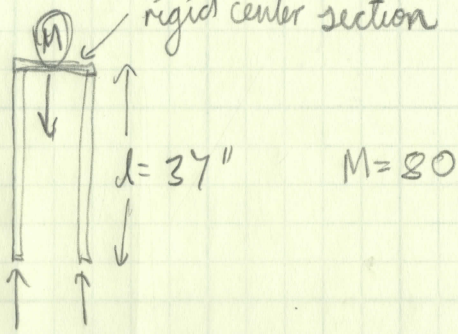

CROSS-SECTION

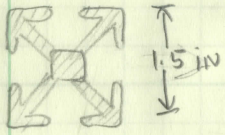

$I = 0.2691 in^4$

$A = 1.26 in^2$

Compressive Stress:

$$\sigma = \frac{40lb}{1.26in^2} = 32psi \quad FOS = \frac{39e3psi}{32psi} = \boxed{1200}$$

CRITICAL LOAD FOR BUCKLING

$$F = \frac{n\pi^2 EI}{L^2}, \Rightarrow \text{worst case: } n=1, \text{ pinned-pinned}$$

for 6105-T5, $E = 10e6 psi$

$$F = \frac{(1)(\pi)^2(10e6 psi)(0.2691 in^4)}{(37in)^2}$$

$$\underline{F = 19400 lbf}$$

$$FOS = \frac{19400}{40} = \boxed{485}$$

$P = 120$ psi

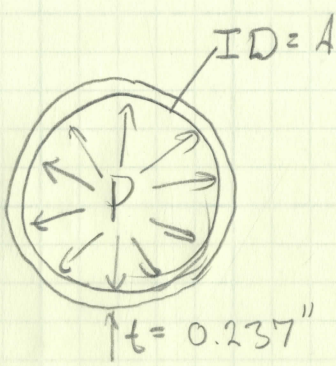

Hoop:

$\sigma_h = pd/2t$

$\sigma_h = \frac{(120\text{psi})(4.026\text{in})}{(2)(0.237\text{in})}$

$\sigma_h = 1019$ psi] FOS $= \frac{73200}{1019} = 72$]

Longitudinal

$\sigma_l = pd/4t = \frac{1}{2}\sigma_h$

$\sigma_l = 510$ psi] , FOS = 144]

Minimum tipping force.

MASS of Nozzle assembly: 66lb + 11lb = 77lb ≈ 80lb

mass of frame: 80lb

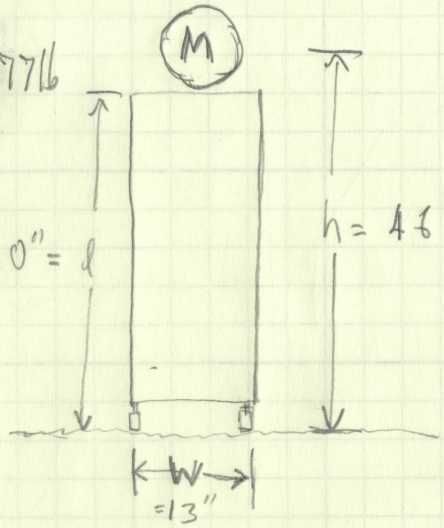

FBD

when $R_R = 0$, it will tip

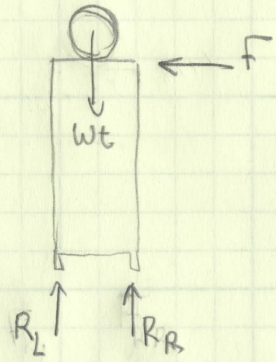

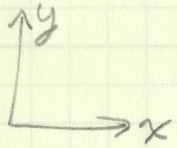

Sum moments:

$$\circlearrowleft \Sigma M_{R_L} = -W_t \cdot \frac{W}{2} + F \cdot l = 0$$

$$F = \frac{W_t W}{2 l}$$

$$F = \frac{(160\text{lb})(13'')}{(2 \cdot 40'')}$$

$$\boxed{F = 26\text{lb}}$$ ← stone nozzle at bottom of cart when not in use and during transportation

TORQUE ON MICRORAT

ISAAC THOMAS

AXIAL FLOW TURBINE

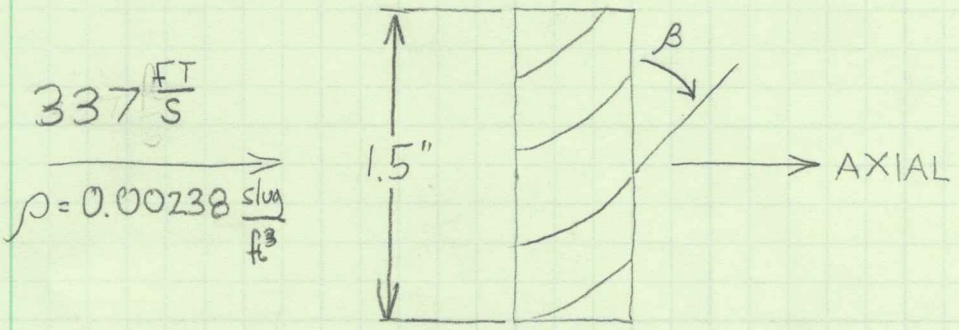

MEAN RADIUS: $r \approx 0.5$ IN

LET $\omega \approx 20000$ RPM (ESTIMATE)

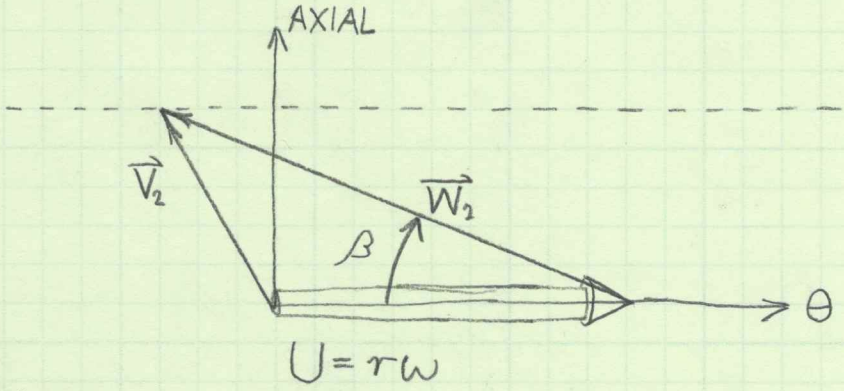

$$\tan\beta = \frac{V_{2\,axial}}{-V_{2\theta} + U}$$

$$U = r\omega = \left(\frac{.5}{12}\,ft\right)\left(20000\frac{rev}{min}\cdot\frac{2\pi\,rad}{rev}\cdot\frac{min}{60s}\right) = 87.3\,ft/s$$

$$T_{SHAFT} = \rho Q (r V_{2\theta}) \quad \text{(NO SWIRL INLET)}$$

$$T_{SHAFT} = \left(0.00238\frac{slug}{ft^3}\right)\left(337\frac{ft}{s}\right)\left(\frac{\pi}{4}(1.5^2 - .5^2)\frac{1}{12^2}ft^2\right)\left(\frac{5}{12}ft\right)V_{\theta 2}$$

$$T_{SHAFT} = 0.0003646\,V_{\theta 2}$$

$$V_{\theta 2} = 87.3\,ft/s - 337\,ft/s\,\frac{1}{\tan\beta}$$

$$T_{SHAFT} = 0.0003646\left(87.3\,ft/s - \frac{337\,ft/s}{\tan\beta}\right)\cdot\frac{12\,in}{ft}$$

for $\beta = 35°$:

$$T_{SHAFT} = -1.72\,in\text{-}lbf = -27.6\,oz\text{-}in$$

U.S. Patent Feb. 20, 1996 Sheet 1 of 4 5,492,313

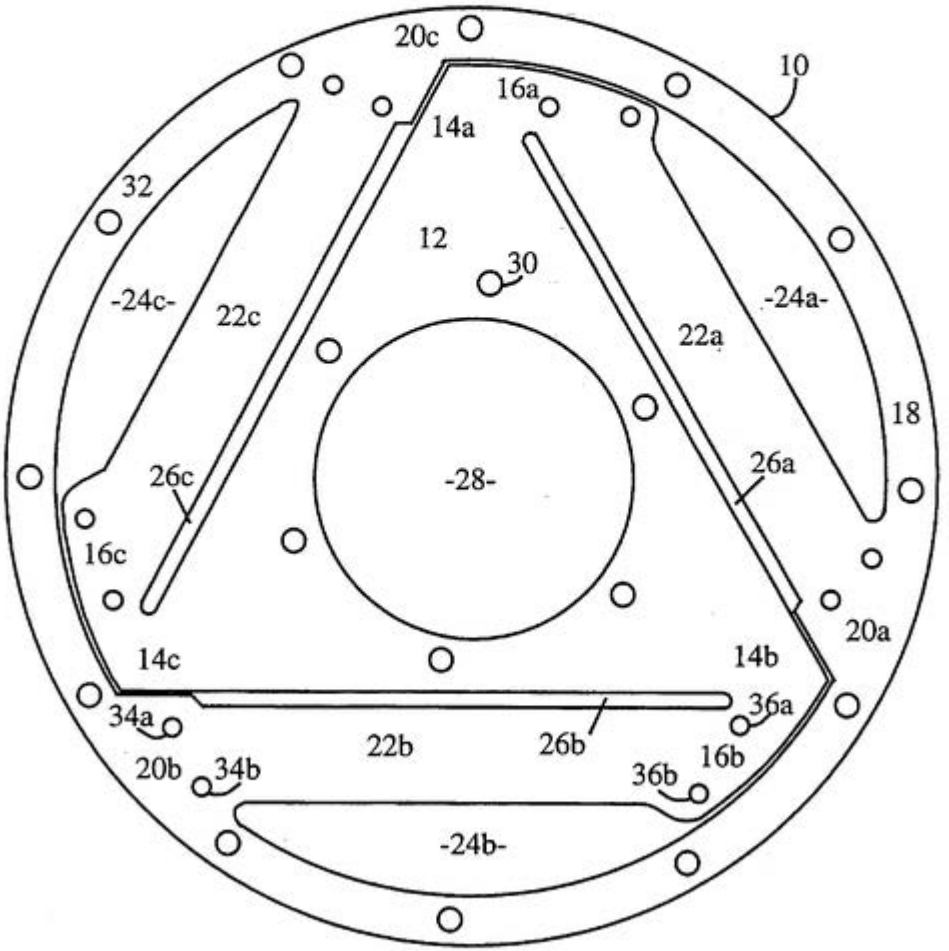

FIG. 1

Pugh Matrix

RAT Drag Measurement

Concept / Criteria	Cantilever	Linear slide	90° Lever arm with a single pivot	Cantilever arm with a four bar linkage	Cantilever arm with an adjustable load cell location
	1	2	3	4	6
Effective Mounting	D	S	S	S	S
Safe operating procedure		S	S	S	S
Retrieves sufficient test data	A	-	+	+	+
Measurement of unloaded vs. loaded		S	S	S	S
Durability	T	-	-	-	-
Affordability		-	-	-	-
Manufacturability	U	-	-	-	-
Reproducability of test environment	M	-	+	+	+
POSITIVE	N/A	0	2	2	2
NEGATIVE	N/A	5	3	3	3
NUETRAL	N/A	3	3	3	3

Pugh Matrix

RAT Torque Measurement

Concept / Criteria	Cantilever	Linear slide	90° Lever arm with a single pivot	Cantilever arm with a four bar linkage	Cantilever arm with an adjustable load cell location
	1	2	3	4	6
Effective Mounting	D	S	S	S	S
Safe operating procedure		S	S	S	S
Retrieves sufficient test data	A	-	+	+	+
Measurement of unloaded vs. loaded		S	S	S	S
Durability	T	-	S	-	S
Affordability		-	-	-	-
Manufacturability	U	-	-	-	-
Reproducability of test environment	M	-	S	S	S
POSITIVE	N/A	0	2	2	2
NEGATIVE	N/A	5	3	3	3
NUETRAL	N/A	3	3	3	3

Pugh Matrix

Straightener

Concept / Criteria	Honeycomb	Wire mesh	Perforated metel sheet	Combination of honeycomb and wire mesh	Small tube	Vortex generator
	1	2	3	4	5	6
Real world wind velocity	D	-	-	+	S	+
Envelopment of wind turbine in air stream		S	S	S	S	S
Utilization of Cal Poly air supply	A	S	S	S	S	S
Safe operating procedure		-	-	-	S	S
Hard stop safety		S	-	S	-	S
Symmetric air stream	T	-	-	S	S	+
Durability		+	+	+	S	+
Affordability	U	+	+	S	+	-
Manufacturability		+	+	S	+	-
Reproducability of test environment	M	-	-	+	-	+
POSITIVE	N/A	3	3	3	2	4
NEGATIVE	N/A	4	5	1	2	2
NUETRAL	N/A	3	2	6	6	4

Pugh Matrix

Nozzle

Concept / Criteria	Threaded reducer	Machined with bolted flange	Machined with quick clamp flange	PVC	Composite	3-D print and cast
	1	2	3	4	5	6
Real world wind velocity	D	S	S	S	S	S
Envelopment of wind turbine in air stream		S	S	S	S	S
Utilization of Cal Poly air supply	A	S	S	-	S	S
Safe operating procedure		S	-	-	-	-
Hard stop safety		S	-	-	-	-
Symmetric air stream	T	S	S	S	S	S
Durability		S	-	-	-	-
Affordability	U	-	-	+	-	-
Manufacturability		-	-	+	+	-
Reproducability of test environment	M	S	S	S	S	S
POSITIVE	N/A	0	0	2	1	0
NEGATIVE	N/A	2	5	4	4	5
NUETRAL	N/A	8	5	4	5	5

SENIOR PROJECT CONCEPT DESIGN REVIEW HAZARD IDENTIFICATION CHECKLIST

Y	N	
☐	☑	Will any part of the design create hazardous revolving, reciprocating, shearing, punching, pressing, squeezing, drawing, cutting, rolling, mixing, or similar actions, including pinch points and shear points?
☑	☐	Can any part of the design undergo high accelerations/decelerations?
☐	☑	Will the system have any large moving masses or large forces?
☐	☑	Will the system produce a projectile?
☐	☑	Is it possible for the system to fall under gravity creating injury?
☐	☑	Will a user be exposed to overhanging weights as part of the design?
☐	☑	Will the system have any sharp edges?
☐	☑	Will the system have any ungrounded electrical systems?
☐	☑	Will there be any large batteries or electrical voltage in the system above 40 V (either AC or DC)?
☐	☑	Will there be any stored mechanical energy in the system such as flywheels, hanging weights or pressurized fluids?
☐	☑	Will the system produce high heat (>120°F) at any location?
☐	☑	Will there be any explosive or flammable liquids, gases, or dust as part of the system?
☐	☑	Will the user of the design be required to exert any abnormal effort or physical posture during the use of the design?
☐	☑	Will there be any materials known to be hazardous to humans involved in either the design or the manufacturing of the design?
☑	☐	Might the system generate high levels of noise?
☐	☑	Is the system easy to use unsafely?
☐	☑	Will the system be used in extreme environmental conditions such as fog, humidity, cold, high temperatures, etc…?
☐	☑	Are there any other potential hazards not listed above? If yes, please explain below.

REVISIONS				
ZONE	REV.	DESCRIPTION	APPROVED	DATE
	A	INITIAL RELEASE	-	-

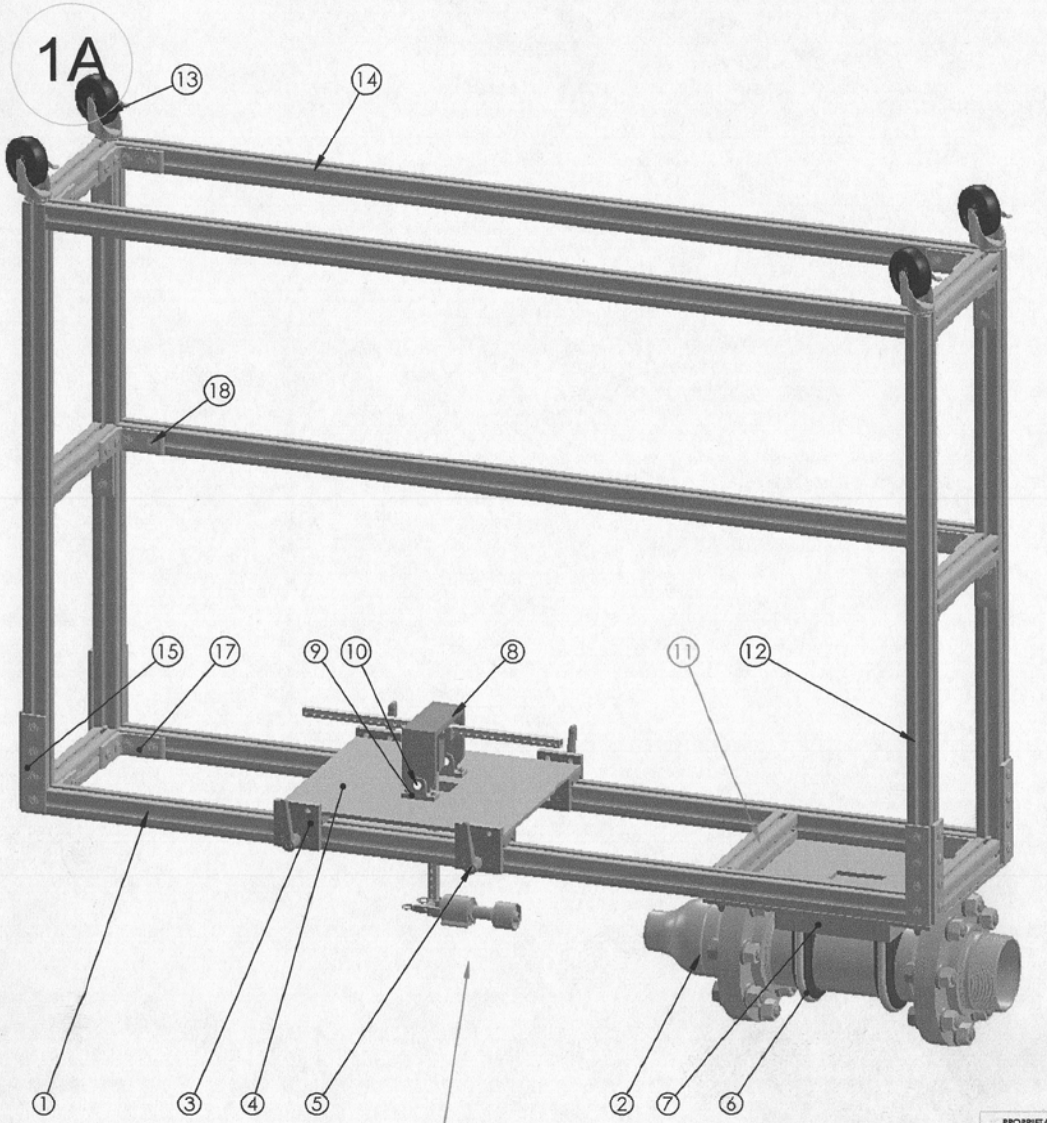

ITEM NO.	PART NUMBER	DESCRIPTION	QTY.
1	t-slot 56'"	56" TOP EXTRUDED ALUMINUM RAILS	2
2	nozzle assembly	4" NPT PIPE/FITTINGS	1
3	60585K33	1.5" ALUMINUM EXTRUSION LINEAR BEARING MOUNT	4
4	sliding surface	C-ARM MOUNTING PLATE	2
5	60585K32	HANDLE CLAMP FOR LINEAR BEARING	4
6	3176T41	4" NPT PIPE U-BOLT CLAMP WITH DAMPER	2
7	nozzle block	NOZZLE BLOCK SPACER MOUNT	1
8	Micro-Rat Mounting Assembly	flexure bearing pivot	1
9	Bearing Block	HOUSING FOR FLEXURE BEARING	2
10	gd-10	FLEXURE BEARING	2
11	t-slot 10	SMALL ALUMINUM EXTRUSION BRACE	7
12	t-slot leg	BOTTOM LENGTH ALUMINUM EXTRUSION	4
13	2834T34	CASTER	4
14	t-slot bottom	BOTTOM LENGTH ALUMINUM EXTRUSION	3
15	47065T42	ALUMINUM LEG BRACE FOR CORNER	8
17	47065T51	ANGLE BRACKET	18
18	47065T97	ANGLE BRACKET FASTENER	104

UNLESS OTHERWISE SPECIFIED:
DIMENSIONS ARE IN INCHES
TOLERANCES:
ANGULAR: ±.5°
ONE PLACE DECIMAL ± .03
TWO PLACE DECIMAL ± .01
THREE PLACE DECIMAL ± .005
CUSTOMER: RUSSEL WESTPHAL
USED ON: FINAL ASSEMBLY
MATERIAL: MIXED
FINISH:
DO NOT SCALE DRAWING

	NAME	DATE
DRAWN	-	-
CHECKED		
ENG APPR.		
MFG APPR.		
COMMENTS:		

TITLE: **FINAL ASSEMBLY**

SIZE	DWG. NO.	REV
B	A	A

SCALE: 1:12 SHEET 1 OF 2

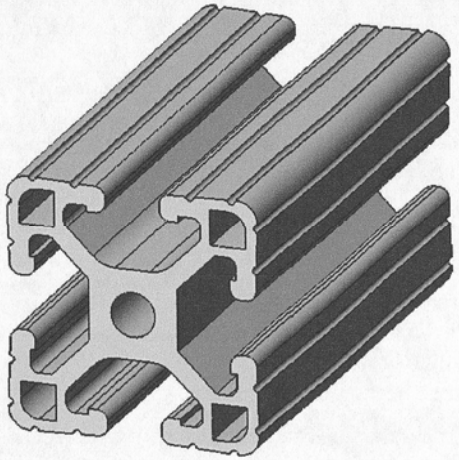

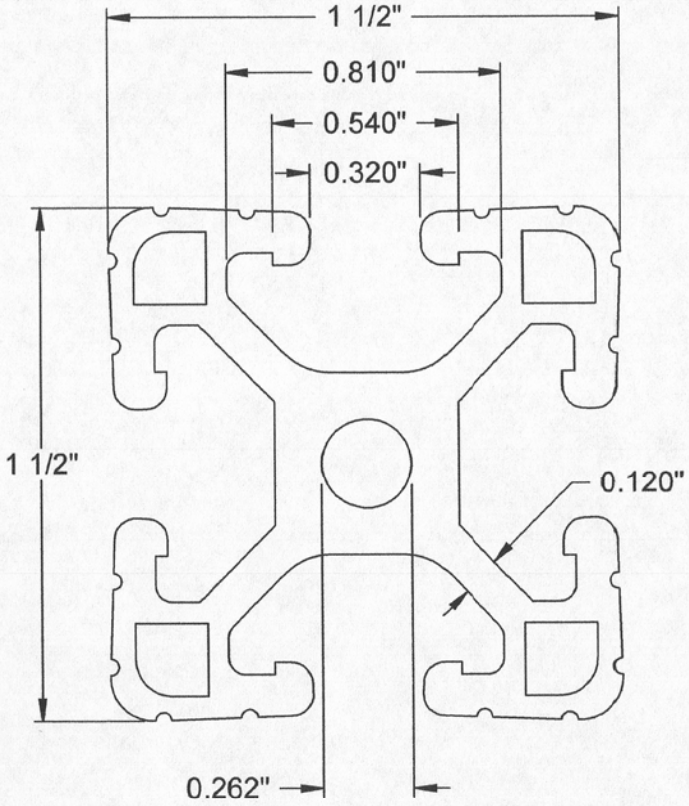

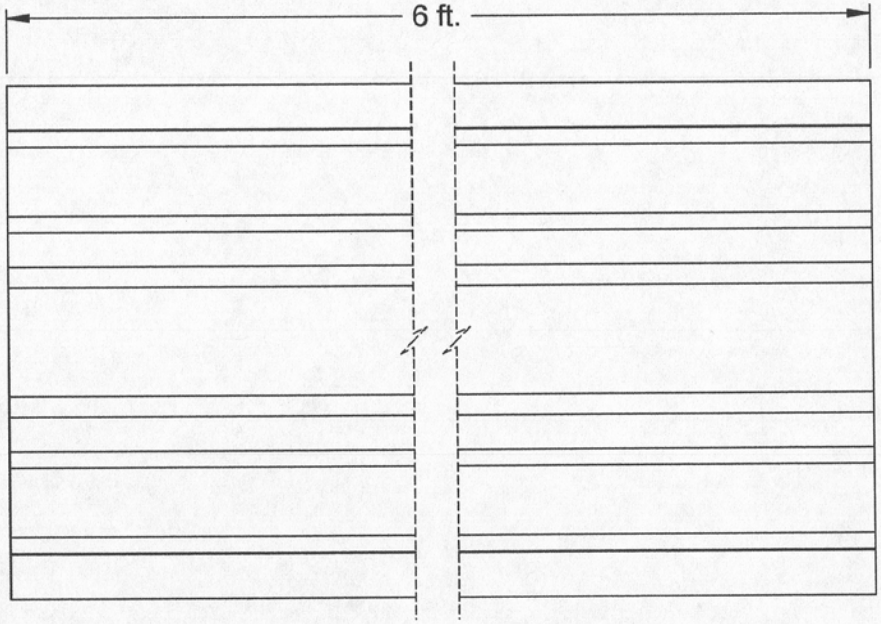

ITEM 1

McMASTER-CARR® CAD

http://www.mcmaster.com

PART NUMBER 47065T148

Aluminum Four-Slot Single Extrusion

1A

REVISIONS				
ZONE	REV.	DESCRIPTION	APPROVED	DATE
	A	INITIAL RELEASE	-	-

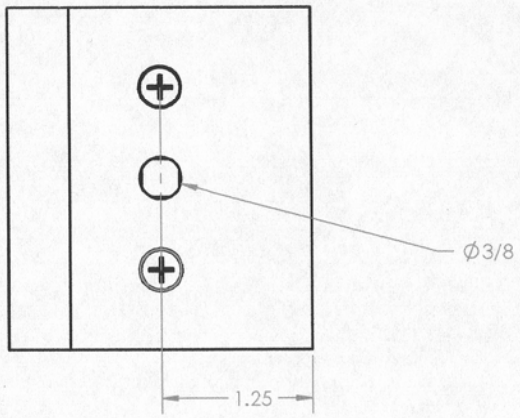

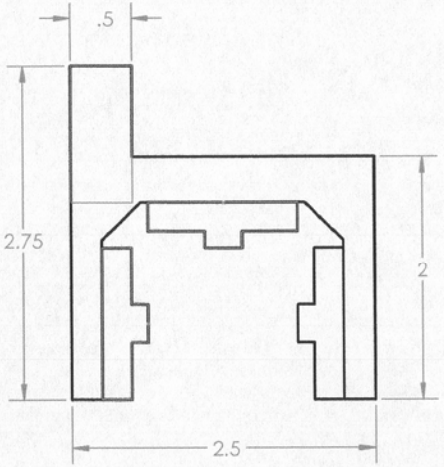

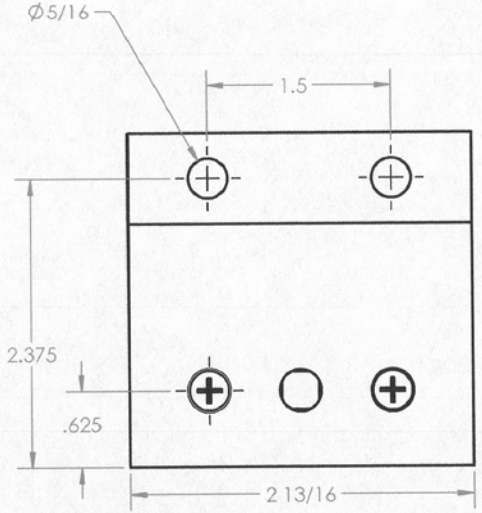

BENCHMARK MANUFACTURING
RELEASE FOR PRODUCTION

PROD LEAD_____ DATE_____

ENGR LEAD_____ DATE_____

PROPRIETARY AND CONFIDENTIAL

THE INFORMATION CONTAINED IN THIS DRAWING IS THE SOLE PROPERTY OF BENCHMARK ELECTRONICS. ANY REPRODUCTION IN PART OR AS A WHOLE WITHOUT THE WRITTEN PERMISSION OF BENCHMARK ELECTRONICS IS PROHIBITED.

UNLESS OTHERWISE SPECIFIED:
DIMENSIONS ARE IN INCHES
TOLERANCES:
ANGULAR: ±.5°
ONE PLACE DECIMAL ± .03
TWO PLACE DECIMAL ± .01
THREE PLACE DECIMAL ± .005

CUSTOMER: RUSSEL WESTPHAL
USED ON: MICRO-RAT MOUNTING
MATERIAL: 6061 ALUMINUM
FINISH:
DO NOT SCALE DRAWING

	NAME	DATE
DRAWN	-	-
CHECKED		
ENG APPR.		
MFG APPR.		

COMMENTS: GLIDEWAYS MADE OF TEFLON

ITEM 3

TITLE:
LINEAR BEARING CARRIAGE FOR T-SLOTTED FRAMING

SIZE	DWG. NO.	REV
B	60585K33	A

SCALE: 1:1 SHEET 1 OF 2

REVISIONS				
ZONE	REV.	DESCRIPTION	APPROVED	DATE
	A	INITIAL RELEASE	-	-

1A

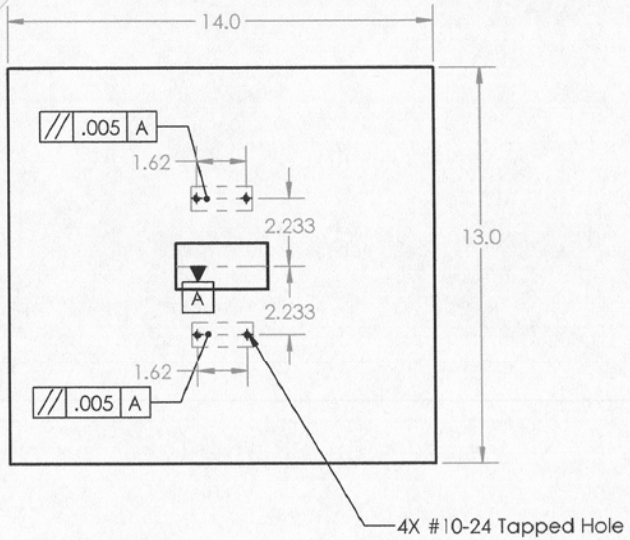

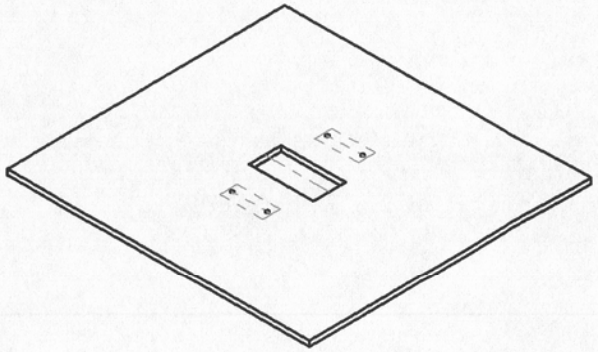

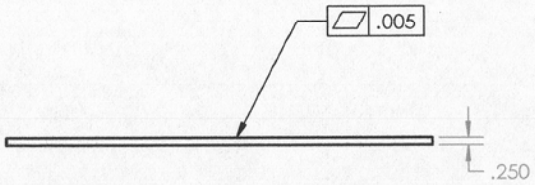

		NAME	DATE
UNLESS OTHERWISE SPECIFIED:	DRAWN	-	-
DIMENSIONS ARE IN INCHES TOLERANCES: ANGULAR: ±.5° ONE PLACE DECIMAL ±.03 TWO PLACE DECIMAL ±.01 THREE PLACE DECIMAL ±.005	CHECKED		
	ENG APPR.		
	MFG APPR.		
CUSTOMER: RUSSEL WESTPHAL	COMMENTS:		
USED ON: MICRO-RAT MOUNTING			
MATERIAL: 6061 ALUMINUM			
FINISH			
DO NOT SCALE DRAWING			

ITEM 4

TITLE:
C-ARM MOUNTING PLATE

SIZE	DWG. NO.	REV
B	1	A

SCALE: 1:4 SHEET 1 OF 2

1A

REVISIONS				
ZONE	REV.	DESCRIPTION	APPROVED	DATE
	A	INITIAL RELEASE	-	-

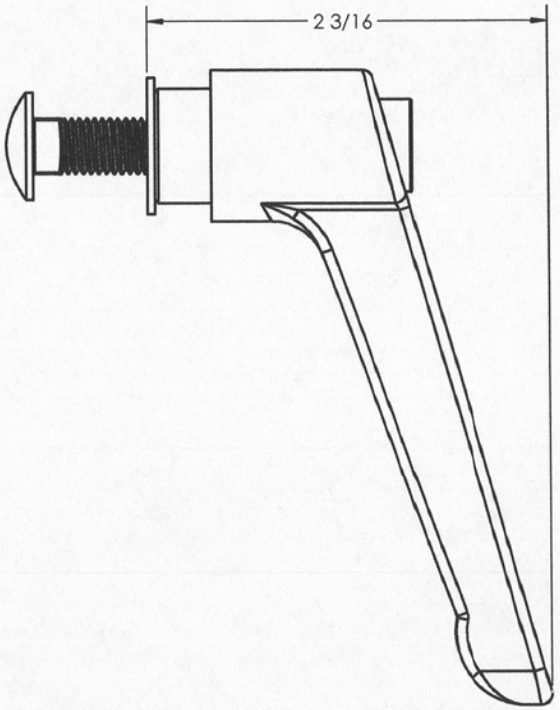

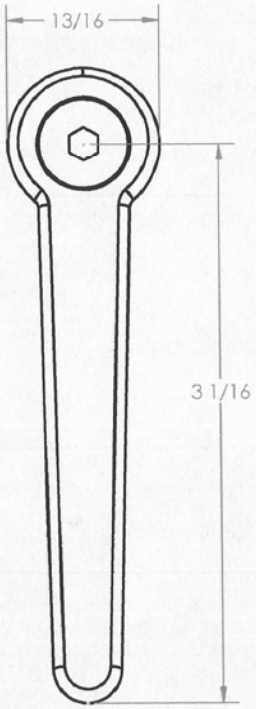

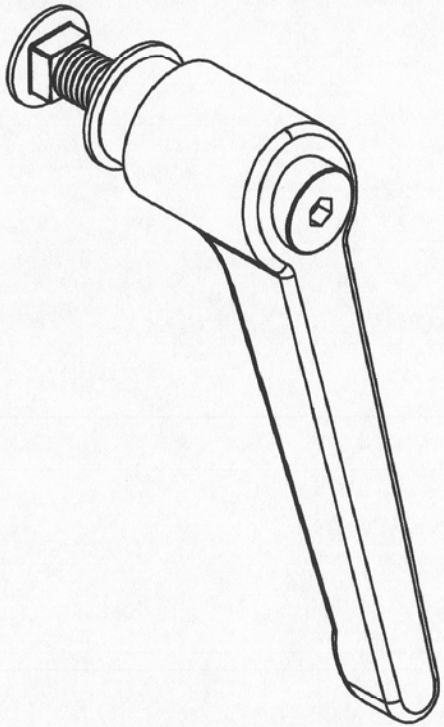

BENCHMARK MANUFACTURING
RELEASE FOR PRODUCTION

PROD LEAD_____ DATE_____

ENGR LEAD_____ DATE_____

UNLESS OTHERWISE SPECIFIED:
DIMENSIONS ARE IN INCHES
TOLERANCES:
ANGULAR: ±.5°
ONE PLACE DECIMAL ± .03
TWO PLACE DECIMAL ± .01
THREE PLACE DECIMAL ± .005

CUSTOMER: RUSSEL WESTPHAL
USED ON: MICRO-RAT MOUNTING
MATERIAL: INJECTION PLASTIC
FINISH:
DO NOT SCALE DRAWING

	NAME	DATE
DRAWN	-	-
CHECKED		
ENG APPR.		
MFG APPR.		
COMMENTS:		

ITEM 5

TITLE:
HANDLE CLAMP FOR
LINEAR BEARINGLINE
AR BEARING HAND
BRAKE FOR T-SLOTTED
FRAMING

SIZE	DWG. NO.	REV
B	[illegible]	A

SCALE: 1:1 SHEET 1 OF 2

1A

REVISIONS				
ZONE	REV.	DESCRIPTION	APPROVED	DATE
	A	INITIAL RELEASE	-	-

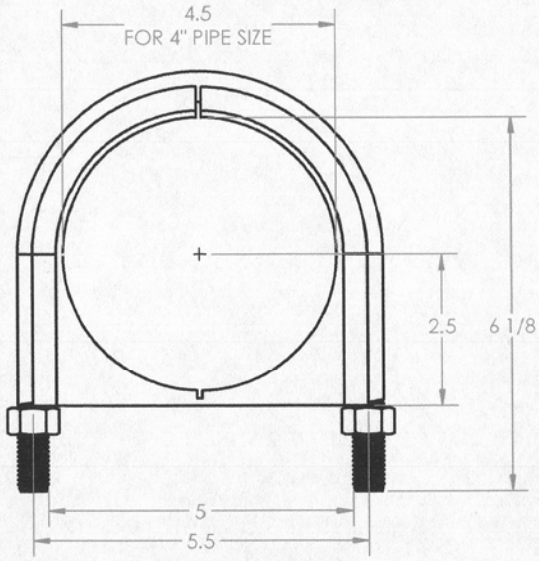

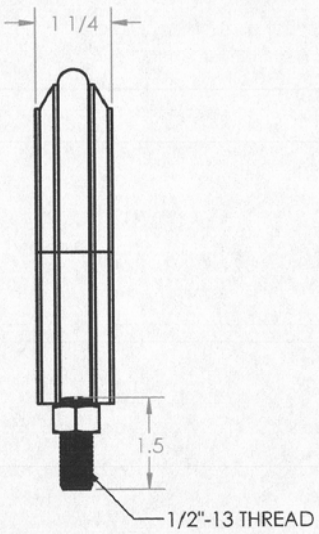

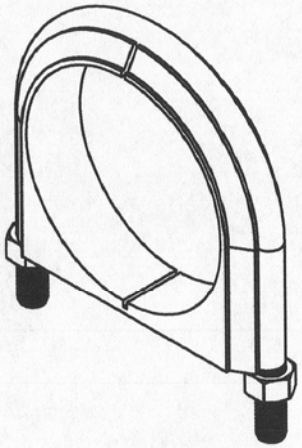

BENCHMARK MANUFACTURING
RELEASE FOR PRODUCTION

PROD LEAD_____ DATE_____

ENGR LEAD_____ DATE_____

UNLESS OTHERWISE SPECIFIED:
DIMENSIONS ARE IN INCHES
TOLERANCES:
ANGULAR: ±.5°
ONE PLACE DECIMAL ±.03
TWO PLACE DECIMAL ±.01
THREE PLACE DECIMAL ±.005

CUSTOMER: RUSSEL WESTPHAL
USED ON: FLOW STRAIGHTENER
MATERIAL: ZINC-PLATED STEEL
FINISH:
DO NOT SCALE DRAWING

	NAME	DATE
DRAWN	-	-
CHECKED		
ENG APPR.		
MFG APPR.		
COMMENTS:		

ITEM 6

TITLE:
ZINC-PLATED STEEL VIBRATION DAMPING U-BOLT

SIZE	DWG. NO.	REV
B	3176T41	A

SCALE: 1:2 SHEET 1 OF 2

REVISIONS				
ZONE	REV.	DESCRIPTION	APPROVED	DATE
	A	INITIAL RELEASE	-	-

1A

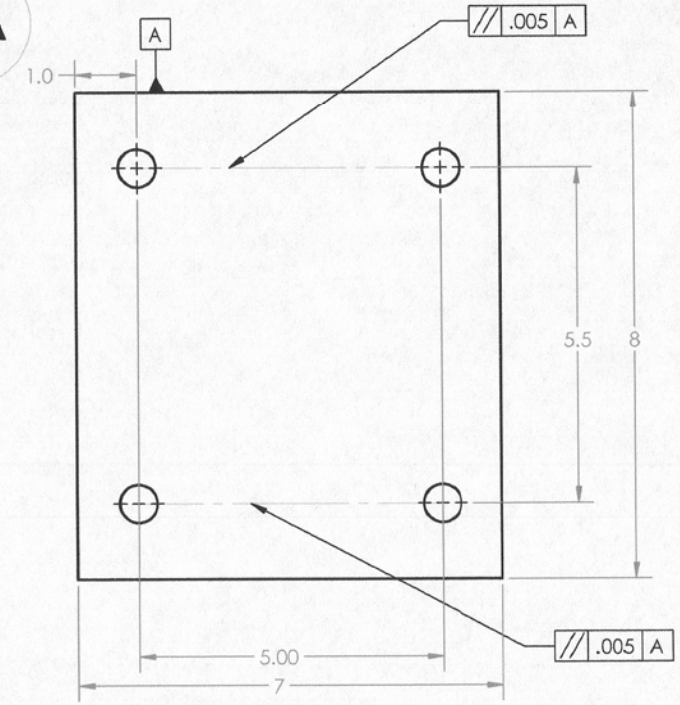

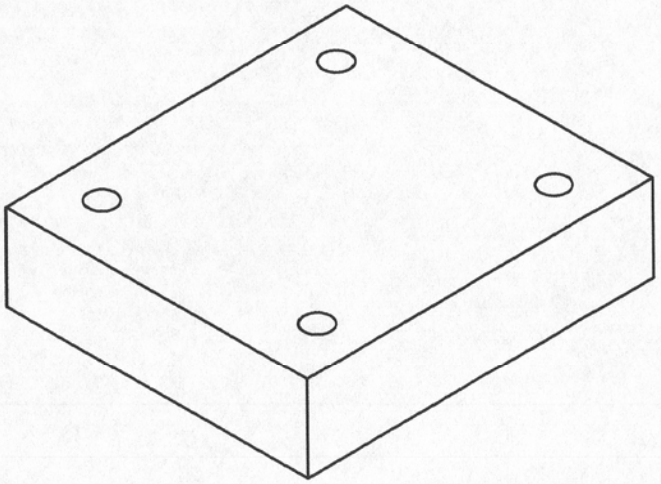

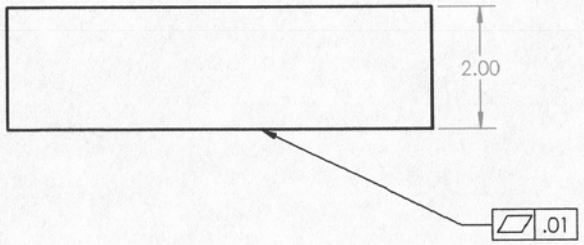

UNLESS OTHERWISE SPECIFIED:		NAME	DATE
DIMENSIONS ARE IN INCHES TOLERANCES: ANGULAR: ±.5° ONE PLACE DECIMAL ± .03 TWO PLACE DECIMAL ± .01 THREE PLACE DECIMAL ± .005	DRAWN	-	-
	CHECKED		
	ENG APPR.		
	MFG APPR.		
CUSTOMER: RUSSEL WESTPHAL	COMMENTS:		
USED ON: MICRO-RAT MOUNTING			
MATERIAL: 6061 ALUMINUM			
FINISH			
DO NOT SCALE DRAWING			

ITEM 7

TITLE:
NOZZLE BLOCK SPACER MOUNT

SIZE	DWG. NO.	REV
B	1	A

SCALE: 1:4 SHEET 1 OF 2

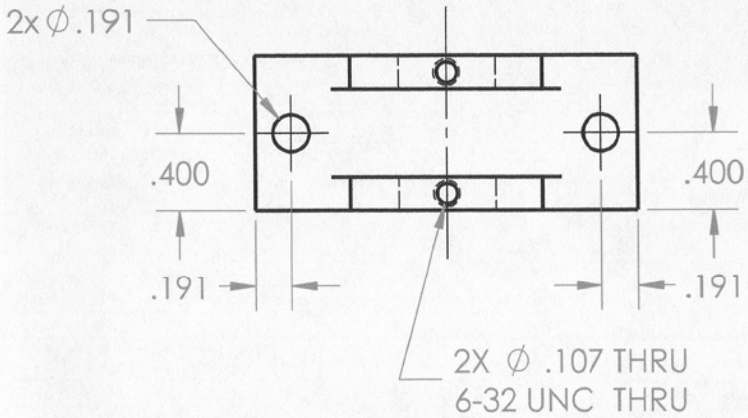

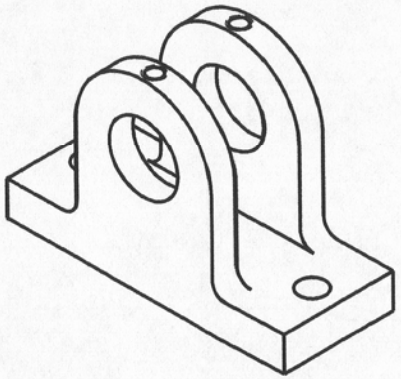

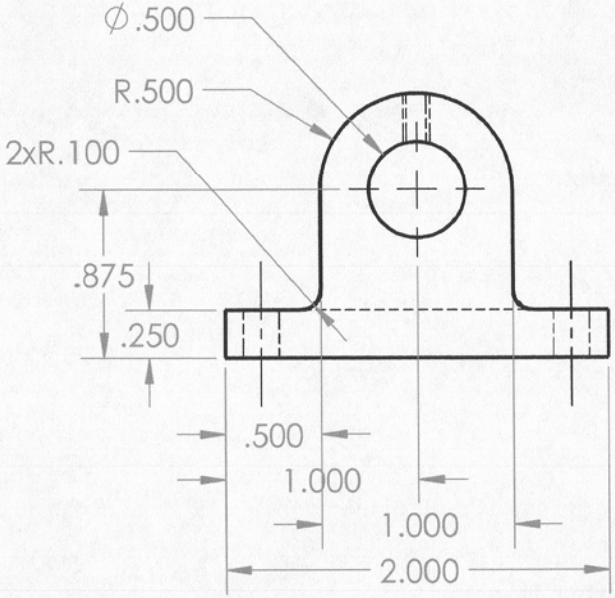

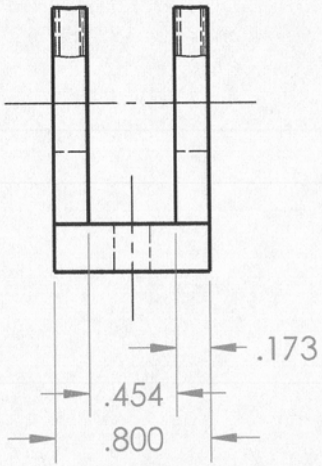

UNLESS OTHERWISE SPECIFIED:		NAME	DATE
DIMENSIONS ARE IN INCHES TOLERANCES: .005	DRAWN	I. THOMAS	04/14/15
	CHECKED		
	ENG APPR.		
	MFG APPR.		
INTERPRET GEOMETRIC TOLERANCING PER:	Q.A.		
MATERIAL 6061-T6 ALUMINUM	COMMENTS:		
FINISH 64			
NEXT ASSY / USED ON			
APPLICATION / DO NOT SCALE DRAWING			

ITEM 9

TITLE:

Bearing Block

SIZE	DWG. NO.	REV
A		1
SCALE: 1:1	WEIGHT:	SHEET 1 OF 1

REVISIONS				
ZONE	REV.	DESCRIPTION	APPROVED	DATE
	A	INITIAL RELEASE	-	-

1A

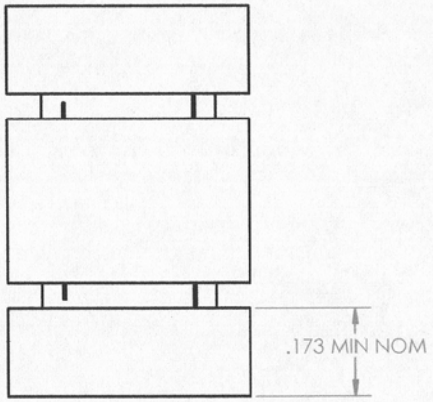

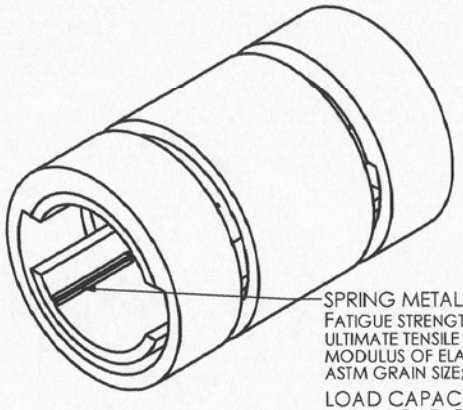

SPRING METAL PROPERTIES:
FATIGUE STRENGTH: 75,000 PSI
ULTIMATE TENSILE STRENGTH: 294,000 PSI
MODULUS OF ELASTICITY: 29,000,000PSI
ASTM GRAIN SIZE: #6 OR FINER

LOAD CAPACITY: 35 LBF
AXIAL LOAD CAPACITY: 91.84 LBF
TORSIONAL SPRING RATE: .0148B LBF-IN/DEGREE

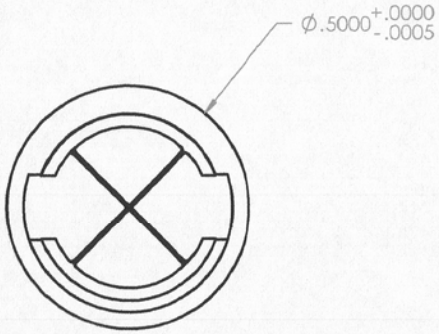

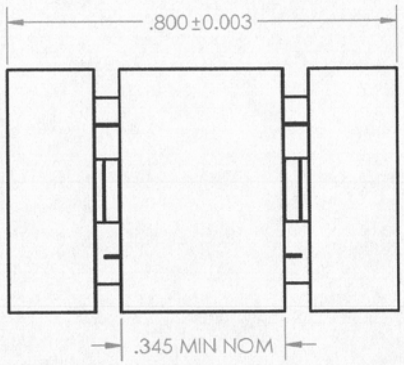

BENCHMARK MANUFACTURING
RELEASE FOR PRODUCTION

PROD LEAD_____ DATE_____

ENGR LEAD_____ DATE_____

UNLESS OTHERWISE SPECIFIED:		NAME	DATE
DIMENSIONS ARE IN INCHES TOLERANCES: ANGULAR: ±.5° ONE PLACE DECIMAL ± .03 TWO PLACE DECIMAL ± .01 THREE PLACE DECIMAL ± .005	DRAWN	-	-
	CHECKED		
	ENG APPR.		
	MFG APPR.		
CUSTOMER: RUSSEL WESTPHAL	COMMENTS: ITEM 10		
USED ON: MOUTING			
MATERIAL: 416 SST/ 410			
FINISH			
DO NOT SCALE DRAWING			

Benchmark electronics precision technologies

TITLE:
DOUBLE ENDED FLEXURE BEARING

SIZE	DWG. NO.	REV
B	GD-10	A
SCALE: 16:1		SHEET 1 OF 2

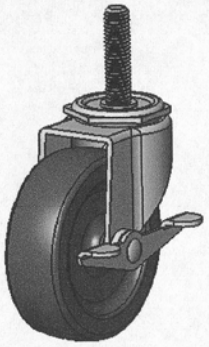

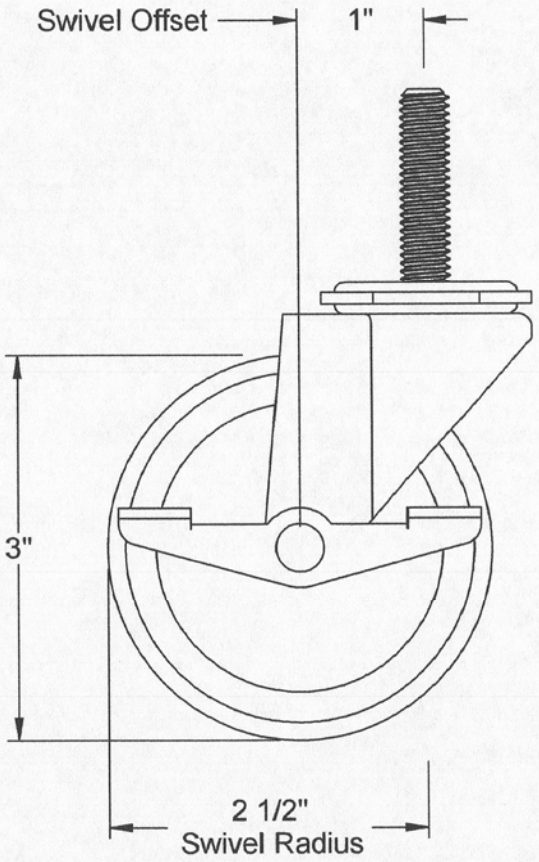

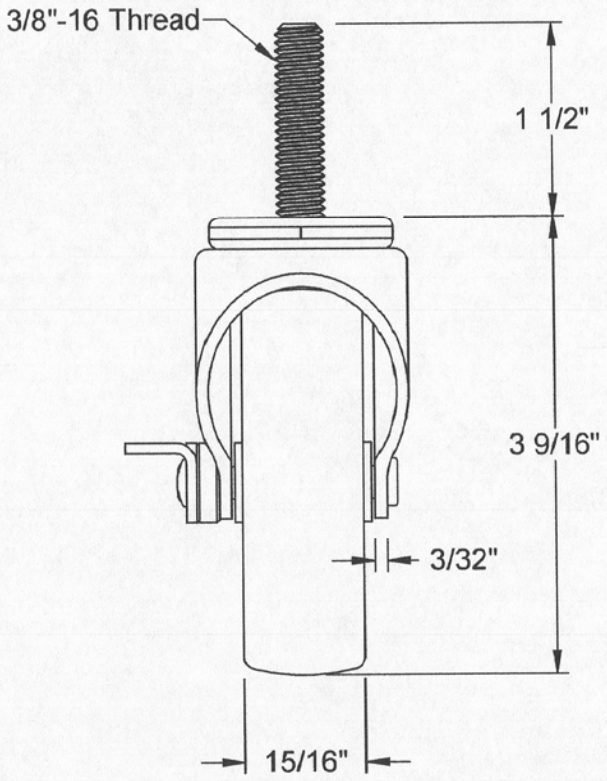

ITEM 13

McMASTER-CARR® CAD

PART NUMBER **2834T34**

http://www.mcmaster.com

Threaded-Stem
Swivel Caster with Brake

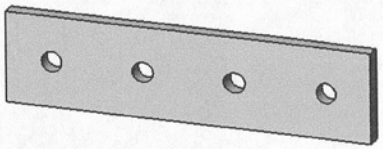

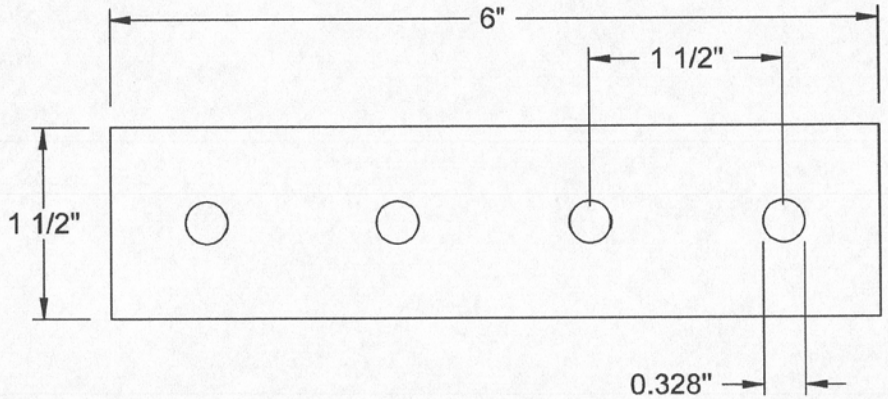

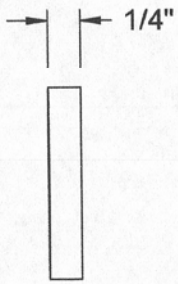

ITEM 15

McMASTER-CARR® CAD	PART NUMBER 47065T42
http://www.mcmaster.com © 2011 McMaster-Carr Supply Company Information in this drawing is provided for reference only.	Aluminum Single Extended Plate

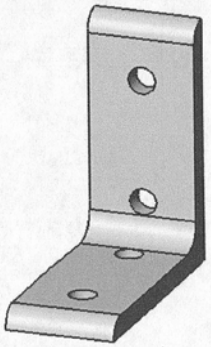

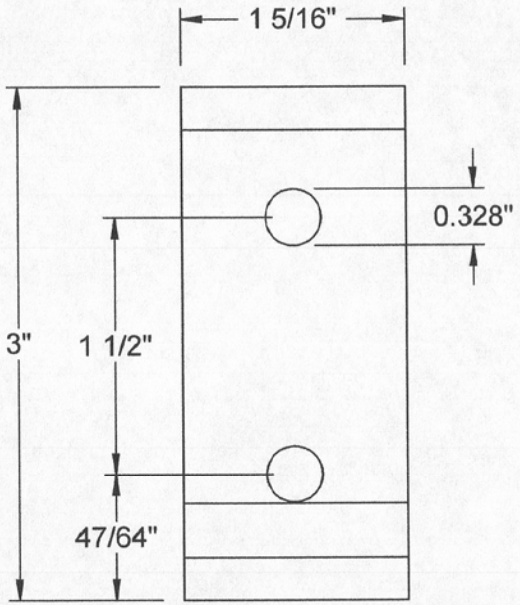

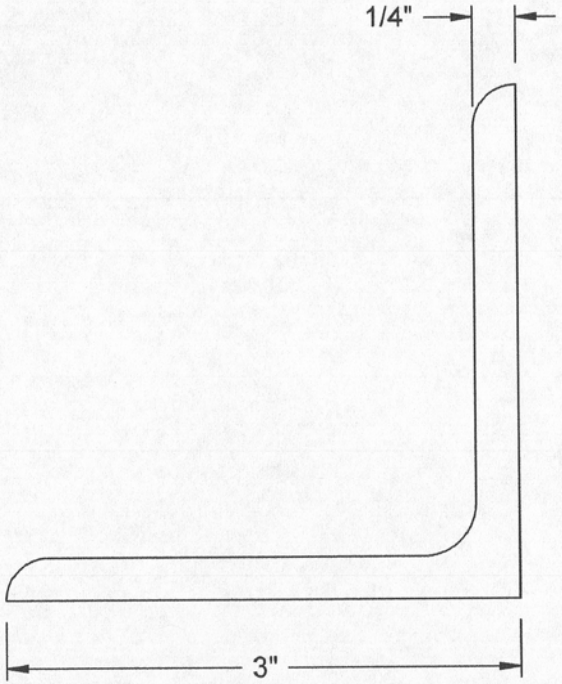

ITEM #17

McMASTER-CARR® CAD	PART NUMBER 47065T51
http://www.mcmaster.com © 2012 McMaster-Carr Supply Company Information in this drawing is provided for reference only.	Aluminum Single Extended 90° Bracket

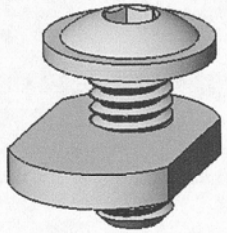

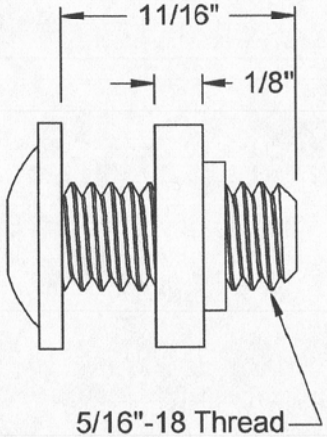

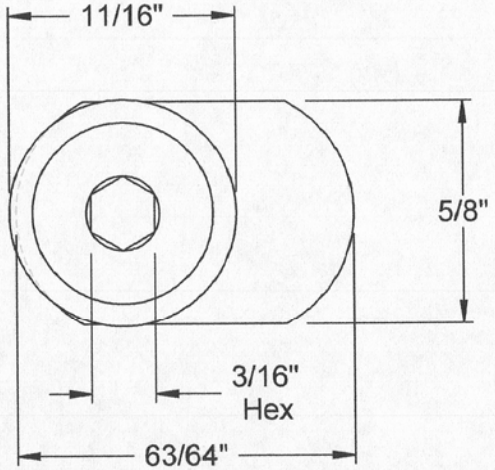

ITEM 18

McMASTER-CARR® CAD	PART NUMBER 47065T97
http://www.mcmaster.com © 2010 McMaster-Carr Supply Company Information in this drawing is provided for reference only.	Zinc-Plated Steel End-Feed Slotted Framing Fastener

1A

ITEM NO.	PART NUMBER	DESCRIPTION	QTY.
1	45605K122	NOZZLE 316 SST	1
2	43505K359	4" NPT SST THREADED PIPE FLANGE	4
3	9157K603	2 1/2" LENGTH SINGLE END 4" NPT PIPE NIPPLE SST	1
4	mesh	STRAIGHTENING MESH	1
5	honeycomb	ALUMINUM HONEYCOMB MESH	1
6	4830K382	12" LENGTH DOUBLE ENDED 4"NPT PIPE NIPPLE SST	1
7	4830K207	3" LENGTH DOUBLE END 4' NPT PIPE NIPPLE SST	1
8	93827A259	5/8" NUT GRADE 8 STEEL ZINC PLATED	16
9	98023A036	5/8" WASHER GRADE 5 ZINC PLATED STEEL	32
10	92620A845	2 1/4" LENGTH 5/8" NUT GRADE 8 STEEL ZINC PLATED	16

REVISIONS				
ZONE	REV.	DESCRIPTION	APPROVED	DATE
	A	INITIAL RELEASE	-	-

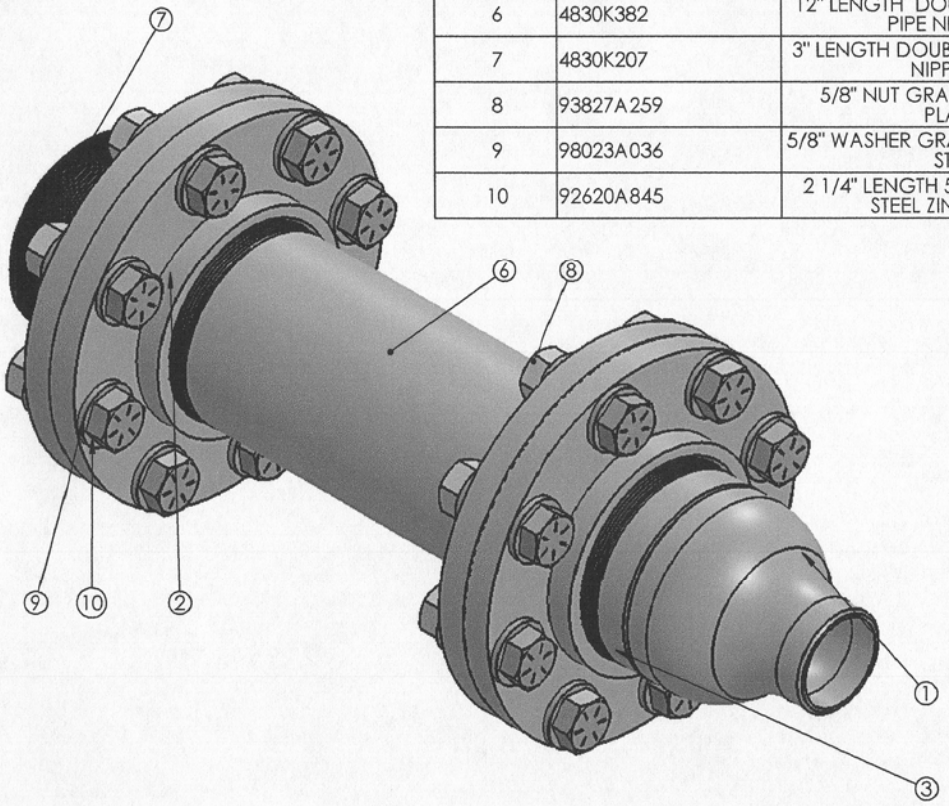

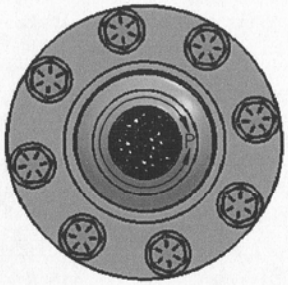

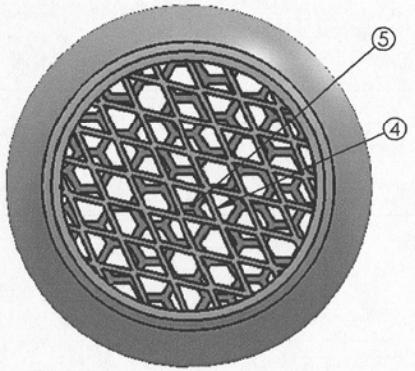

DETAIL P
SCALE 1 : 1

UNLESS OTHERWISE SPECIFIED:		NAME	DATE
DIMENSIONS ARE IN INCHES TOLERANCES: ANGULAR: ±.5° ONE PLACE DECIMAL ±.03 TWO PLACE DECIMAL ±.01 THREE PLACE DECIMAL ±.005	DRAWN	-	-
	CHECKED		
	ENG APPR.		
	MFG APPR.		
CUSTOMER: RUSSEL WESTPHAL	COMMENTS:		
USED ON: FINAL ASSEMBLY			
MATERIAL: 316 SST			
FINISH			
DO NOT SCALE DRAWING			

TITLE:
4" NPT PIPE/FITTINGSFLO W STRAIGTENING FINAL ASSEMBLY

SIZE	DWG. NO.	REV
B	1	A
SCALE: 1:8		SHEET 1 OF 2

REVISIONS				
ZONE	REV.	DESCRIPTION	APPROVED	DATE
	A	INITIAL RELEASE	-	-

1A

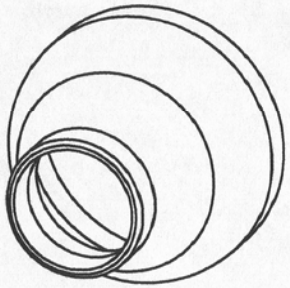

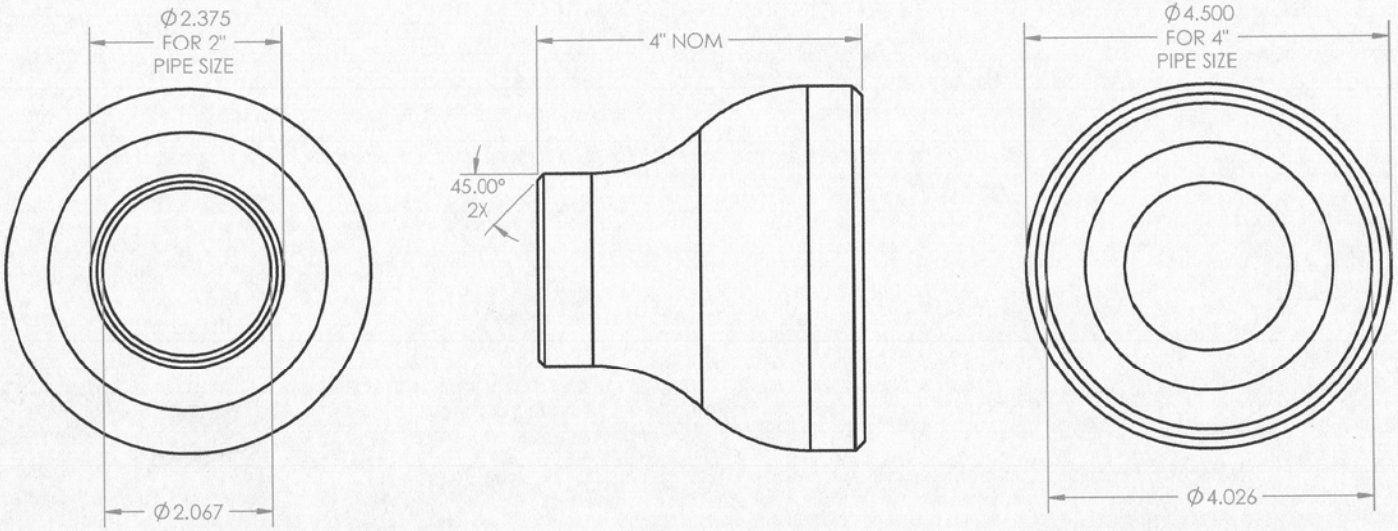

BENCHMARK MANUFACTURING
RELEASE FOR PRODUCTION

PROD LEAD_____ DATE_____

ENGR LEAD_____ DATE_____

PROPRIETARY AND CONFIDENTIAL

THE INFORMATION CONTAINED IN THIS DRAWING IS THE SOLE PROPERTY OF BENCHMARK ELECTRONICS. ANY REPRODUCTION IN PART OR AS A WHOLE WITHOUT THE WRITTEN PERMISSION OF BENCHMARK ELECTRONICS IS PROHIBITED.

UNLESS OTHERWISE SPECIFIED:
DIMENSIONS ARE IN INCHES
TOLERANCES:
ANGULAR: ±.5°
ONE PLACE DECIMAL ± .03
TWO PLACE DECIMAL ± .01
THREE PLACE DECIMAL ± .005
CUSTOMER RUSSEL WESTPHAL
USED ON FLOW STRAIGHTENER
MATERIAL 316 SST
FINISH
DO NOT SCALE DRAWING

	NAME	DATE
DRAWN	-	-
CHECKED		
ENG APPR.		
MFG APPR.		

COMMENTS: ITEM 1

Benchmark electronics precision technologies

TITLE:
TYPE 316 SST BUTT-WELD CONCENTRIC REDUCING COUPLING

SIZE	DWG. NO.	REV
B	45555K122	A

SCALE: 1:3 SHEET 1 OF 2

1A

REVISIONS				
ZONE	REV.	DESCRIPTION	APPROVED	DATE
	A	INITIAL RELEASE	-	-

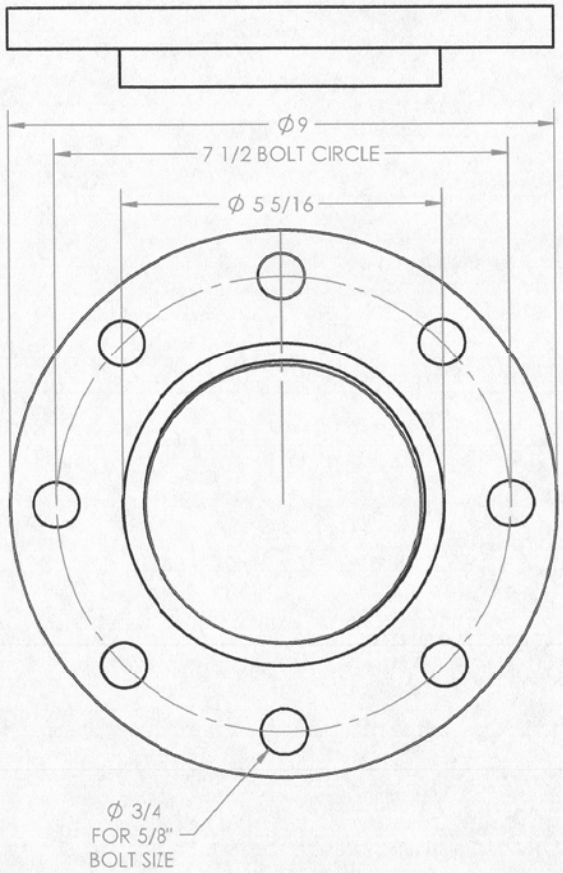

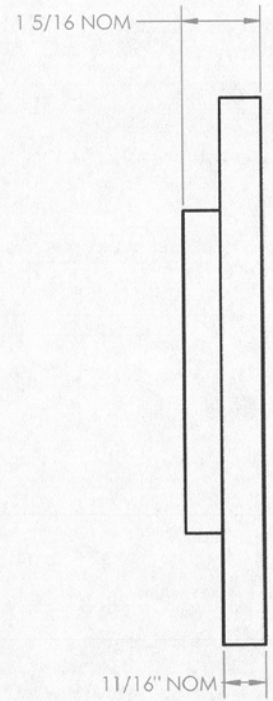

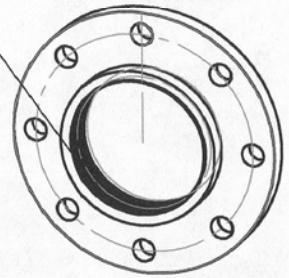

BENCHMARK MANUFACTURING
RELEASE FOR PRODUCTION

PROD LEAD_____ DATE_____

ENGR LEAD_____ DATE_____

PROPRIETARY AND CONFIDENTIAL

THE INFORMATION CONTAINED IN THIS DRAWING IS THE SOLE PROPERTY OF BENCHMARK ELECTRONICS. ANY REPRODUCTION IN PART OR AS A WHOLE WITHOUT THE WRITTEN PERMISSION OF BENCHMARK ELECTRONICS IS PROHIBITED.

UNLESS OTHERWISE SPECIFIED:
DIMENSIONS ARE IN INCHES
TOLERANCES:
ANGULAR: ±.5°
ONE PLACE DECIMAL ± .03
TWO PLACE DECIMAL ± .01
THREE PLACE DECIMAL ± .005
CUSTOMER RUSSEL WESTPHAL
USED ON FLOW STRAIGHTENER
MATERIAL 316 SST
FINISH
DO NOT SCALE DRAWING

	NAME	DATE
DRAWN	-	-
CHECKED		
ENG APPR.		
MFG APPR.		

COMMENTS: ITEM 2

Benchmark electronics precision technologies

TITLE:
TYPE 316 SST THREADED CAST FLANGE

SIZE	DWG. NO.	REV
B	43615K569	A

SCALE: 1:3 SHEET 1 OF 2

REVISIONS				
ZONE	REV.	DESCRIPTION	APPROVED	DATE
	A	INITIAL RELEASE	-	-

1A

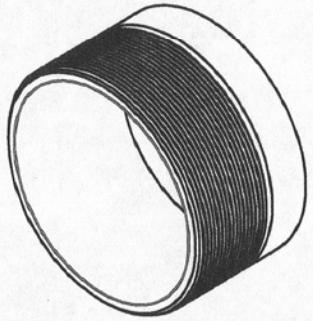

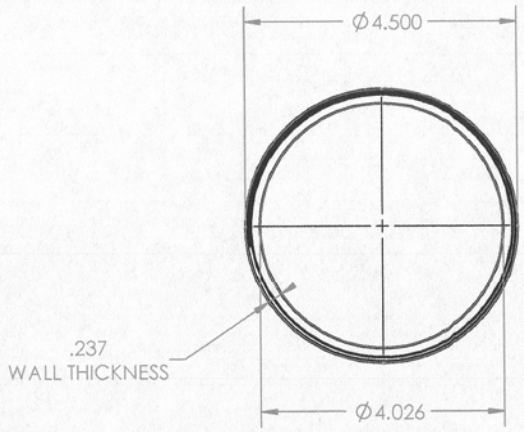

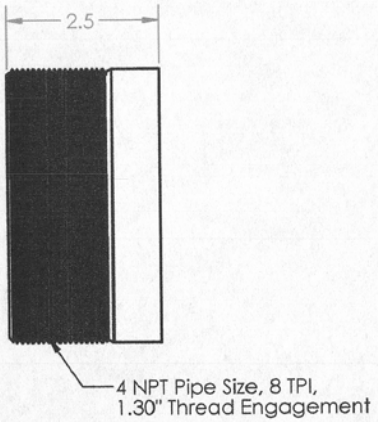

BENCHMARK MANUFACTURING
RELEASE FOR PRODUCTION

PROD LEAD_____ DATE_____

ENGR LEAD_____ DATE_____

UNLESS OTHERWISE SPECIFIED:
DIMENSIONS ARE IN INCHES
TOLERANCES:
ANGULAR: ±.5°
ONE PLACE DECIMAL ±.03
TWO PLACE DECIMAL ±.01
THREE PLACE DECIMAL ±.005

CUSTOMER: RUSSEL WESTPHAL
USED ON: FLOW STRAIGHTENER
MATERIAL: 316/316L SST
FINISH:
DO NOT SCALE DRAWING

	NAME	DATE
DRAWN	-	-
CHECKED		
ENG APPR.		
MFG APPR.		

COMMENTS: ITEM 3

Benchmark electronics precision technologies

TITLE:
TYPE 316/316L STAINLESS STEEL PIPE NIPPLE 2-1/2"

SIZE	DWG. NO.	REV
B	9110T82	A

SCALE: 1:2 SHEET 1 OF 2

McMASTER-CARR® OVER 555,000 PRODUCTS
(562) 692-5911
(562) 695-2323 (fax)
la.sales@mcmaster.com
Text 75930

ITEM 4

Strainer Grade Wire Cloth

304 Stainless Steel, 30 x 30 Mesh, .0130" Wire Diameter

In stock
$8.95 Each
9241T41

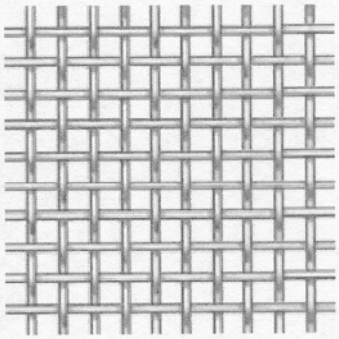

Mesh Size	30 × 30
Opening Size	
Length	0.02"
Width	0.02"
Open Area	37%
Wire Diameter	0.013"
Sheet Size	12"×12"
Additional Specifications	Choosing the Correct Wire Cloth Mesh Size

Maximize flow when straining your liquid process lines—woven from thin wire, this wire cloth has a larger percentage of open area than other wire cloth with the same mesh size. Type 304 stainless steel has good corrosion resistance.

McMASTER-CARR. OVER 555,000 PRODUCTS
(562) 692-5911
(562) 695-2323 (fax)
la.sales@mcmaster.com
Text 75930

ITEM 5

Corrosion-Resistant Formable 3003 Aluminum

Honeycomb Core, 3/4" Thick, 12" x 12"

In stock
$26.40 Each
9635K941

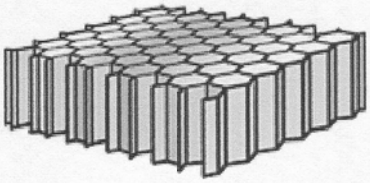

Alloy	3003
Shape	Honeycomb Core
Finish	Unpolished
Overall Thickness	3/4"
Thickness Tolerance	±0.008"
Width	12"
Width Tolerance	±1/8"
Length	12"
Length Tolerance	±1/8"
Material Composition	
Silicon	0-0.6%
Iron	0-0.7%
Copper	0-0.3%
Manganese	0.3-1.5%
Magnesium	0.2-0.8%
Chromium	0-0.2%
Zinc	0-0.4%
Titanium	0-0.1%
Other	0-0.15%
Aluminum	95.25-99.5%
Nominal Density	0.098 lbs./cu. in.
Modulus of Elasticity	10.0 ksi × 10^3
Elongation	2-5%
Melting Range	900° to 1,210° F
Thermal Conductivity	1100-1500 Btu/hr. × in./sq.ft. @ 77° F
Electrical Resistivity	21-25 Ohm-Cir. Mil/ft. @ 68° F

Often used for tanks, heat exchangers, and general sheet metal work, Alloy 3003 offers excellent corrosion resistance with good formability and weldability. It is nonmagnetic and not heat treatable. Temperature range is -300° to 300° F, unless otherwise stated.

Yield strength is approximate and may vary based on size and shape.

The rigid honeycomb design gives these sheets a high strength-to-weight ratio. Temperature range is -30° to 300° F. Thickness tolerance is ±0.008". Width and length tolerances are ±1/8".

REVISIONS				
ZONE	REV.	DESCRIPTION	APPROVED	DATE
	A	INITIAL RELEASE	-	-

1A

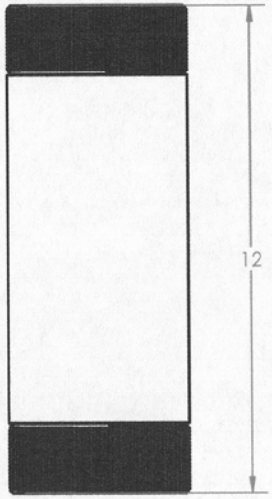

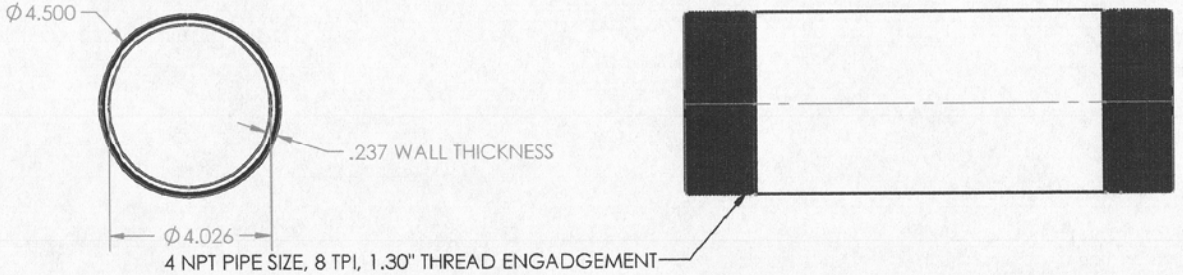

BENCHMARK MANUFACTURING
RELEASE FOR PRODUCTION

PROD LEAD_____ DATE_____

ENGR LEAD_____ DATE_____

UNLESS OTHERWISE SPECIFIED:		NAME	DATE
DIMENSIONS ARE IN INCHES TOLERANCES: ANGULAR: ±.5° ONE PLACE DECIMAL ± .03 TWO PLACE DECIMAL ± .01 THREE PLACE DECIMAL ± .005	DRAWN	-	-
	CHECKED		
	ENG APPR.		
	MFG APPR.		
CUSTOMER RUSSEL WESTPHAL	COMMENTS: ITEM 6		
USED ON FLOW STRAIGHTENER			
MATERIAL 316 SST			
FINISH			
DO NOT SCALE DRAWING			

Benchmark electronics precision technologies

TITLE:
12" LENGTH DOUBLE ENDED 4"NPT PIPE NIPPLE SSTT
YPE 316/316L STAINLESS STEEL PIPE NIPPLE

REV B A

SCALE: 1:3 SHEET 1 OF 2

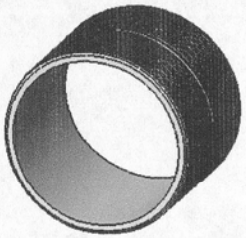

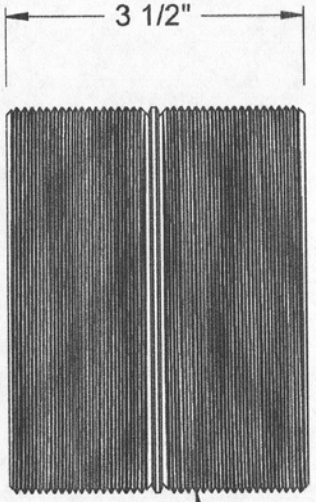

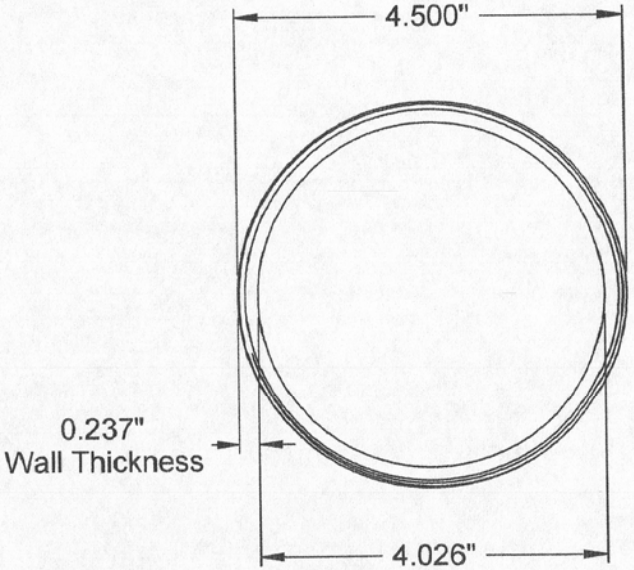

ITEM 7

McMASTER-CARR® CAD

http://www.mcmaster.com

PART NUMBER **4830K207**

Type 304/304L Stainless Steel Pipe Nipple

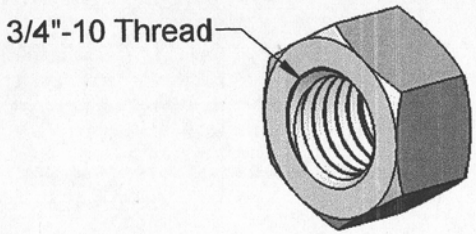

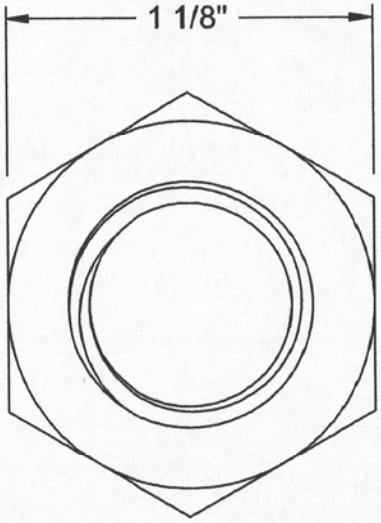

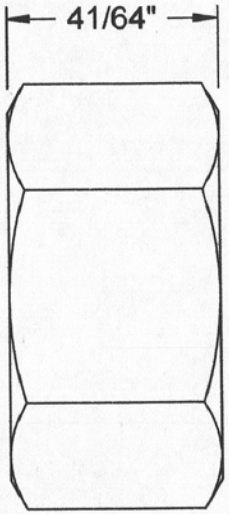

ITEM 8

McMASTER-CARR® CAD	PART NUMBER 93827A259
http://www.mcmaster.com © 2015 McMaster-Carr Supply Company Information in this drawing is provided for reference only.	Hex Nut

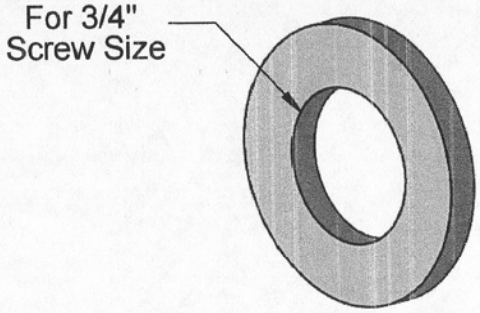

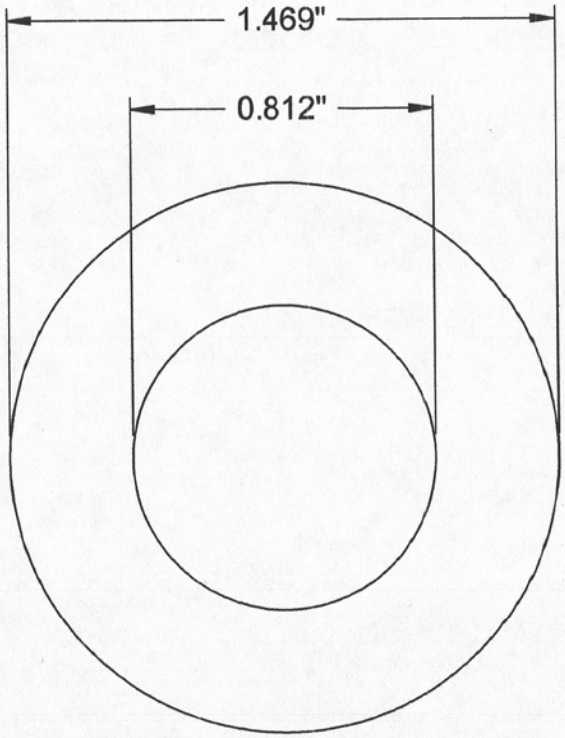

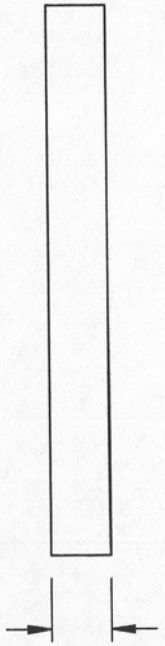

Washer may vary from
0.108" to 0.16" in thickness.

ITEM 9

McMASTER-CARR® CAD	PART NUMBER 98023A036
http://www.mcmaster.com © 2014 McMaster-Carr Supply Company Information in this drawing is provided for reference only.	General Purpose Washer

REVISIONS				
ZONE	REV.	DESCRIPTION	APPROVED	DATE
	A	INITIAL RELEASE	-	-

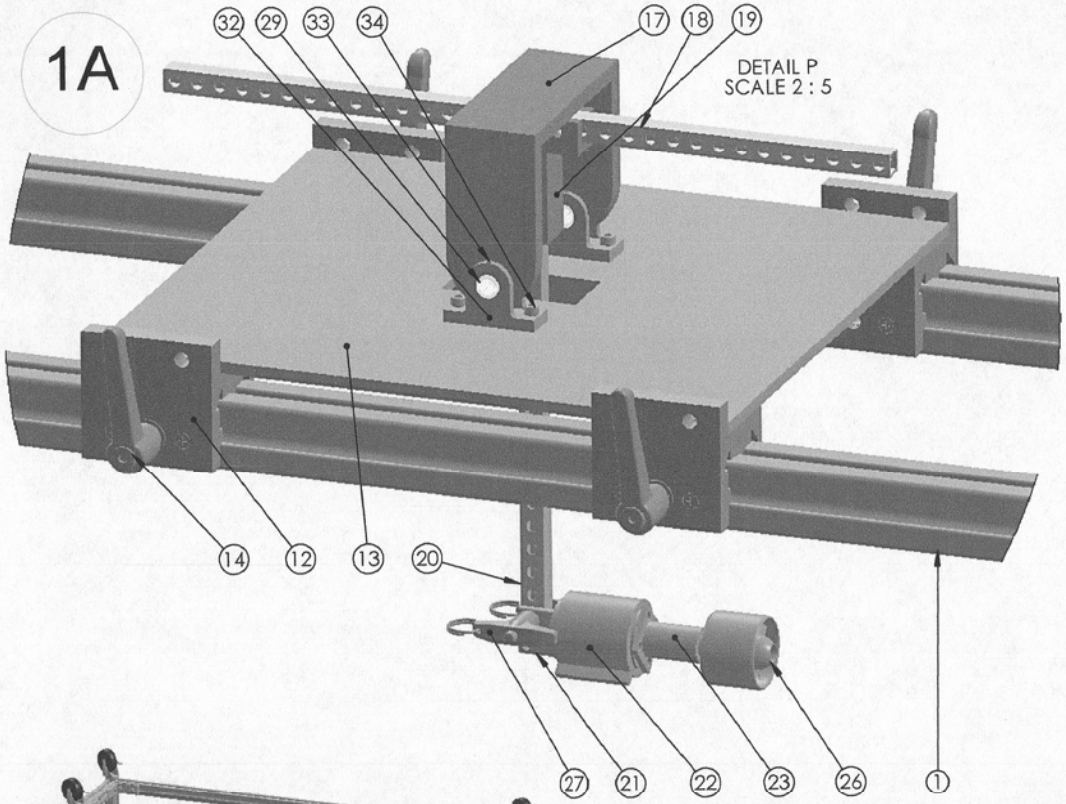

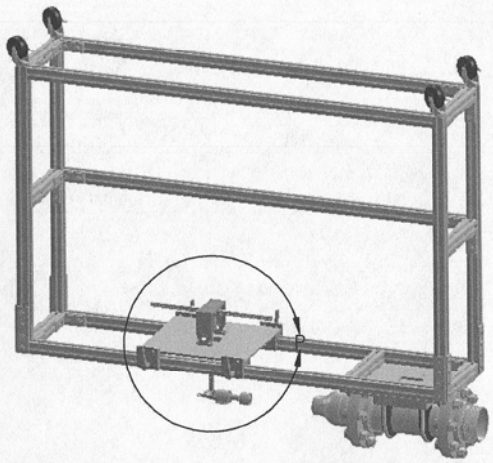

ITEM NO.	PART NUMBER	DESCRIPTION	QTY.
1	t-slot 56""	56" TOP EXTRUDED ALUMINUM RAILS	2
12	60585K33	1.5" ALUMINUM EXTRUSION LINEAR BEARING MOUNT	4
13	sliding surface	C-ARM MOUNTING PLATE	2
14	60585K32	HANDLE CLAMP FOR LINEAR BEARING	4
17	c-arm	C-ARM FOR MICRO RAT MOUNTING	1
18	0.5x0.5-alluminum-tube 1_16-wall-thickness 10	DRILLED ALUMINUM BAR STOCK FOR MOUNTING MICRO RAT	1
19	90 degree brace	ALUMINUM MACHINED BILLET	1
20	0.5x0.5-alluminum-tube 1_16-wall-thickness	FOR LOAD CELL POSITIONING	1
21	torque cell to arm	SECURES TORQUE CELL TO ALUMINUM BAR	1
22	torque sensor	TRANSDUCER TECHNIQUES RTS	1
23	generator holder	SECURES MICRO RAT TO TORQUE SENSOR	1
26	Turbine Blisk - Rev6 - No shaft	TURBINE BLADE	1
27	90293A135	QUICK CONNECT PIN	2
28	gd-10_01	FLEXURE BEARING	4
32	Bearing Block	SUPPORT MECHANISM FOR C-ARM	2
33	92313A144	CUP POINT SET SCREWS	4
34	91251A345	HEX CAP SCREW FOR BEARING BLOCK	4

UNLESS OTHERWISE SPECIFIED:
DIMENSIONS ARE IN INCHES
TOLERANCES:
ANGULAR: ±.5°
ONE PLACE DECIMAL ±.03
TWO PLACE DECIMAL ±.01
THREE PLACE DECIMAL ±.005

CUSTOMER: RUSSEL WESTPHAL
USED ON: FINAL ASSEMBLY
MATERIAL: MIXED
FINISH:
DO NOT SCALE DRAWING

	NAME	DATE
DRAWN	-	-
CHECKED		
ENG APPR.		
MFG APPR.		
COMMENTS:		

TITLE:
MICRO-RAT MOUNTING SUB-ASSEMBLY BILL OF MATERIALS

SIZE	DWG. NO.	REV
B	1	A

SCALE: 1:12 SHEET 1 OF 2

REVISIONS				
ZONE	REV.	DESCRIPTION	APPROVED	DATE
	A	INITIAL RELEASE	-	-

1A

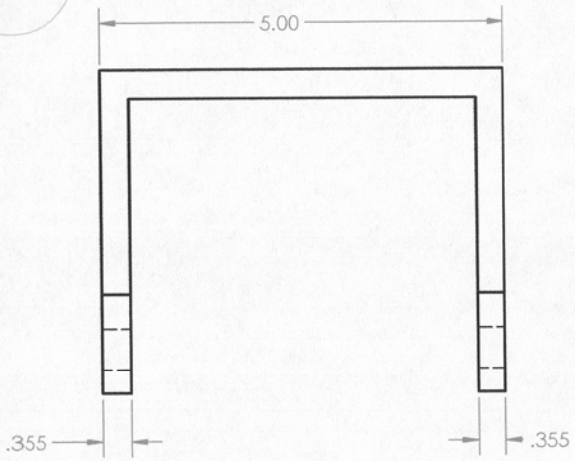

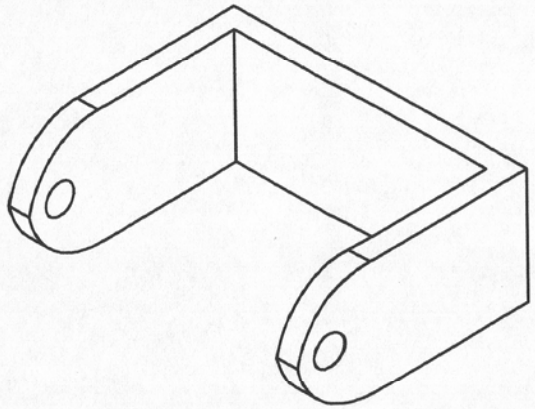

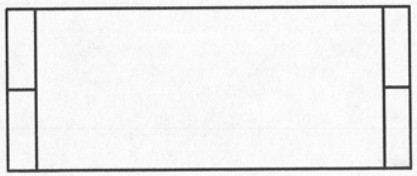

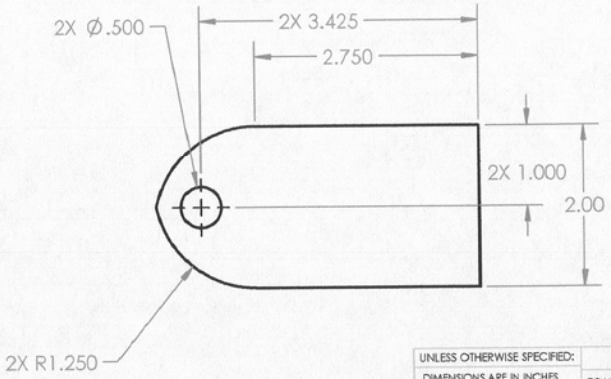

		NAME	DATE
UNLESS OTHERWISE SPECIFIED:	DRAWN	-	-
DIMENSIONS ARE IN INCHES	CHECKED		
TOLERANCES: ANGULAR: ±.5°	ENG APPR.		
ONE PLACE DECIMAL ± .03	MFG APPR.		
TWO PLACE DECIMAL ± .01	COMMENTS:		
THREE PLACE DECIMAL ± .005	ITEM 17		
CUSTOMER: RUSSEL WESTPHAL			
USED ON: MICRO-RAT MOUNTING			
MATERIAL: 6061 ALUMINUM			
FINISH			
DO NOT SCALE DRAWING			

TITLE:
C-ARM FOR MICRO RAT MOUNTING

SIZE	DWG. NO.	REV
B	1	A

SCALE: 1:2 SHEET 1 OF 2

REVISIONS				
ZONE	REV.	DESCRIPTION	APPROVED	DATE
	A	INITIAL RELEASE	-	-

1A

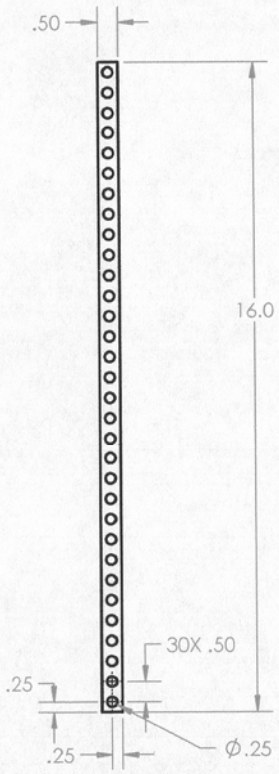

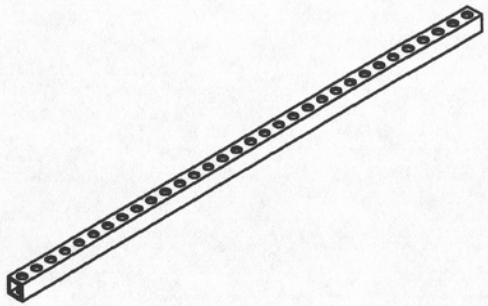

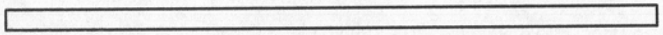

ITEM 18/20

UNLESS OTHERWISE SPECIFIED:		NAME	DATE
DIMENSIONS ARE IN INCHES TOLERANCES: ANGULAR: ±.5° ONE PLACE DECIMAL ± .03 TWO PLACE DECIMAL ± .01 THREE PLACE DECIMAL ± .005	DRAWN	-	-
	CHECKED		
	ENG APPR.		
	MFG APPR.		
CUSTOMER: RUSSEL WESTPHAL	COMMENTS:		
USED ON: MICRO-RAT MOUNTING			
MATERIAL: 6061 ALUMINUM			
FINISH			
DO NOT SCALE DRAWING			

TITLE: **C-ARM BALANCE BEAM**

SIZE	DWG. NO.	REV
B	1	A

SCALE: 1:8 SHEET 1 OF 2

REVISIONS				
ZONE	REV.	DESCRIPTION	APPROVED	DATE
	A	INITIAL RELEASE	-	-

1A

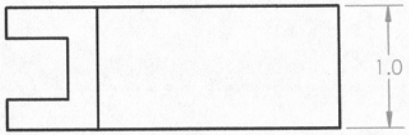

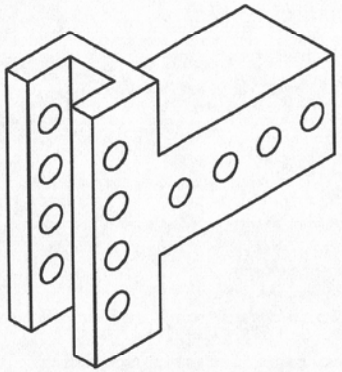

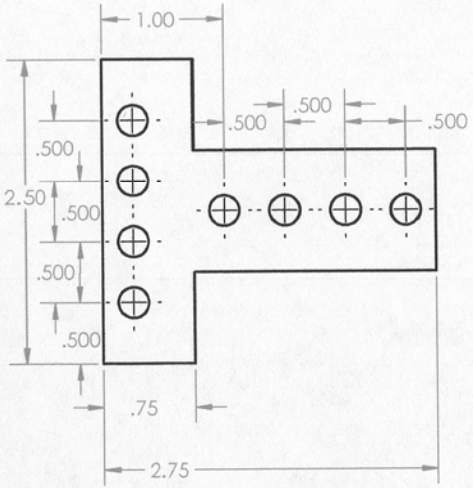

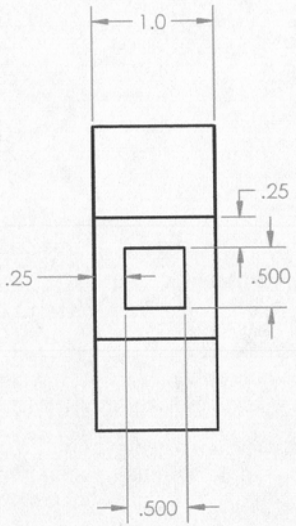

ITEM 19

UNLESS OTHERWISE SPECIFIED:		NAME	DATE
DIMENSIONS ARE IN INCHES TOLERANCES: ANGULAR: ±.5° ONE PLACE DECIMAL ±.03 TWO PLACE DECIMAL ±.01 THREE PLACE DECIMAL ±.005	DRAWN	-	-
	CHECKED		
	ENG APPR.		
	MFG APPR.		
CUSTOMER: RUSSEL WESTPHAL	COMMENTS: ITEM 19		
USED ON: MICRO-RAT MOUNTING			
MATERIAL: 6061 ALUMINUM			
FINISH			
DO NOT SCALE DRAWING			

TITLE: **C-ARM BALANCE BAR**

SIZE	DWG. NO.	REV
B	1	A

SCALE: 1:1 SHEET 1 OF 2

REVISIONS				
ZONE	REV.	DESCRIPTION	APPROVED	DATE
	A	INITIAL RELEASE	-	-

1A

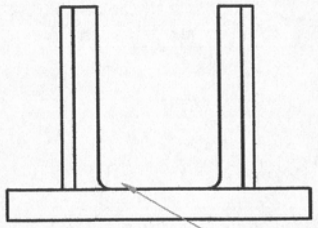

R.050 OR TOOL RADIUS

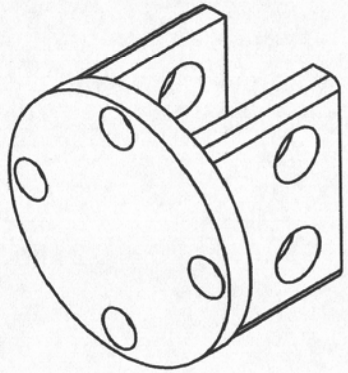

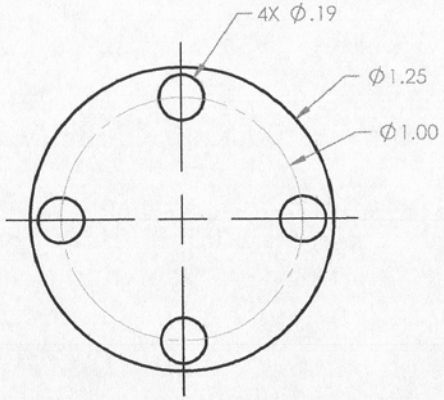

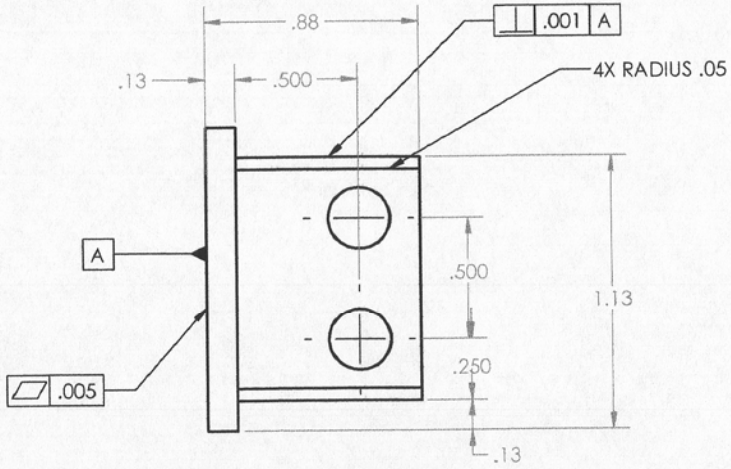

ITEM 28

UNLESS OTHERWISE SPECIFIED:		NAME	DATE
DIMENSIONS ARE IN INCHES TOLERANCES: ANGULAR: ±.5° ONE PLACE DECIMAL ± .03 TWO PLACE DECIMAL ± .01 THREE PLACE DECIMAL ± .005	DRAWN	-	-
	CHECKED		
	ENG APPR.		
	MFG APPR.		
CUSTOMER: RUSSEL WESTPHAL	COMMENTS:		
USED ON: MICRO-RAT MOUNTING			
MATERIAL: 6061 ALUMINUM			
FINISH			
DO NOT SCALE DRAWING			

TITLE: **TORQUE CELL MOUNTING BRACKET**

SIZE	DWG. NO.	REV
B	1	A

SCALE: 2:1 SHEET 1 OF 2

ITEM 22

LOW CAPACITY (INCH-OUNCE) REACTION TORQUE SENSOR

RTS SERIES

MADE IN USA

CAPACITY RANGES:
5, 10, 25, 50, 100, 200, 500, 1,000 in-oz

The RTS Series torque sensors were designed to fill the need for accurate torque measurements below 62.5 in.lbs. without giving up stiffness or sensitivity to forces from other directions. They are manufactured from sensor quality aluminum and anodized for long term durability. Bonded foil strain gages and materials of the highest quality are installed assuring high reliability. The four bolt hole pattern with the use of our O.D. or I.D. pilots on either end allows simple adaptation to any application.

AMX-4 10ft mating cable included.

Specifications

al

°F

Temp. Effect on Zero: 0.005% of R.O./°F
Terminal Resistance: 350 ohms nominal
Excitation Voltage: 10 VDC
Safe Overload: 150% of R.O.

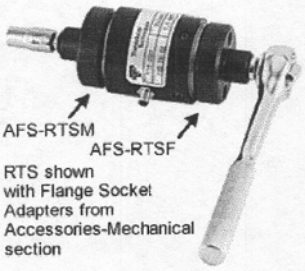

RTS shown with Flange Socket Adapters from Accessories-Mechanical section

Dimensions in Inches, RTS-5 through 1,000

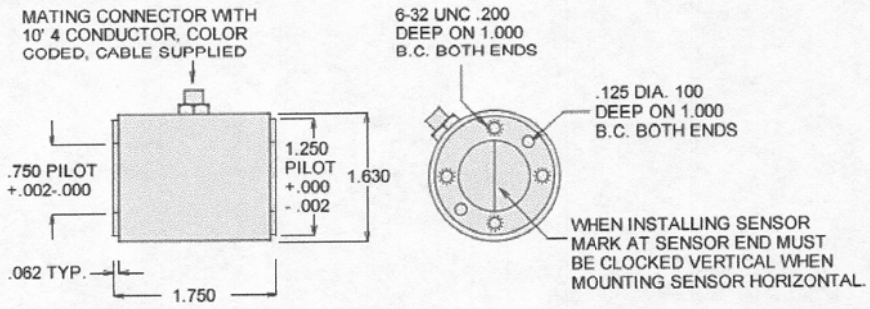

1A

REVISIONS				
ZONE	REV.	DESCRIPTION	APPROVED	DATE
	A	INITIAL RELEASE	-	-

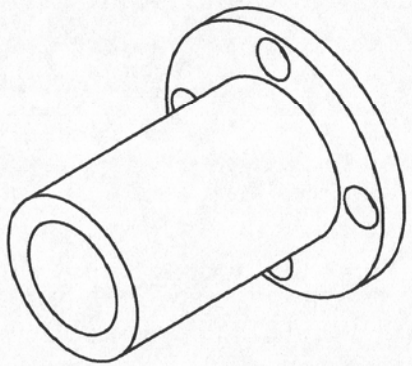

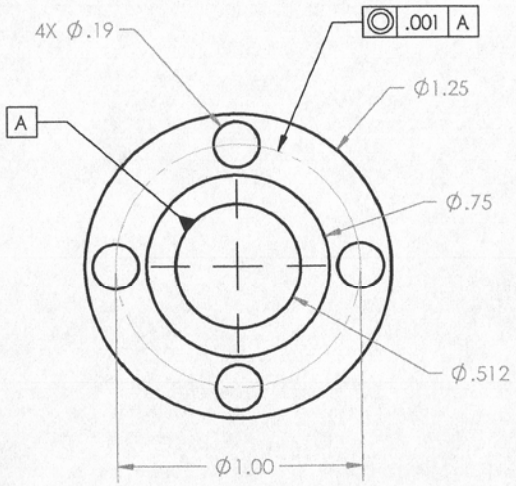

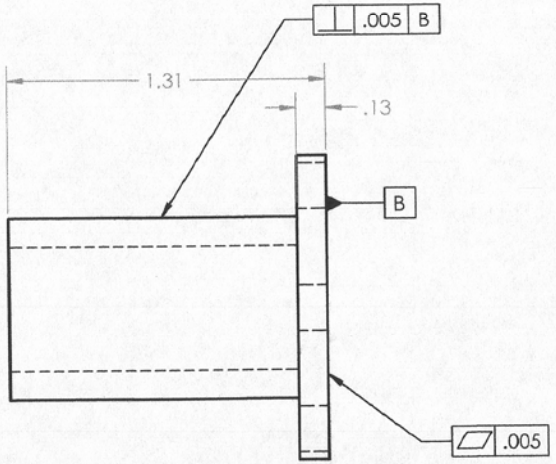

ITEM 23

		NAME	DATE
UNLESS OTHERWISE SPECIFIED:			
DIMENSIONS ARE IN INCHES	DRAWN	-	-
TOLERANCES:	CHECKED		
ANGULAR: ±.5°	ENG APPR.		
ONE PLACE DECIMAL ±.03	MFG APPR.		
TWO PLACE DECIMAL ±.01			
THREE PLACE DECIMAL ±.005			
CUSTOMER: RUSSEL WESTPHAL	COMMENTS:		
USED ON: MICRO-RAT MOUNTING	ITEM 23		
MATERIAL: 6061 ALUMINUM			
FINISH			
DO NOT SCALE DRAWING			

TITLE:
MICRO-RAT TO TORQUE CELL FIXTURE

SIZE	DWG. NO.	REV
B	1	A

SCALE: 2:1 SHEET 1 OF 2

REVISIONS			
REV.	DESCRIPTION	DATE	APPROVED
A	INTITIAL RELEASE	3/7/2011	RV

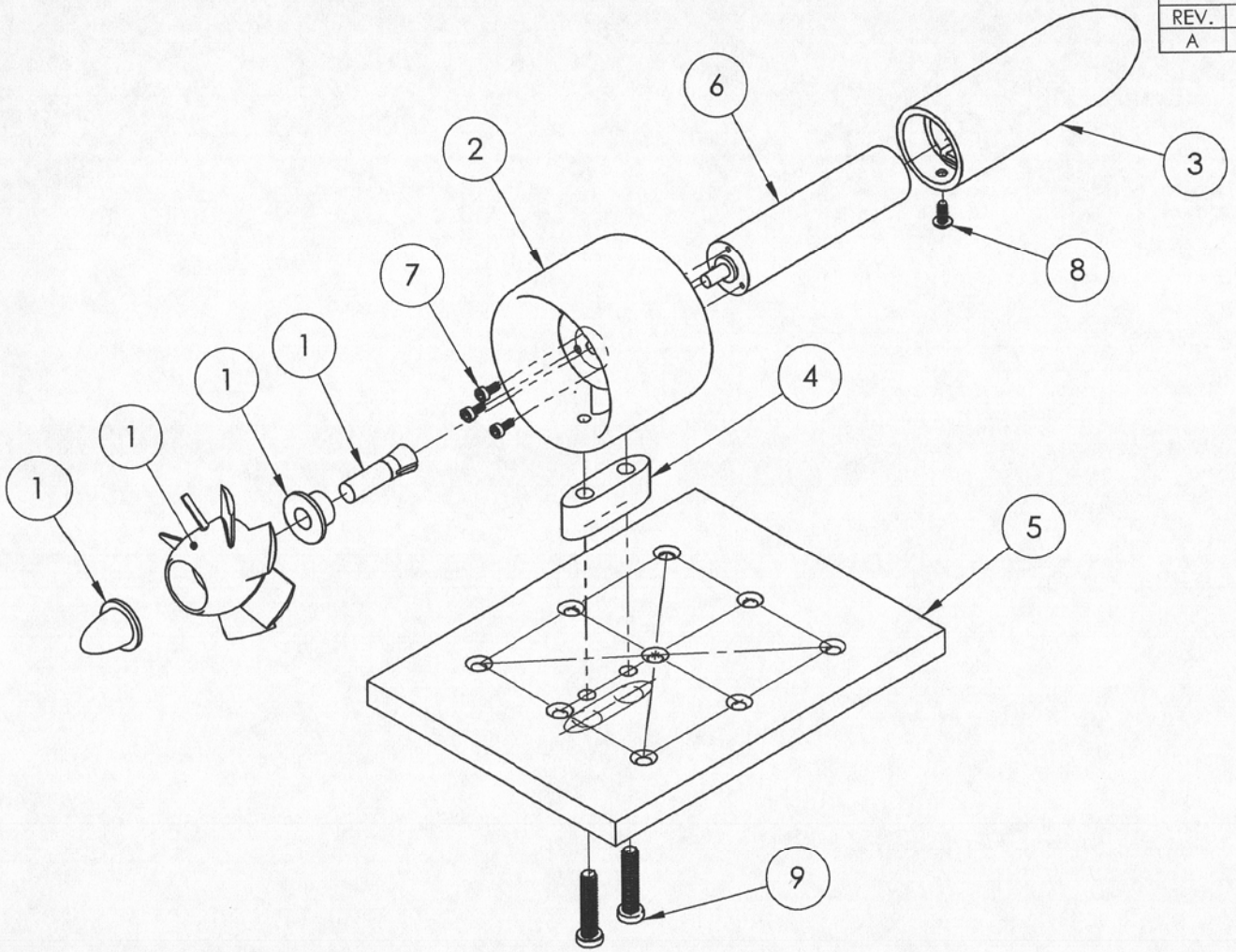

ITEM #	PART #	DESCRIPTION	QTY.
1	1001	BLISK ASSEMBLY	1
2	1002	COWLING	1
3	1003	NUCELLE	1
4	1004	SUPPORT STRUT	1
5	1005	MOUNTING PLATE	1
6	1006	GENERATOR	1
7	1007	91290A021	3
8	1008	91255A076	1
9	1009	92220A144	2

ITEM 26 ASSMB.

UNLESS OTHERWISE SPECIFIED:
DIMENSIONS ARE IN INCHES

	NAME	DATE
DRAWN		
CHECKED		

COMMENTS:

Linear Tolerances:	Angular Tolerances:
x. ±	x. ±
x.x ±	x.x ±
x.xx ±	x.xx ±
x.xxx ±	

MATERIAL: Aluminum 6061

FINISH: XXXXXXX

DO NOT SCALE DRAWING

ICEPICK

TITLE:
ASSEMBLY,
BLDS HEATING DEVICE

SIZE	DWG. NO.	REV
A	1000	A

SCALE: 2:3	WEIGHT:	SHEET 1 OF 1

REVISIONS			
REV.	DESCRIPTION	DATE	APPROVED
A	INTIIAL RELEASE	3/7/2011	RV

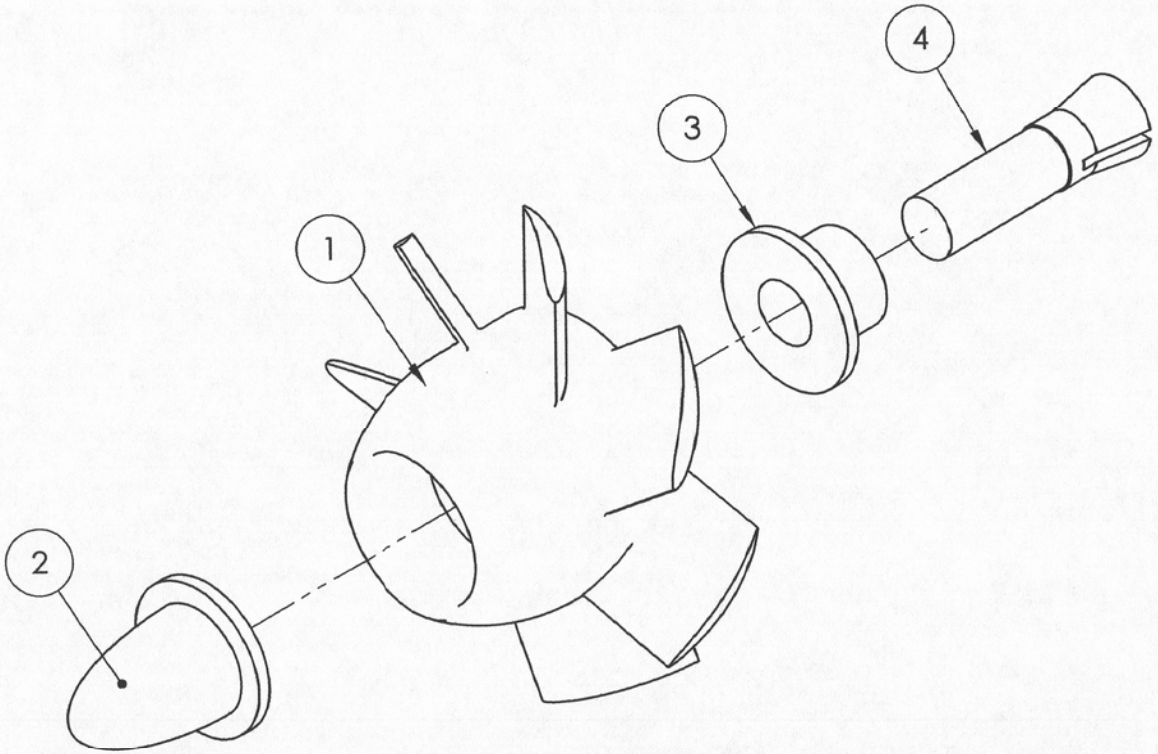

ITEM 26 ASSMB.

ITEM #	PART #	DESCRIPTION	QTY.
1	1001A	BLISK	1
2	1001B	COLLETHEAD	1
3	1001C	COLLET COLLAR	1
4	1001D	COLLET BODY	1

UNLESS OTHERWISE SPECIFIED:
DIMENSIONS ARE IN INCHES

	NAME	DATE
DRAWN		
CHECKED		

COMMENTS:

Linear Tolerances:
x. ±
x.x ±
x.xx ±
x.xxx ±

Angular Tolerances:
x. ±
x.x ±
x.xx ±

MATERIAL: Aluminum 6061

FINISH: XXXXXXX

DO NOT SCALE DRAWING

ICEPICK

TITLE:
ASSEMBLY,
BLISK

SIZE	DWG. NO.	REV
A	1001	A

SCALE: 2:1 | WEIGHT: | SHEET 1 OF 1

5 4 3 2 1

REVISIONS			
REV.	DESCRIPTION	DATE	APPROVED
A	INITIAL RELEASE	3/7/2011	RV

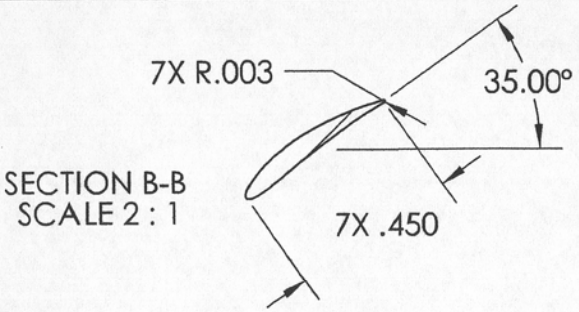

SECTION B-B
SCALE 2 : 1

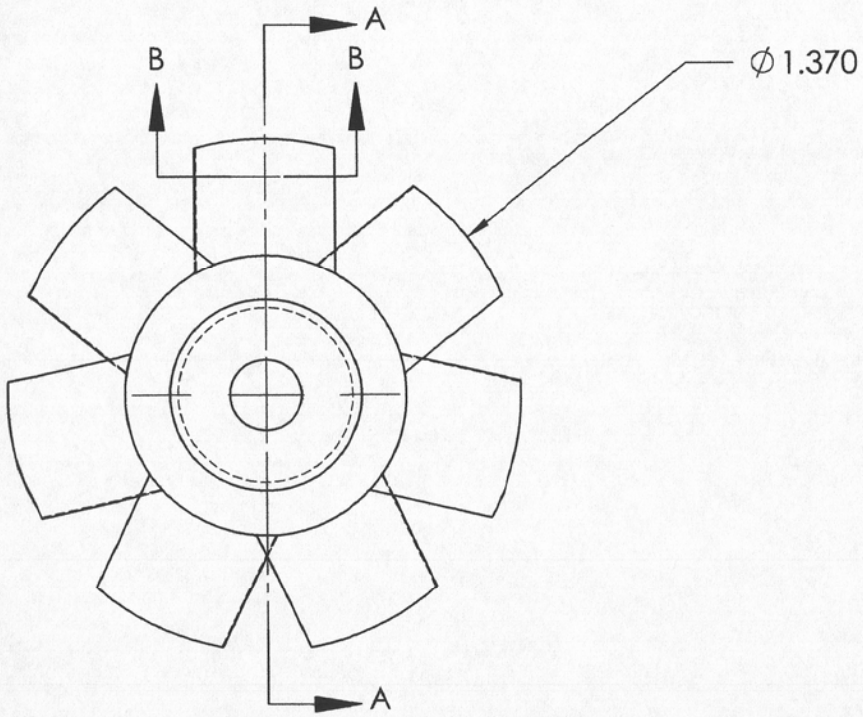

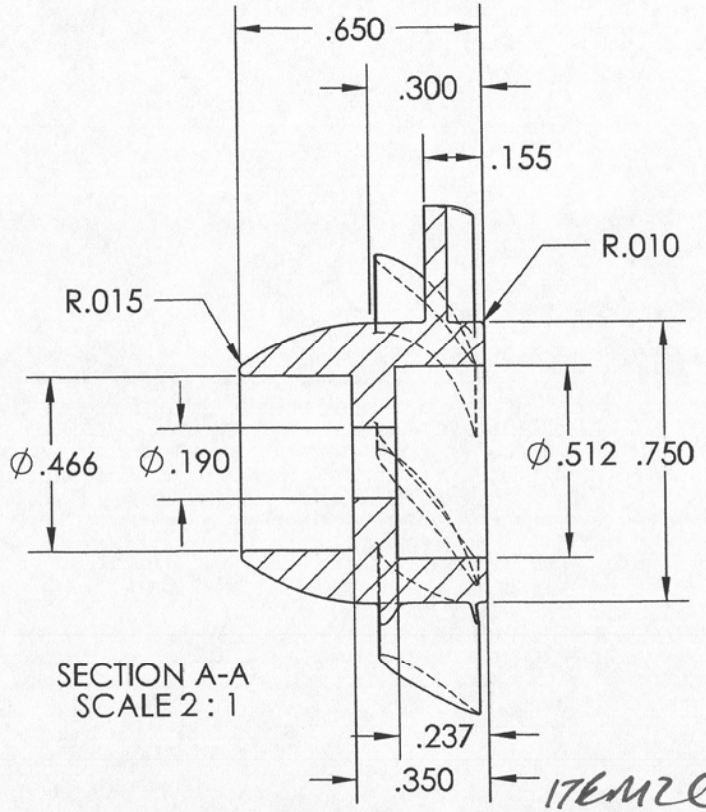

SECTION A-A
SCALE 2 : 1

ITEM 26

UNLESS OTHERWISE SPECIFIED: DIMENSIONS ARE IN INCHES Linear Tolerances: x.xx ± .01 x.xxx ± .002		NAME	DATE
	DRAWN	J. Hsu	3/7/2011
	CHECKED		
	COMMENTS:		
MATERIAL: Aluminum 6061			
FINISH: None			
DO NOT SCALE DRAWING			

PROPRIETARY AND CONFIDENTIAL
THE INFORMATION CONTAINED IN THIS DRAWING IS THE SOLE PROPERTY OF TEAM ICE PICK. ANY REPRODUCTION IN PART OR AS A WHOLE WITHOUT THE WRITTEN PERMISSION OF TEAM ICE PICK IS PROHIBITED. PROPRIETARY AND CONFIDENTIAL

ICEPICK

TITLE: Blisk

SIZE	DWG. NO.	REV
A	1001A	A

SCALE: 2:1	WEIGHT:	SHEET 1 OF 1

REVISIONS			
REV.	DESCRIPTION	DATE	APPROVED
A	INITIAL RELEASE	3/7/2011	RV

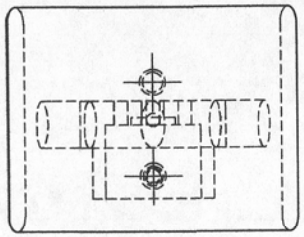

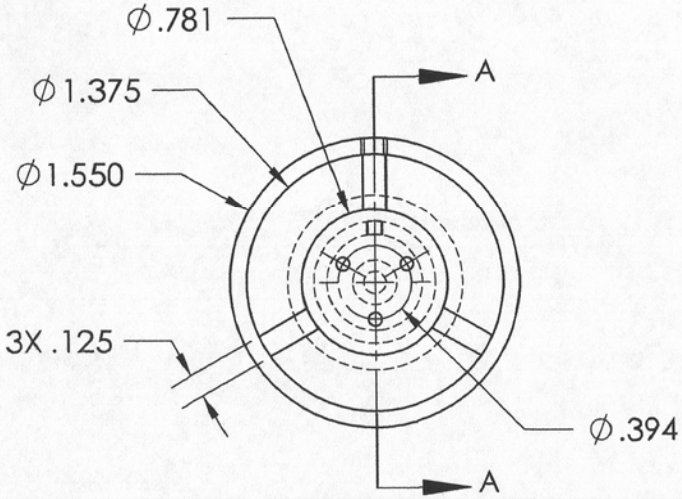

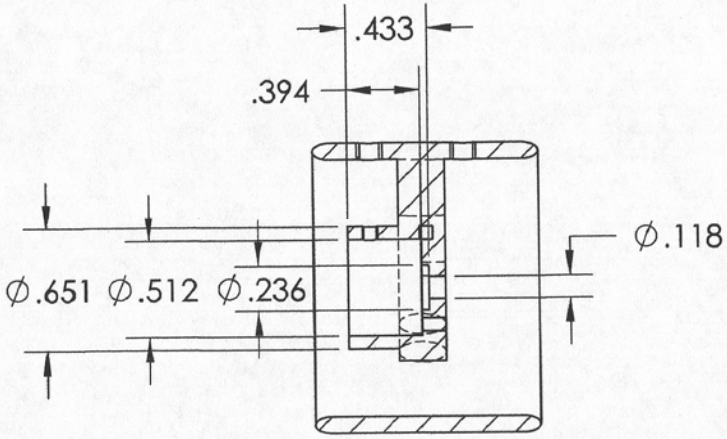

SECTION A-A

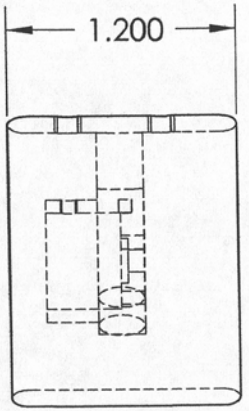

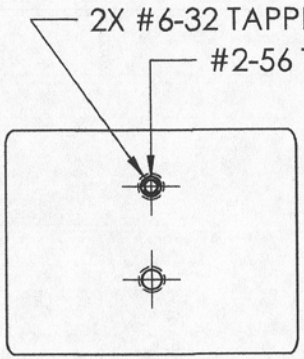

ITEM 26

UNLESS OTHERWISE SPECIFIED: DIMENSIONS ARE IN INCHES Linear Tolerances: x.xx ± .01 x.xxx ± .002		NAME	DATE
	DRAWN	J. Hsu	3/7/2011
	CHECKED		
	COMMENTS:		
MATERIAL: Aluminum 6061	PROPRIETARY AND CONFIDENTIAL THE INFORMATION CONTAINED IN THIS DRAWING IS THE SOLE PROPERTY OF TEAM ICE PICK. ANY REPRODUCTION IN PART OR AS A WHOLE WITHOUT THE WRITTEN PERMISSION OF TEAM ICE PICK IS PROHIBITED. PROPRIETARY AND CONFIDENTIAL		
FINISH: None			
DO NOT SCALE DRAWING			

ICEPICK

TITLE: CNC COWLING

SIZE	DWG. NO.	REV
A	1002	A

SCALE: 1:1	WEIGHT:	SHEET 1 OF 1

REVISIONS			
REV.	DESCRIPTION	DATE	APPROVED
A	INITIAL RELEASE	3/7/2011	RV

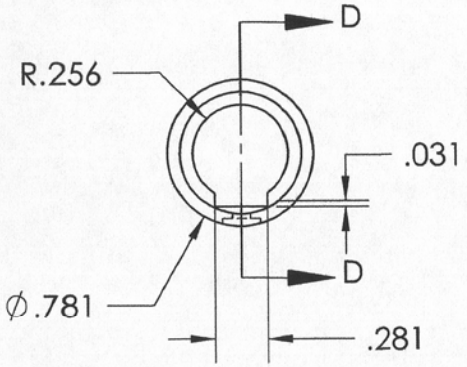

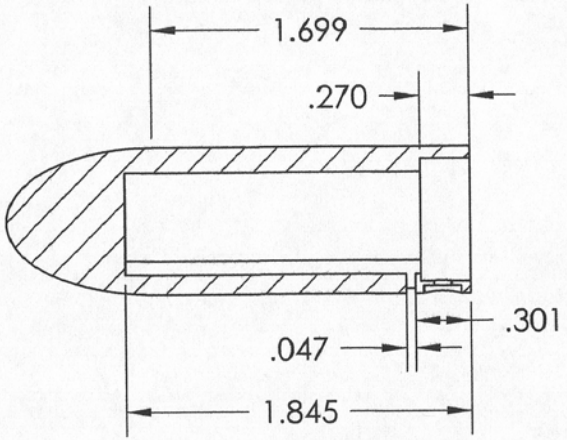

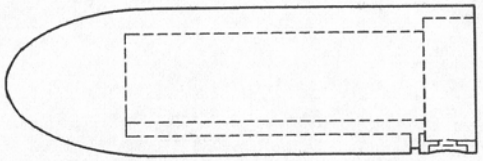

SECTION D-D
SCALE 1 : 1

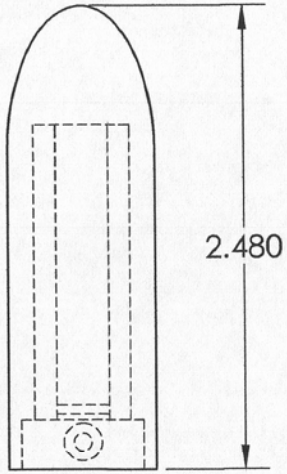

ITEM 26

		NAME	DATE
UNLESS OTHERWISE SPECIFIED: DIMENSIONS ARE IN INCHES	DRAWN	J. Hsu	3/7/2011
Linear Tolerances: x.xx ± .01 x.xxx ± .002	CHECKED		
	COMMENTS:		

PROPRIETARY AND CONFIDENTIAL
THE INFORMATION CONTAINED IN THIS DRAWING IS THE SOLE PROPERTY OF TEAM ICE PICK. ANY REPRODUCTION IN PART OR AS A WHOLE WITHOUT THE WRITTEN PERMISSION OF TEAM ICE PICK IS PROHIBITED. PROPRIETARY AND CONFIDENTIAL

MATERIAL: Aluminum 6061
FINISH: None
DO NOT SCALE DRAWING

ICEPICK

TITLE: NUCELLE

SIZE	DWG. NO.	REV
A	1003	A

SCALE: 1:2 | WEIGHT: | SHEET 1 OF 1

REVISIONS			
REV.	DESCRIPTION	DATE	APPROVED
A	INITIAL RELEASE	3/7/2011	RV

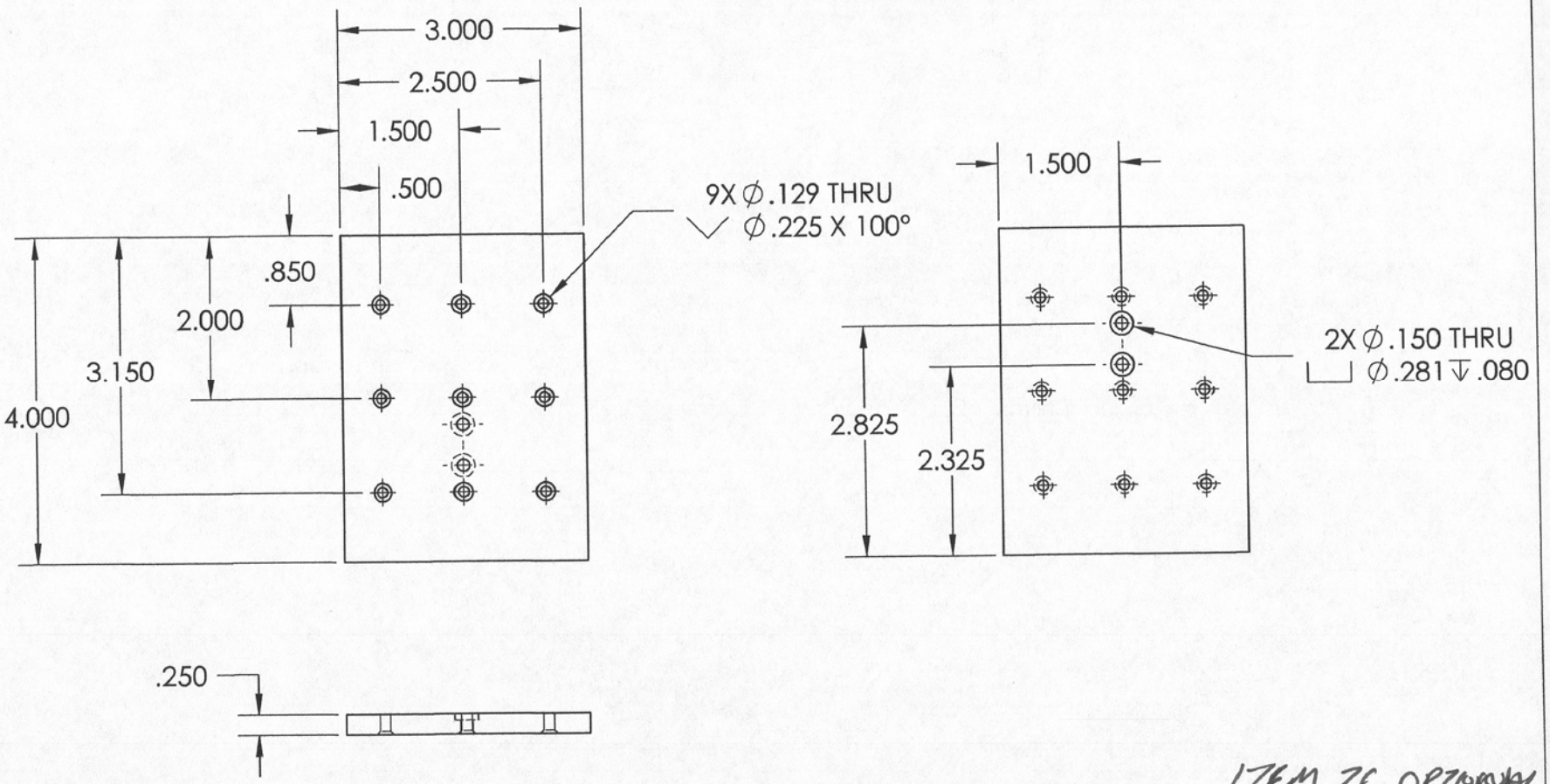

ITEM 2C OPTIONAL

UNLESS OTHERWISE SPECIFIED: DIMENSIONS ARE IN INCHES		NAME	DATE
	DRAWN	J. Hsu	3/7/2011
Linear Tolerances: x.xx ± .01 x.xxx ± .002	CHECKED		
	COMMENTS:		
MATERIAL: Aluminum 6061	PROPRIETARY AND CONFIDENTIAL THE INFORMATION CONTAINED IN THIS DRAWING IS THE SOLE PROPERTY OF TEAM ICE PICK. ANY REPRODUCTION IN PART OR AS A WHOLE WITHOUT THE WRITTEN PERMISSION OF TEAM ICE PICK IS PROHIBITED. PROPRIETARY AND CONFIDENTIAL		
FINISH: None			
DO NOT SCALE DRAWING			

ICEPICK

TITLE: Mounting Plate

SIZE	DWG. NO.	REV
A	1005	A

SCALE: 1:2	WEIGHT:	SHEET 1 OF 1

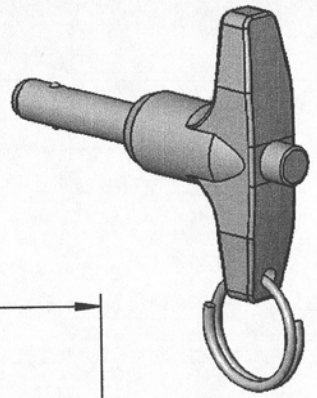

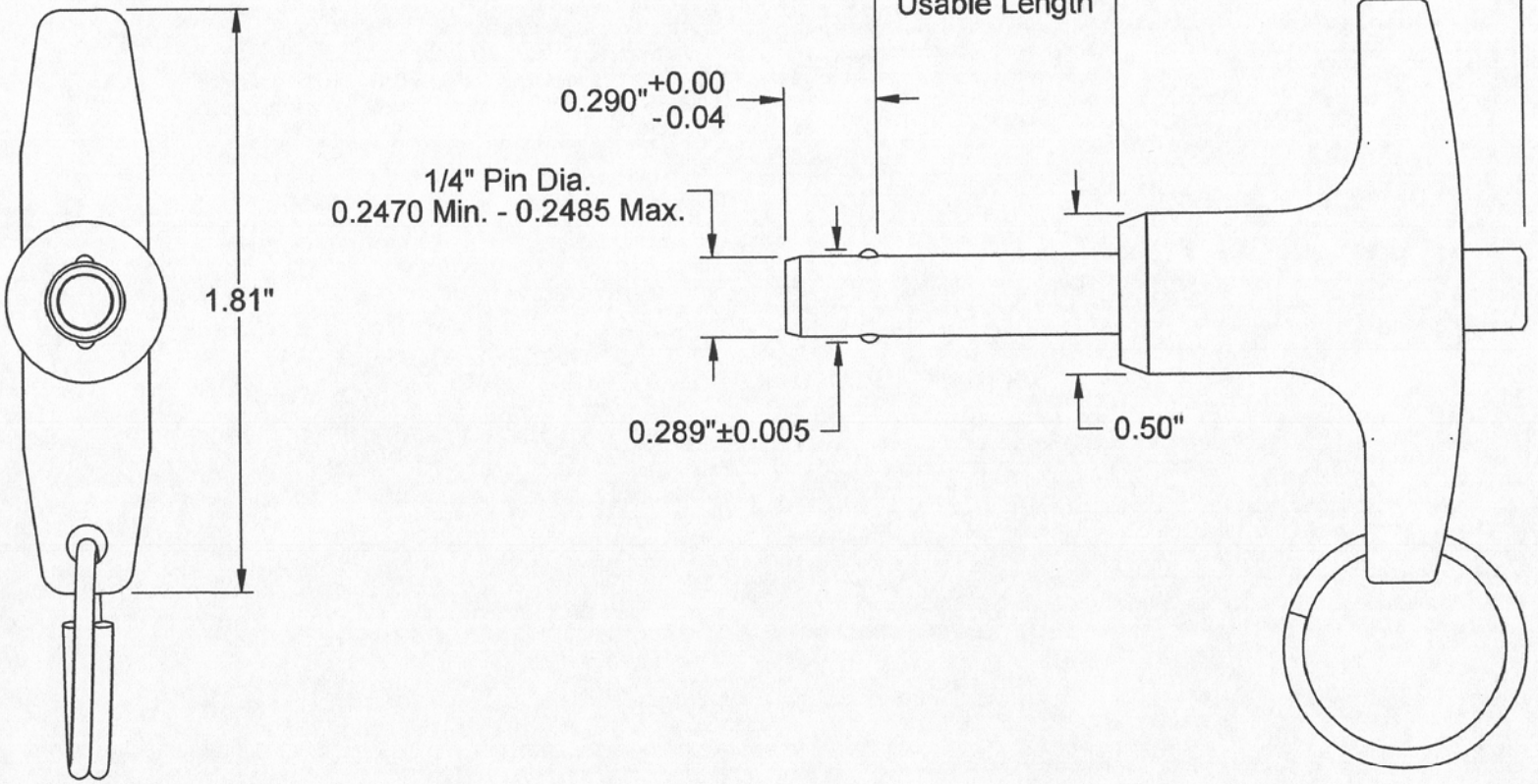

ITEM 27

McMASTER-CARR® CAD	PART NUMBER 90293A135
http://www.mcmaster.com © 2012 McMaster-Carr Supply Company Information in this drawing is provided for reference only.	Aluminum-Handle Push-Button Quick-Release Pin

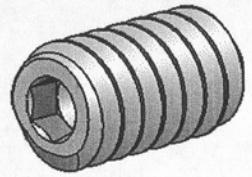

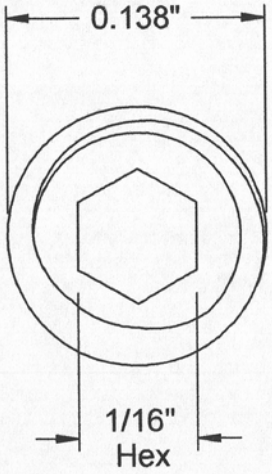

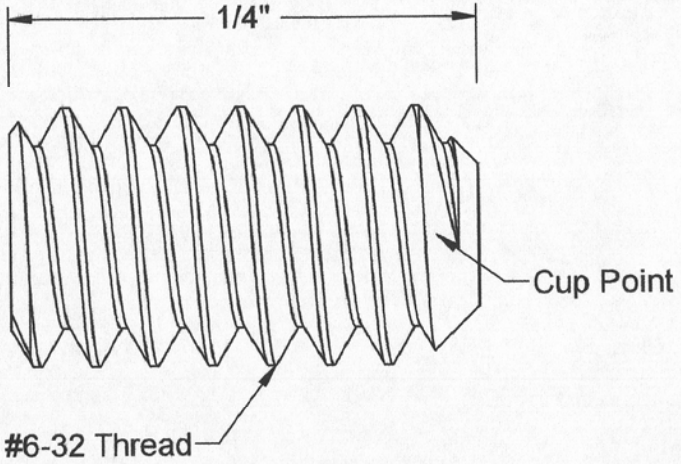

ITEM 33

McMASTER-CARR® CAD	PART NUMBER 92313A144
http://www.mcmaster.com © 2013 McMaster-Carr Supply Company Information in this drawing is provided for reference only.	Cup Point Set Screw

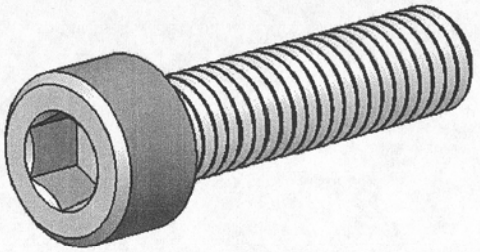

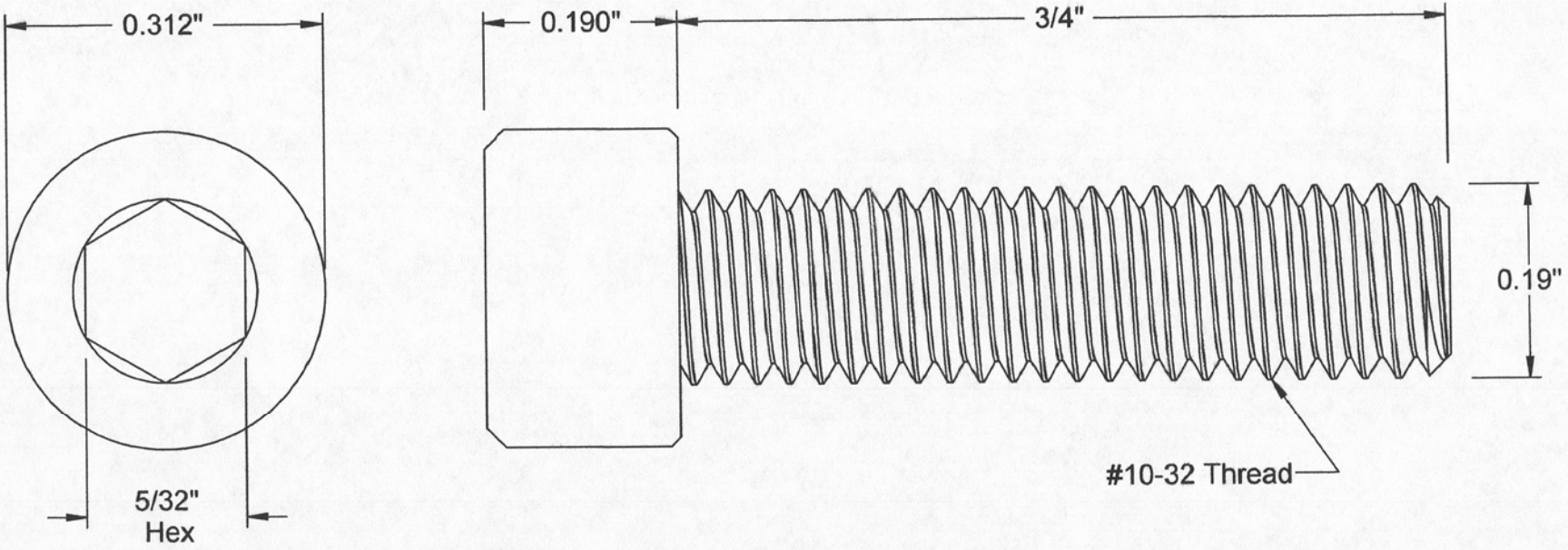

ITEM 34

McMASTER-CARR® CAD	PART NUMBER 91251A345
http://www.mcmaster.com © 2013 McMaster-Carr Supply Company Information in this drawing is provided for reference only.	Alloy Steel Socket Head Cap Screw

Vendor	Contact Information	Materials	Part Number	Price	Quantity	Extended Cost
McMaster-Carr	(562)-692-5911 9630 Norwalk Blvd. Santa Fe Springs, CA 90670-2932 www.mcmastercarr.com	2 1/2" LENGTH SINGLE END 4" NPT PIPE NIPPLE SST	9157K603	$32.68	1	$32.68
		3" Length Double End 4" NPT Pipe Nipple SST	4830K207	$35.22	1	$35.22
		Grade 8, 5/8"-11 Zinc Aluminum Coated Steel Hex Nut	93827A253	$0.64	20	$12.74
		Grade 8, 5/8" Zinc Yellow-Chromate Plated Steel Flat Washer	98023A035	$0.37	50	$18.30
		5/8"-11 Thread, 4-1/2" Long, Zinc-Plated, High-Strength Grade 8 Steel Cap Screw	91257A812	$2.73	16	$43.68
		1.5" Aluminum Extrusion Linear Bearing Mount	60585K33	$55.35	4	$221.40
		Handle Clamp for Linear Bearing	60585K32	$15.50	4	$62.00
		4" Pipe U-Bolt Clamp with Damper	3176T41	$15.35	2	$30.70
		0.5" Square Tubing 6061 Aluminum	6546K49	$2.50	3	$7.50
		Quick Connect Pin	90293A135	$17.35	2	$34.70
		Cup Point Set Screws	92313A144	$0.24	10	$2.35
		1/4-20 Hex Cap Screw for Bearing Block	91251A345	$0.52	20	$10.35
		Caster	2834T34	$10.65	4	$42.60

Amazon Supply	800-220-4242 www.amazon.com	Nozzle 316 SST	45605K122	$18.75	1	$18.75
		4" NPT SST Threaded Pipe Flange	435505K359	$84.95	4	$339.80
		12" Length Double Ended 4" NPT Pipe Nipple SST	4830K382	$24.78	1	$24.78
Transducer Techniques	(951)-719-3900 42480 Rio Nedo Temecula, CA 92590 www.transducertechniques.com	Transducer Techniques RTS	torque sensor	$850.00	1	$850.00
		Load Cell	Force Transducer	$90.00	1	$90.00
C-Flex	(315)-895-7454 104 Industrial Drive Frankfort, New York 13340 www.c-flex.com	Flexure Bearing	gd-10_01	$85.76	2	$171.52
80/20	(260)-248-8030 1701 South 400 East Columbia City, IN 46725 www.8020.net	Aluminum Extrusion	t-slot leg	$35.00	4	$140.00
		Angle Bracket	47065T51	$4.89	18	$88.02
		Angle Bracket Fastener	47065T97	$0.69	104	$71.24

ITEM NO.	PART NUMBER	DESCRIPTION	QTY.	IND. COST	TOTAL COST	VENDOR
1	t-slot 56""	56" TOP EXTRUDED ALUMINUM RAILS	2	35.00	70.00	80/20
2	45605K122	NOZZLE 316 SST	1	18.75	18.75	AMAZON SUPPLY
3	43505K359	4" NPT SST THREADED PIPE FLANGE	4	84.95	365.28	AMAZON SUPPLY
4	9157K603	2 1/2" LENGTH SINGLE END 4" NPT PIPE NIPPLE SST	1	0	0	MCMASTER CARR
5	mesh	STRAIGHTENING MESH	1	8.95	8.95	MCMASTER CARR
6	honeycomb	ALUMINUM HONEYCOMB MESH	1	0.	0.	CAL POLY
7	4830K382	12" LENGTH DOUBLE ENDED 4"NPT PIPE NIPPLE SST	1	24.78	49.56	AMAZON SUPPLY
8	4830K207	3" LENGTH DOUBLE END 4' NPT PIPE NIPPLE SST	1	35.22	35.22	MCMASTER CARR
9	93827A259	5/8" NUT GRADE 8 STEEL ZINC PLATED	16	1.09	17.45	MCMASTER CARR
10	98023A036	5/8" WASHER GRADE 5 ZINC PLATED STEEL	32	8.96/20	17.92	MCMASTER CARR
11	92620A845	2 1/4" LENGTH 5/8" NUT GRADE 8 STEEL ZINC PLATED	16	15.06/15	15.06	MCMASTER CARR
12	60585K33	1.5" ALUMINUM EXTRUSION LINEAR BEARING MOUNT	4	55.35	221.40	MCMASTER CARR
13	sliding surface	C-ARM MOUNTING PLATE	2	0.	0.	CAL POLY MANUFACTURE
14	60585K32	HANDLE CLAMP FOR LINEAR BEARING	4	15.50	62.00	MCMASTER CARR
15	3176T41	4" NPT PIPE U-BOLT CLAMP WITH DAMPER	2	15.35	61.40	MCMASTER CARR
16	nozzle block	NOZZLE BLOCK SPACER MOUNT	1	0.	0.	CAL POLY MANUFACTURE
17	c-arm	C-ARM FOR MICRO RAT MOUNTING	1	0.	0.	CAL POLY MANUFACTURE
18	0.5x0.5-alluminum-tube 1_16-wall-thickness 10	DRILLED ALUMINUM BAR STOCK FOR MOUNTING MICRO RAT	1	5.35	5.35	MCMASTER CARR
19	90 degree brace	ALUMINUM MACHINED BILLET	1	0.	0.	CAL POLY MANUFACTURE
20	0.5x0.5-alluminum-tube 1_16-wall-thickness	FOR LOAD CELL POSITIONING	1	5.35	5.35	MCMASTER CARR

ITEM NO.	PART NUMBER	DESCRIPTION	QTY.	IND. COST	TOTAL COST	VENDOR
21	torque cell to arm	SECURES TORQUE CELL TO ALUMINUM BAR	1	0.	0.	CAL POLY MANUFACTURE
22	torque sensor	TRANSDUCER TECHNIQUES RTS	1	850.00	850.00	TRANSDUCER TECHNIQUES
23	generator holder	SECURES MICRO RAT TO TORQUE SENSOR	1	0.	0.	CAL POLY MANUFACTURE
26	Turbine Blisk - Rev6 - No shaft	TURBINE BLADE	1	0.	0.	BLDS TEAM
27	90293A135	QUICK CONNECT PIN	2	17.35	34.70	MCMASTER CARR
28	gd-10_01	FLEXURE BEARING	2	85.76	85.76	C-FLEX
32	Bearing Block	SUPPORT MECHANISM FOR C-ARM	2	0.	0.	CAL POLY MANUFACTURE
33	92313A144	CUP POINT SET SCREWS	4	2.35/10	2.34	MCMASTER CARR
34	91251A345	HEX CAP SCREW FOR BEARING BLOCK	4	10.35/20	10.35	MCMASTER CARR
35	t-slot 10	SMALL ALUMINUM EXTRUSION BRACE	7	35.00	35.00	80/20
36	t-slot leg	BOTTOM LENGTH ALUMINUM EXTRUSION	4	35.00	35.00	80/20
37	2834T34	CASTER	4	10.65	10.65	MCMASTER CARR
38	t-slot bottom	BOTTOM LENGTH ALUMINUM EXTRUSION	3	35.00	70.00	80/20
39	47065T42	ALUMINUM LEG BRACE FOR CORNER	8	0.	0.	CAL POLY MANUFACTURE
40	47065T51	ANGLE BRACKET	18	4.89	88.02	80/20
41	47065T97	ANGLE BRACKET FASTENER	104	2.74/4	71.24	80/20
42	force transducer	LOAD CELL	1	90.00	90.00	TRANSDUCER TECHNIQUES
43	TOTAL COST			2473.02		

DO NOT SCALE DRAWING

COMMENTS:

TITLE: COSTING AND VENDOR INFORMATION

SIZE	DWG. NO.	REV
B		

SCALE: 1:4	DATE:	SHEET 2 OF 2

Datum / Date: 2/2/2015

PROJECT PROPOSAL REQUIREMENTS:

- FOLLOW SUCCESS GUIDE
- MAKE SURE PDF
- BY 12 PM TUESDAY MORNING
- FILL IN TABLE CONTENTS
- STAMPER

2/3/2015

- CREATIVE FUNCTIONS.
- STATEMENT OF FUNCTION SHOULD BE GENERAL.
  - " INCREASE VELOCITY"
  - " STRAIGHTEN FLOW "
  - " MEASURE THRUST "
  - " MEASURE TORQUE "
  - " RE-CREATE FLIGHT-

PRIMARY:

- MEASURE THRUST FUNC.
- INCREASE VELOCITY. FUNC
- MEASURE THRUST FUNC
- RE-CREATE WIND ENVIRONMENT. ATT
- EASILY INTERCHANGE ATT
- ADAPT TO AIR SYSTEM ATT
- REDUCE LOSSES. ATT
- MOUNT READILY. ATT
- ENVELOPE MICRO-RAT FUNC
- IMPRESS NORTHROP. ATT

SECONDARY.

- MEASURE TORQUE FUNC
- LOOK PRETTY ATT
- HAVE AN ENCLOSURE ATT
- HAVE 3-5 FACTOR ATT OF SAFETY.
- MINIMIZE AIR STREAM % DIFFERENCE ATT
- CREATE FORCE AMPLIFICATION. ATT

FUNCTIONS / ATTRIBUTES:

ATTRIBUTES:

- THIS DEVICE WILL BE SAFE
- THIS DEVICE WILL QUALITY OF DEVICE.

FUNCTIONS.

BRAIN STORMING:

STRAIGHTENING

- STRAWS
- CLOTH
- MESH
- HONEYCOMB
- TREE ROOTS
- VORTEX GENERATORS
- SOCKS.
- SLEEVES
- HAIR.
- PAPER
- TRAFFIC CONE
- STREAMERS
- RED SOLO CUPS W/ HOLES.
- PVC PIPES.
- SMALL DEVICE W WINGS/FINS.
- ATTRACT SOMEONE IS HAVING FUN
  - MOUTHS
  - EMPTY SUPERSOAKER
  - SPONGE.
  - GARDEN HOSE
  - KEVLAR.
  - LONG STRETCH OF STRIPE
  - DONT BEND OF HEAT. / COOLING

Datum / Date: 2/3/2015

- MUFFLER
- GLASS PACK.
- MAZE
- SWISS CHEESE
- ALGEA.
- WIRE
- ION STRAIGHTENING
- CHARGES
- FRUIT.
- FRUIT LOOPS.
- DONUTS.
- PRESSURE.
- TUBE MICRO RAT.
- PIPE COATINGS
- NOODLES.
- SIDE GRABBERS.
- CENTRIFUGE
- FANS
- HOVER BOARDS
- NEGATOIDS
- NOZZLE
- PIPE SLITS
- AEROSOL.
- MARBLES
- GRASS
- BIO FILTERS
- CHOPSTICKS
- ELECTRICITY.
- ADJACENT AIR STREAMS
- EDDY CREATORS
- PAPAYA.
- COFFEE
- MIST
- TEFLON.
- BOUNDARY LAYER REDUCTION
- EXPANSION CHAMBER
- TOILET PAPER ROLES
- BLOW DRYERS
- PENCILS.
- UNDER DOOR GAPS
- BOUNDARY LAYER HAIR.
- MITOCHONDRIA
- AIR SINKS
- PIPE CLEANERS

BRAINWRITING:
ON PAPER

SCAMPER:

SUBSTITUTE - UNSTRAIGHT FOR STRAIGHT.
- AIR FOR WATER.

COMBINE: VORTEX W/ HONEYCOMB
CLOTH OVER MESH.
MESH W/ TREE ROOTS
EXPANSION CHAMBER W/ NOZZLE.
BOUNDARY LAYER REDUCTION W/ HEAT.
ION STRAIGHTENING W/ SLITS)
EDDY CREATORS /W VORTEX!
ALGEA W/ CHOPSTICKS.
TEFLON W/ SPONGE.

ADAPT: - USE SKEWERS POSSIBLY INSTEAD OF
- CHOPSTICKS.
- MAKE SLITS INTO AIR SINKS.
- GARDEN HOSE INTO A NOZZLE
- LIKE A WIND TUNNEL
- DYSON VACUUM!
- AIR GUN ON COMPRESSOR

MODIFY: SQUARE AIR STREAM.
MAKE IT WHISTLE
MAKE NOZZLE AIR STRAIGHTENER
MAKE NOZZLE THE SHAPE OF AN ASTERISK!

PUT TO OTHER USES: - TO BLOW DANDILIONS
- TEACH PEOPLE ABOUT AIR SAFETY KITE BOARDING
- HAND DRYER
- GOLF BALL LAUNCHER
- BASEBALL LAUNCHER

Datum / Date: 2/3/2015

ELIMINATE - THE NOZZLE
- NO- MICRO RAT USE BETTER BATTERIES.
- TEAMATES
- TORQUE MEASUREMENT

RE-ARRANGE - VACUUM CHAMBER LETS BLOW AIR OVER RAT INTO CHAMBER
- CREATE A CENTRIFUGE MOVE RAT INSTEAD.
- PUT IT ON A CAR. MOVING 230 MPH

- USE EPOXY/SCREW TO PERMANETLY ATTATCH MICRO RAT TO A SLIDER WITH SQUEEZE CLAMPS TO ADJUST POSITION FROM AIR STREAMLINE

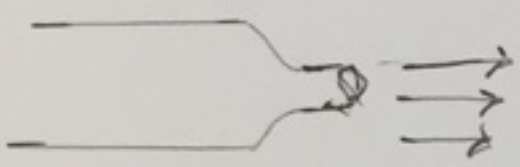

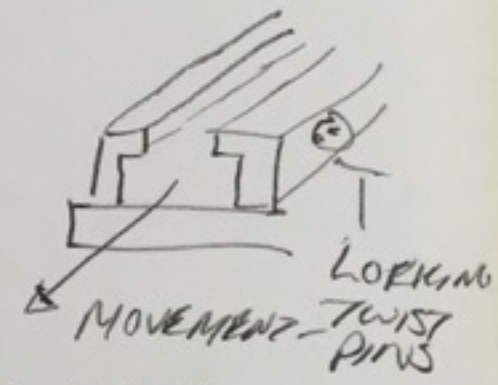

Add extension to the mounting guide

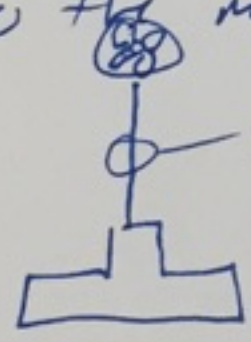

Measure thrust with strain gauge & minimize interference with flow.

- Use an array of screw holes that the MICRO RAT can be moved around and screwed down for adjustability

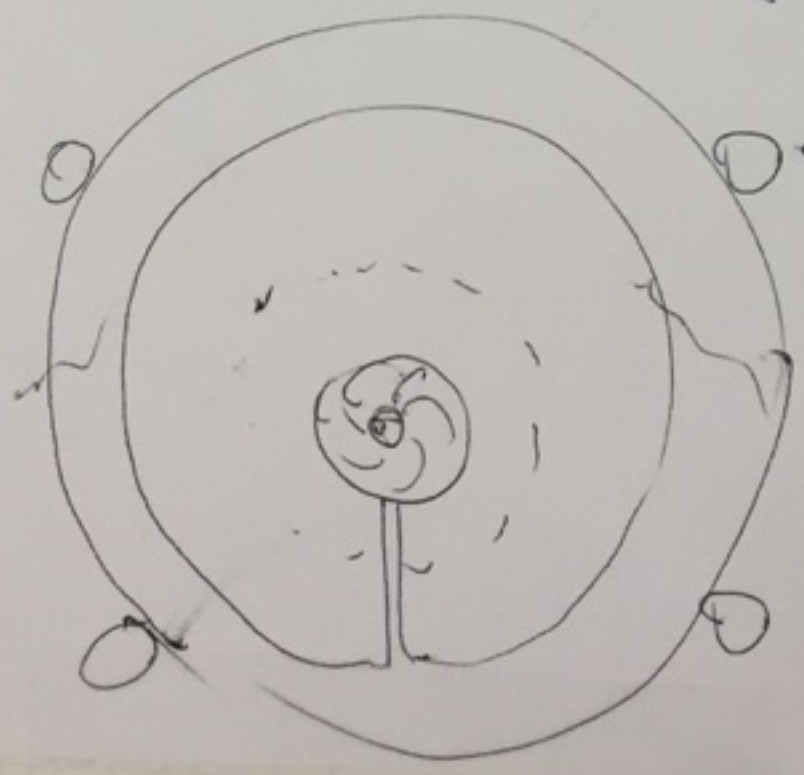

← bearing support

- minimal interference w/ rotor

Pneumatic Test Procedure

Pneumatic tests are potentially more dangerous than hydrostatic because of the higher level of potential energy. Pneumatic tests may be performed only when at least one of the following conditions exists:

- When pressure systems are so designed that they cannot be filled with water.
- When pressure systems are to be used in services where traces of the testing medium cannot be tolerated.

In addition to a justification, a piping schematic for pneumatic pressure test is required. A recommended typical piping schematic for pneumatic test is shown in Figure 1. In our case a hydrostatic test is impossible at system pressure due to sealing problems in our wire mesh interface.

Important Installation of a pressure relief valve is required for a pneumatic test.

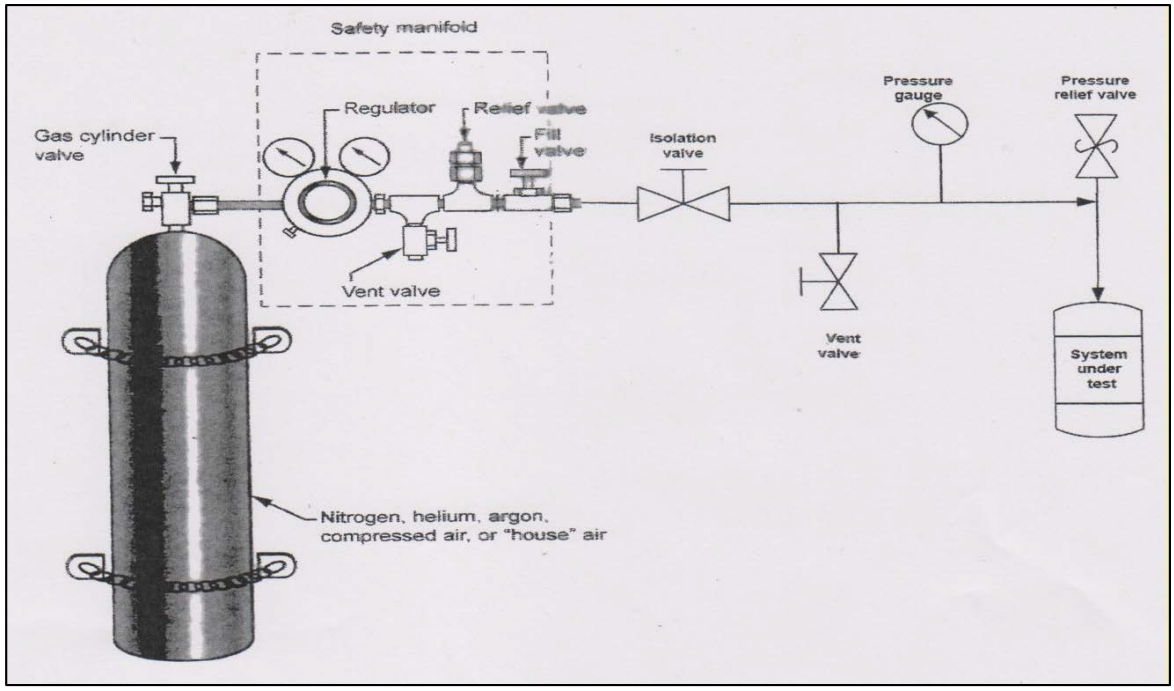

Figure 1. Recommended Typical Piping Schematic for Pneumatic Testing

Step	Person	Action
Planning		
1.	Mechanic	Obtains test pressure after consulting the Russell Westphal/ Jim Gerhardt *Note: ensures that the pneumatic test pressure does not exceed the established test pressure of the system, unless otherwise specified in the design documents.*
2.	Mechanic	Completes pressure test plan, including justification for pneumatic testing and a piping schematic for the test, and submits for approval
3.	Supervisor	Approves plan
4.	Russell Westphal	Approves plan
Performing		
5.	Mechanic	Ensures that the test gauge has a current calibration sticker. (A pressure relief valve or non-reclosing relief device may be installed in the test medium supply line to ensure that this limit is not exceeded.)
6.	Mechanic	Ensures that the test area is properly flagged, barricaded, or otherwise controlled to prevent unauthorized personnel entry
7.	Mechanic	Removes from the immediate area all persons not directly involved in the test
8.	Mechanic	Installs the calibrated test gauge so it is visible at all times
9.	Mechanic	Verifies that the pressure is continually monitored to ensure that pressure never exceeds the designated test pressure of the system
10.	Mechanic	Removes relief devices from the system to be tested, where the test pressure will exceed the set pressure of the device OR Holds down each valve disk by an appropriate test clamp and equalizes pressure on non-reclosing relief devices
11.	Mechanic	Pressurizes the system, raising pressure in the system gradually until not more than 1/2 of the test pressure is achieved
12.	Mechanic	Increases the pressure slowly in steps of approximately 1/10 of the test pressure until the required test pressure has been reached
13.	Mechanic	Reduces the pressure to the maximum operating pressure before proceeding with the inspection; holds the pressure for a sufficient period of time to permit inspection of the system
14.	Mechanic	Checks the pressure gauge periodically for indications of leakage
15.	Mechanic	Applies a soap solution to accessible welds, screwed pipe joints, flanges, et cetera where leakage is suspected
16.	Mechanic	If there is evidence of structural distortion, either rejects the system or repairs as advised by the inspector
17.	Mechanic	If there is leakage in the system, performs the following as appropriate: ▪ Ensures repair is performed and return to Step 11 or

Step	Person	Action
		▪ Rejects the system
18.	Mechanic	When the test is completed, vents the test medium to approved discharge vicinity
Recording		
19.	Inspector	Signs pressure test record
20.	Mechanic	Completes pressure test record and submits copy to the DVP
21.	Mechanic	Submits copies of the test plan and test record to the Report

ME428 DVP&R Format

Report Date		Dr. Westphal				Mount			REPORTING ENGINEER:		
TEST PLAN								**TEST REPORT**			
Item No	Specification or Clause Reference	Test Description	Acceptance Criteria	Test Responsibility	Test Stage	TIMING		TEST RESULTS			NOTES
						Start date	Finish date	Test Result	Quantity Pass	Quantity Fail	
1	Flexure Bearing	In order to verify the rotational spring constant for calibration of instrumentation a micro-Rat will be hung from a cantilever location. This sample mass will help us "tare" our load cell to a zero drag absolute zero position.	After calibration, changes in mass of the micro rat, up to five pounds, should be recorded accuratly within a percent difference of known weight. This method will confirm that hysterisis has negligeable effect inside the flexure bearing.	Cameron	PV	9/25/2015	10/10/2015				
2	Drag	Maximum drag force range must be known to stay within the bounds of the fixtures capabilities. The maximum range of our load cell setup must be determined. Hanging additional known mass from the micro-RAT in a vertical plane will allow gravity to simultate additional drag force and test the range of input force correctly measured by our fixture setup.	After calibration, changes in mass of the micro rat should be recorded accuratly within a percent difference of known weight. This method will confirm that hysterisis has negligeable effect inside the flexure bearing. The max moment and minimum moment locations will be used to set this input range.	Ken	PV	9/25/2015	10/10/2015				
3	Torque	Maximum transducer torque	Dimensionless group graphs for shaft torque with varying free stream velocity will be visually inspected for congruence to theory.	Cameron	PV	9/25/2015	10/10/2015				
4	Wind velocity	Maximum velocity, average as well as maximum percent difference. A pitot-static probe will be used to determine the velocity in the 4" pipe. A 230 mph free stream velocity corresponds to a 95 mph 4" tube velocity.	Pass/Fail 230 mph minumum free stream velocity.	Issac	PV	9/25/2015	10/10/2015				
5	Full Test Operation Time	The test must be set up and run. The micro-RAT must be mounted, the measurement system calibrated, the flow straightener bolted on to the air supply, the trial run with data collected, and the system removed and stored in the fluids lab.	2-3 Hours.	Ken	PV	9/25/2015	10/10/2015				
6	Pressure Test	Test is outlined in Appendix entry test procedure	pass with minimal leakage	Ken	PV	9/25/2015	10/10/2015				
7											
8											
9											
10											
11											
12											
15											
16											
17											
18											
19											
20											
21											
22											
23											
24											
25											
26											
27											
28											
29											
30											

Potential Failure Mode and Effect Analysis of Flow System

Prepared By: Cameron Naugle, Kenny Enstrom, Cody Lee, and Isaac Thomas

FMEA Date (03/10/2015)

Item / Function	Potential Failure Mode	Potential Effect(s) of Failure	Sev	Potential Cause(s) / Mechanism(s) of Failure	Occur	Crit	Recommended Action(s)	Responsibility & Target Completion Date	Action Results			
									Actions Taken	Sev	Occur	Crit
Expanision Chamber	Corrosion	Rupture, Loss of pressure, Flow Loss	10	Moisture in air stream	1	10	Powder Coating	5/27/2015 Cody				
	Fatigue	Rupture, Loss of pressure	10	Extended use	1	10	Higher Pipe Schedule/ Increased support structure	5/27/2015 Cody				
	Brittle Fracture	Rupture, Loss of pressure	10	Overpressurization	3	30	Higher Pipe Schedule/ Increased support structure	5/27/2015 Cody				
	Thermal Expansion	Rupture, Loss of pressure	10	Exposure to high heat	1	10	Reflective coating	5/27/2015 Cody				
Flow Straightening	Dislodging	Micro-RAT destruction, Loss of Function, Personal Injury	10	Vibration, Fracture, fouling	3	30	Secure Mounting Technique, Bolstering	6/5/2015 Cameron				
	Fouling	Loss of flow, Loss of function, loss of repeatability, Increased Back pressure	5	Impurity in airstream, corrosion, bending	5	25	Routine Inspection Procedure	6/5/2015 Cameron				
Nozzeling	Explosive Dislodging	loss of function, personal injury, micro-RAT destruction	10	Vibration, brittle fracture, fatigue, back pressure	4	40	Routine Inspection Procedure	6/5/2015 Ken				
	Corrosion	loss of flow, loss of repeatability, weakening	4	Moisture in air stream	2	8	absorber material	6/5/2015 Ken				
	Brittle Fracture	loss of function, potential dislodging, personal injury	10	Vibration, brittle fracture, fatigue	1	10	Routine Inspection Procedure	6/5/2015 Ken				

Potential Failure Mode and Effect Analysis of Mounting System

Prepared By: Cameron Naugle, Kenny Enstrom, Cody Lee, and Isaac Thomas

FMEA Date (03/10/2015)

Item / Function	Potential Failure Mode	Potential Effect(s) of Failure	Sev	Potential Cause(s) / Mechanism(s) of Failure	Occur	Crit	Recommended Action(s)	Responsibility & Target Completion Date	Action Results			
									Actions Taken	Sev	Occur	Crit
Torque Sensor	Exceed Maximum Torque	Loss of device	6	Loss of airstream velocity control	3	18	Robust valve control system, Safe operating procedure	8/10/2015 Isaac				
	Fatigue	Loss of repeatability	5	Cyclic loading/Thermal fatigue	4	20	Minimize cantilever weight	8/10/2015 Isaac				
	Overheating	Loss of repeatability	4	Exposure to high heat	1	4	Cool environment	8/10/2015 Isaac				
Force Transducer	Exceed Maximum Force	Loss of device	6	Loss of airstream velocity control	3	18	Robust valve control system, Safe operating procedure, Static analysis	8/10/2015 Cody				
	Fatigue	Loss of repeatability	5	Cyclic loading/Thermal fatigue	4	20	Robust force transducer	8/10/2015 Cody				
	Overheating	Loss of repeatability	4	Exposure to high heat	1	4	Cool environment	8/10/2015 Cody				
Structure	Fatigue	loss of repeatability, increased likelihood of damage to components	7	Cyclic Loading	5	35	Routine Inspection Procedure	6/5/2015 Ken				
	Brittle Fracture	Loss of function	10	Cyclic Loading	2	20	Routine Inspection Procedure	6/5/2015 Ken				
Flexure Bearing	Fatigue	loss of function	4	Cyclic Loading	4	16	Routine Inspection Procedure	6/5/2015 Cameron				
	Brittle Fracture	loss of function	6	Cyclic Loading	1	6	Routine Inspection Procedure	6/5/2015 Cameron				